MASTER

LTR 20-103
Proj. No. P 394

PRELIMINARY POSTTEST ANALYSIS OF LOFT LOSS-OF-COOLANT EXPERIMENT L2-2

JAMES R. WHITE WILLIAM H. GRUSH
CLINT D. KEELER

June 1979

EG&G Idaho, Inc.

IDAHO NATIONAL ENGINEERING LABORATORY

DEPARTMENT OF ENERGY

IDAHO OPERATIONS OFFICE UNDER CONTRACT DE-AC07-76IDO1570

EG&G Idaho, Inc.

FORM EG&G 398
(Rev. 12-78)

INTERIM REPORT

Accession No. ____________

Report No. LTR 20-103

Contract Program or Project Title:

LOFT Experimental Program Division
Proj. No. P 394

Subject of this Document:

Preliminary Posttest Analysis of LOFT Loss-of-Coolant Experiment L2-2

Type of Document:

LOFT Technical Report

Author(s):

J. R. White, W. H. Grush, and C. D. Keeler

Date of Document:

Responsible NRC Individual and NRC Office or Division:

G. D. McPherson, Director Safety Research, USNRC

This document was prepared primarily for preliminary or internal use. It has not received full review and approval. Since there may be substantive changes, this document should not be considered final.

EG&G Idaho, Inc.
Idaho Falls, Idaho 83401

Prepared for the
U.S. Nuclear Regulatory Commission
and the U.S. Department of Energy
Idaho Operations Office
Under contract No. DE-AC07-76ID01570
NRC FIN No. A6048

INTERIM REPORT

EG&G Idaho, Inc.

LOFT TECHNICAL REPORT
LOFT PROGRAM

FORM EG&G-229
(Rev. 12-76)

TITLE: Preliminary Posttest Analysis of LOFT Loss-of-Coolant Experiment L2-2	REPORT NO.: LTR 20-103
AUTHOR: J. R. White, W. H. Grush, and C. D. Keeler	GWA NO.:
PERFORMING ORGANIZATION: LOFT Experimental Program Division	DATE: June 27, 1979
LOFT APPROVAL: LEPD Manager	

DISPOSITION OF RECOMMENDATIONS

A complete posttest analysis of LOCE L2-2 results will be done as time permits. Additional testing recommended in this report is currently planned on being done in the LOFT Test Support Facility. It was recommended that the experiment prediction for LOFT LOCEs L2-3 and L2-4 be repeated. This will be done prior to performing these experiments. The quality assurance procedures for code input will be reviewed and appropriately revised.

SUMMARY

A preliminary posttest analysis of Loss-of-Coolant Experiment (LOCE) L2-2, which was conducted in the Loss-of-Fluid Test (LOFT) facility, was performed to gain an understanding of the cause of the disparity between predicted and measured fuel rod cladding temperature responses in the LOFT core. LOCE L2-2 was performed as part of the LOFT Experimental Program conducted by EG&G Idaho, Inc., for the U.S. Nuclear Regulatory Commission. LOCE L2-2 is the first experiment in the LOFT Power Ascension Series L2 (first series of LOFT nuclear experiments), which was designed to investigate the response of the LOFT nuclear core to the blowdown, refill, and reflood transients during LOCEs conducted at gradually increasing power levels. LOCE L2-2 was conducted at 50% power (25 MW, 26.38 kW/m).

Results from LOCE L2-2 show that a core-wide rewet occurred early in the transient (during blowdown starting at about 7 s after rupture) which was not calculated in the pretest prediction analysis. This early core-wide rewet resulted in the peak fuel rod cladding temperatures being lower (by a mean value of 166 K for 24 thermocouples) than had been calculated. This preliminary posttest analysis was concerned solely with determining why the early core-wide rewet was not predicted by the RELAP4/MOD6 pretest analysis and by no means is it a complete posttest analysis of LOCE L2-2 results. However, during this analysis, several errors made in the prettest analysis were found, and their impact on the predicted results is assessed.

Three factors were postulated to have caused the disparity between predicted and measured fuel rod cladding temperatures for LOCE L2-2: (a) the initial fuel rod stored energy, (b) the heat transfer surface, and (c) the hydraulics calculation. These factors were examined and are discussed in this report. It was determined that core hydraulics, as influenced by the calculation of broken loop cold leg break flow, was the major factor causing the disparity.

CONTENTS

SUMMARY ii

I. INTRODUCTION 1

II. MEASURED FUEL ROD CLADDING TEMPERATURE RESPONSE 5

1. TYPICAL COMPARISON OF PREDICTED AND LOCE L2-2 DATA . . . 5

2. UNCERTAINTY AND PERTURBATION EFFECT OF THERMOCOUPLES . . 7

III. PREDICTED FUEL ROD CLADDING TEMPERATURE RESPONSE 9

1. FUEL ROD STORED ENERGY 9

2. THE RELAP4/MOD6 HEAT TRANSFER SURFACE 9

2.1 Assessment of RELAP4/MOD6 Heat Transfer Calculation 10
2.2 Heat Transfer Option Selection Sensitivity Study Results 10
2.3 RELAP4/MOD6 Rewet Criteria 18

3. THE RELAP4/MOD6 CALCULATED CORE HYDRAULICS 19

3.1 Evidence of Core Flow Underprediction 19
3.2 Effects of Using Measured Initial Conditions 21
3.3 Break Flow Sensitivity Study Results 27
3.4 Fuel Rod Computation Scheme 44
3.5 Effects of RELAP4/MOD6 Control Volume Corrections 46

IV. CONCLUSIONS 51

V. REFERENCES 54

APPENDIX A - FUEL ROD STORED ENERGY, GAP CONDUCTANCE, AND HEAT TRANSFER SENSITIVITY STUDIES 55

APPENDIX B - CRITICAL FLOW TRANSITION QUALITY 63

APPENDIX C - DETERMINATION OF THE CAUSE OF THE FUEL ROD COMPUTATION SCHEME PROBLEM 77

FIGURES

1. LOFT major components in cold leg break configuration 2

2. LOFT core configuration and instrumentation 3

3. Comparison of predicted and measured fuel rod cladding temperature response near the midplane of the center fuel module during LOCE L2-2 6

4. Predicted versus measured local maximum fuel rod cladding temperature for the Semiscale Mod-1, THTF core base cases, and LOCE L2-2 11

5. Cladding temperature of average-powered fuel rod showing sensitivity due to film boiling correlation choice for lower third of core 12

6. Cladding temperature of average-powered fuel rod showing sensitivity due to film boiling correlation choice for middle third of core 13

7. Cladding temperature of average-powered fuel rod showing sensitivity due to film boiling correlation choice for upper third of core 14

8. Quality in center of core showing sensitivity due to film boiling correlation choice 16

9. Cladding temperature on highest-powered fuel rod showing sensitivity to both film boiling correlation choice and initial conditions 17

10. Comparison of predicted and measured momentum flux above fuel Module 1 20

11. Comparison of predicted and measured momentum flux above fuel Module 3 20

12. Cladding temperature of average-powered fuel rod showing sensitivity due to using measured initial conditions for lower third of core 22

13. Cladding temperature of average-powered fuel rod showing sensitivity due to using measured initial conditions for middle third of core 23

14. Cladding temperature of average-powered fuel rod showing sensitivity due to using measured initial conditions for upper third of core 24

15. Upper plenum pressure showing sensitivity due to using measured initial conditions 25

16. Quality in middle third of core showing sensitivity due to using measured initial conditions 26

17. Comparison of predicted and measured mass flow in the broken loop cold leg 28

18. Cladding temperature of average-powered fuel rod showing sensitivity due to break flow multiplier for lower third of core 29

19. Cladding temperature of average-powered fuel rod showing sensitivity due to break flow multiplier for middle third of core 30

20. Cladding temperature of average-powered fuel rod showing sensitivity due to break flow multiplier for upper third of core 31

21. Quality in middle third of core showing sensitivity due to break flow multiplier 32

22. Core inlet mass flow rate showing sensitivity due to break flow multiplier 33

23. Upper plenum pressure showing sensitivity due to break flow multiplier 34

24. Henry-Fauske/homogeneous equilibrium critical flow model . . 36

25. Henry-Fauske/homogeneous equilibrium critical flow model with linear weighting transition 37

26. Broken loop cold leg mass flow rate showing sensitivity due to critical flow transition quality 38

27. Core inlet mass flow rate showing sensitivity due to critical flow transition quality 39

28. Core inlet mass flow rate showing sensitivity due to critical flow transition quality (expanded scale) 40

29. Cladding temperature of average-powered fuel rod showing sensitivity due to critical flow transition quality for lower third of core 41

30. Cladding temperature of average-powered fuel rod showing sensitivity due to critical flow transition quality for middle third of core 42

31. Cladding temperature of average-powered fuel rod showing sensitivity due to critical flow transition quality for upper third of core 43

32. Core entrance calculated mass flow rate for system model and center, control, and corner fuel module hot rods 45

33. Core entrance mass flow rate showing effects due to control volume corrections 47

34. Core entrance mass flow rate showing effects due to control volume corrections (expanded scale) 48

35. Cladding temperature of average-powered fuel rod showing effects due to control volume corrections for middle third of core 49

A-1. Calculated fuel rod cladding temperature response for LOCEs L2-2, L2-3, and L2-4 58

A-2. Initial fuel rod cladding temperature slope as a function of fuel rod stored energy 59

A-3. Fuel rod cladding temperature history for adiabatic and best-estimate LOCE L2-2 prediction compared with LOCE L2-2 measured data 60

A-4. Fuel rod cladding surface temperature response as a function of fuel-cladding gap conductance for simulated LOCE L2-2 conditions 61

B-1. Ratios of measured break mass flow rates to HEM calculated critical mass flow rates 65

B-2. Stagnation universal quality calculated by MASFLO program 66

B-3. Stagnation quality history for Semiscale Mod-1 Test S-02-4 67

B-4. Ratios of measured break mass flow rates to critical mass flow rates calculated using five critical flow models (t = 0 to 5 s) 68

B-5. Ratios of measured break mass flow rates to critical mass flow rates calculated using five critical flow models (t = 0 to 20 s) 69

B-6. Stagnation quality history for Semiscale Mod-1 Test S-06-5 70

B-7. Comparison of measured break flow rates and calculated critical flow rates for Semiscale Mod-1 Test S-06-5 71

B-8. Ratios of measured to calculated break flow rates for Semiscale Mod-1 Test S-06-5 72

B-9. HEM mass flow ratio as a function of stagnation universal quality for Semiscale Mod-1 Test S-06-5 73

B-10. Henry-Fauske mass flow ratio as a function of stagnation universal quality for Semiscale Mod-1 Test S-06-5 74

C-1. Model schematic of LOFT system showing volumes used to test the hot rod computational scheme 80

C-2. Schematic of junctions connected to plenum volumes for system and hot rod calculations 81

C-3. Schematic depicting the dual time-dependent volume method . . 82

C-4. Volume-averaged velocity for volume below the core 83

C-5. Volume-averaged velocity for volume above the core 84

C-6. Mass flow rate in core inlet 85

C-7. Mass flow rate in upper third of core 86

C-8. Volume quality in middle third of core 87

C-9. Fuel rod cladding surface temperature in lower third of core 88

C-10. Fuel rod cladding surface temperature in middle third of core 89

C-11. Fuel rod cladding surface temperature in upper third of core 90

PRELIMINARY POSTTEST ANALYSIS OF LOFT LOSS-OF-COOLANT EXPERIMENT L2-2

I. INTRODUCTION

A preliminary posttest analysis of Loss-of-Coolant Experiment (LOCE) L2-2, which was conducted in the Loss-of-Fluid Test (LOFT) facility, was performed to gain an understanding of the cause of the disparity between predicted and measured fuel rod cladding temperature responses in the LOFT core. LOCE L2-2 was the first experiment performed in the LOFT Power Ascension Series L2, which is the first series of experiments to be performed in LOFT with the nuclear core producing power. These experiments are all full, double-ended cold leg break experiments and are being conducted by EG&G Idaho, Inc., for the U.S. Nuclear Regulatory Commission.

The specific objectives of LOCE L2-2 were to determine fuel rod-to-coolant heat transfer in the postcritical heat flux regime and to determine whether any cladding perforation occurs as a result of a loss of coolant with the nuclear reactor operating at a 26.25 kW/m maximum linear heat generation rate (50% rated core power). To satisfy these objectives, the LOFT facility was configured and operated to simulate a postulated loss-of-coolant accident resulting from a 200% double-ended offset shear break in the cold leg of the primary coolant system of a large (∿1000 MWe) pressurized water reactor. The major components of LOFT in the cold leg break configuration are shown in Figure 1. Figure 2 shows the LOFT core configuration and the locations and types of in-core instrumentation.

Prior to conducting LOCE L2-2, a pretest prediction analysis[1] was performed using the RELAP4/MOD6[2] and the FRAP-T4[3] computer codes. Results from LOCE L2-2 show that a core-wide rewet occurred early in the transient (during blowdown starting at about 7 s after rupture) which was not calculated in the pretest prediction analysis. This early core-wide rewet resulted in the peak fuel rod cladding

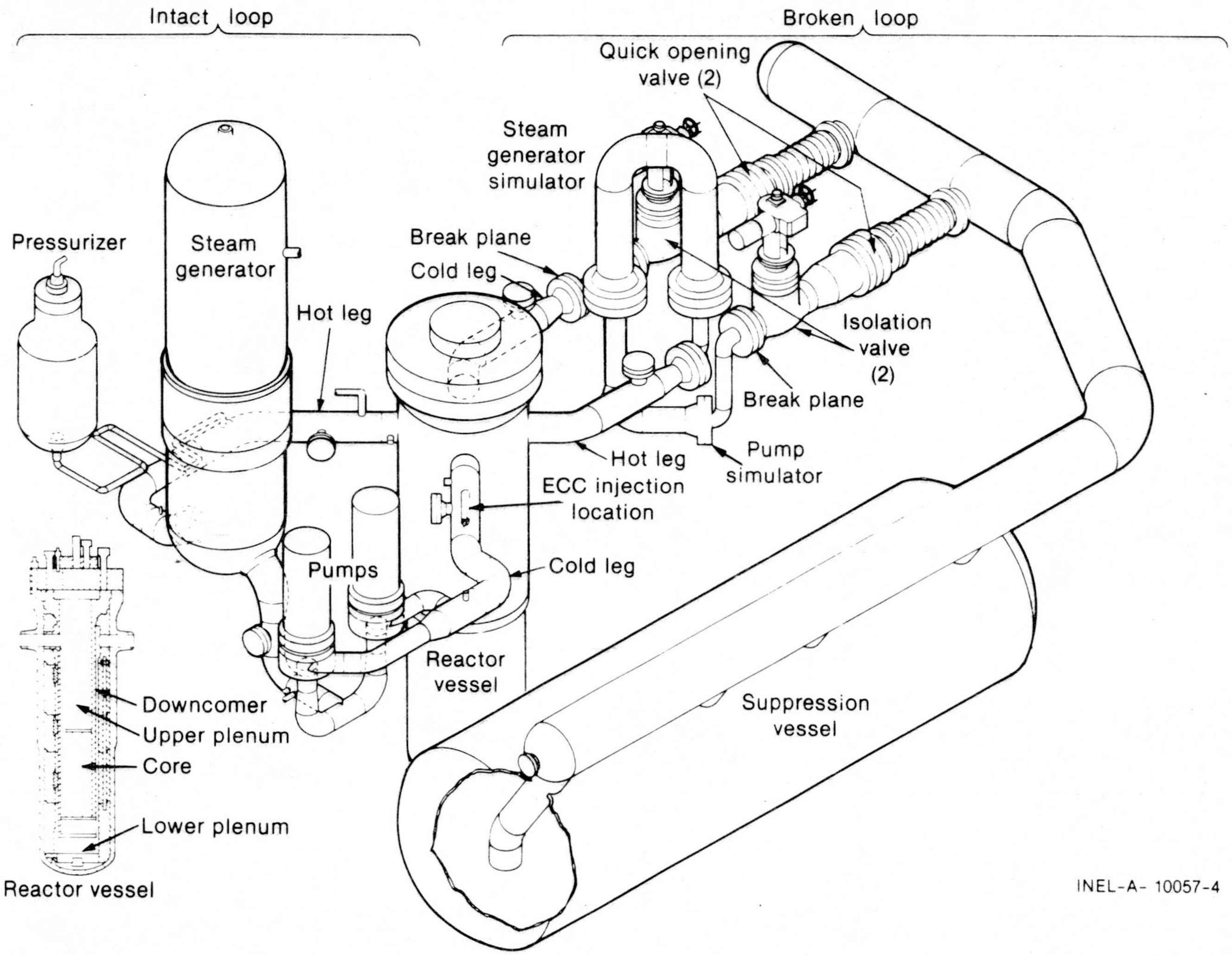

Fig. 1 LOFT major components in cold leg break configuration.

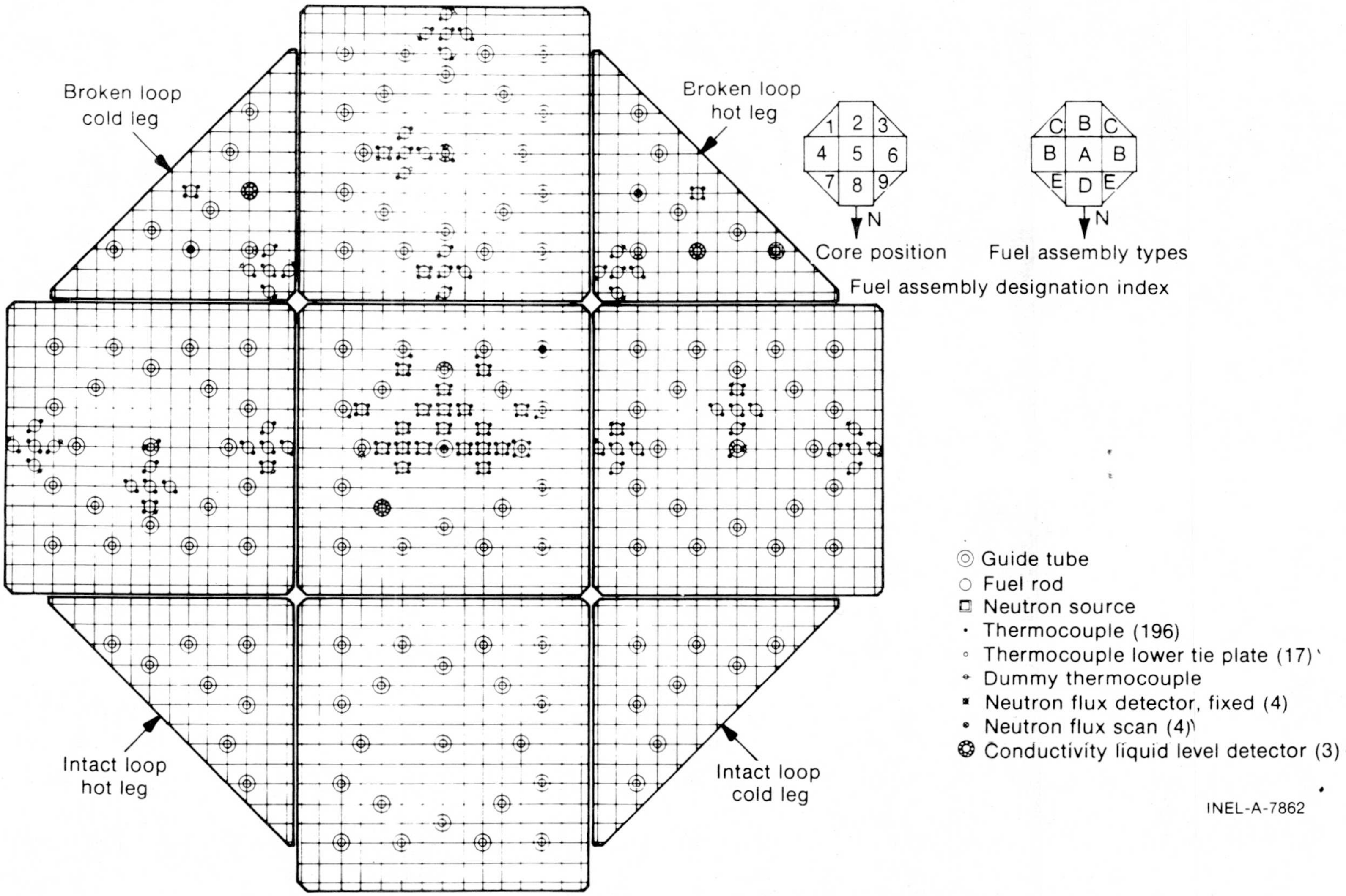

Fig. 2 LOFT core configuration and instrumentation.

temperatures being lower (by a mean value of 166 K for 24 thermocouples) than had been calculated. This preliminary posttest analysis was concerned solely with determining why the early core-wide rewet was not predicted by the RELAP4/MOD6 pretest analysis and by no means is it a complete posttest analysis of LOCE L2-2 results. The results presented in this interim report are facts as presently understood.

Three factors were postulated to have caused the disparity between predicted and measured fuel rod cladding temperatures for LOCE L2-2: (a) the initial fuel rod stored energy, (b) the heat transfer surface, and (c) the hydraulic calculation. These factors were examined and are discussed in this report. The measured and predicted fuel rod cladding temperatures for LOCE L2-2 are discussed in Sections II and III, respectively. The three factors considered as possible causes of the disparity are also discussed and resolved in Section III. Conclusions are presented in Section IV.

II. MEASURED FUEL ROD CLADDING TEMPERATURE RESPONSE

In analyzing the differences between predicted and measured cladding temperatures for LOCE L2-2, it was necessary first to determine whether the cladding thermocouples truly reflected the cladding temperatures on the instrumented rods. The following sections address this subject.

1. TYPICAL COMPARISON OF PREDICTED AND LOCE L2-2 DATA

Figure 3 compares typical predicted and measured fuel rod responses during LOCE L2-2. Additional fuel rod responses are presented in the experiment data report for LOCE L2-2[4]. The measured temperatures in the higher powered regions generally cease rising rapidly at about 7 s. As can be observed from the material presented in Reference 4, the rewet progresses from the bottom to the top of the LOFT core. No core-wide rewet was predicted to occur during the blowdown portion of the transient.

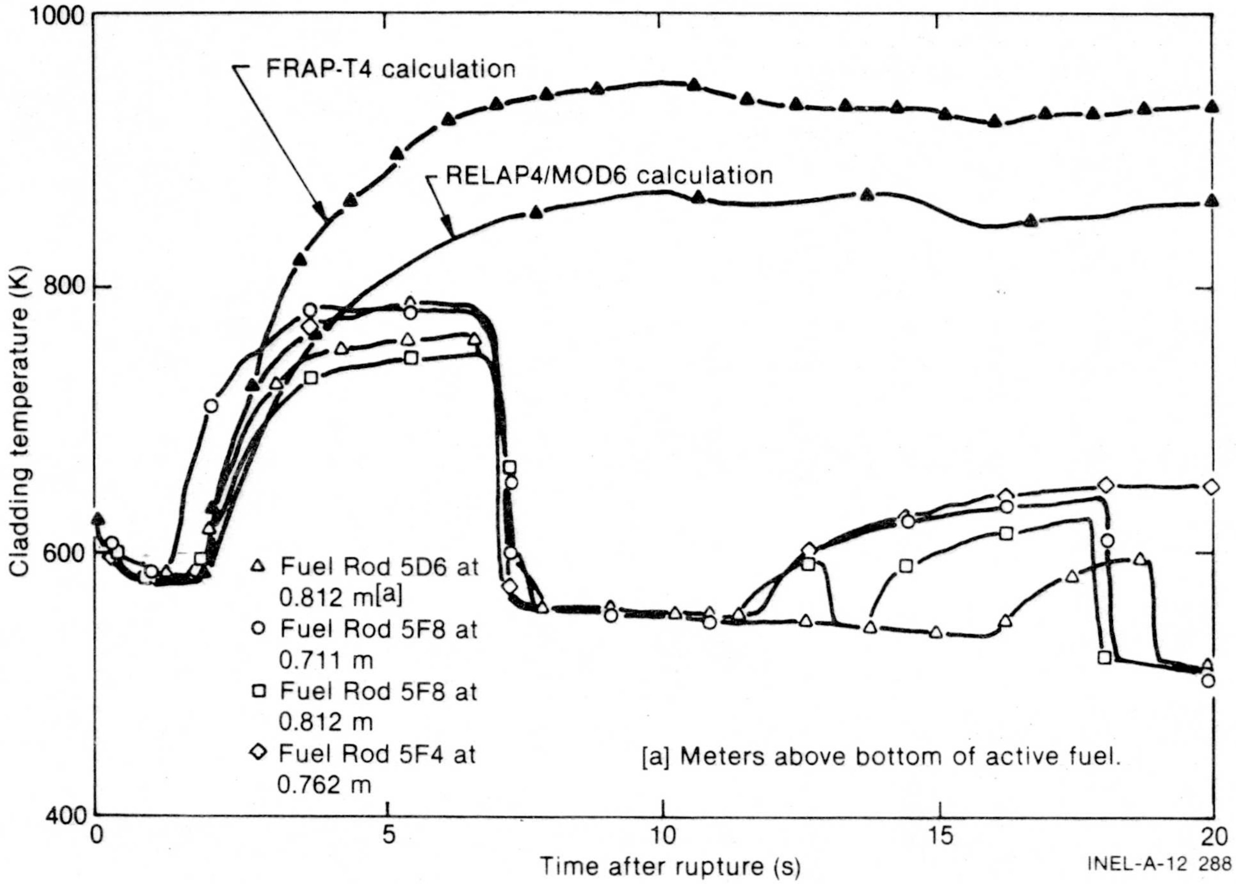

Fig. 3 Comparison of predicted and measured fuel rod cladding temperature response near the midplane of the center fuel module during LOCE L2-2.

2. UNCERTAINTY AND PERTURBATION EFFECT OF THERMOCOUPLES

The observed rewet has been postulated to have been influenced or caused by the presence of thermocouples on the instrumented fuel rods. This postulate would imply that the rewet was a local phenomena observed only on the instrumented fuel rods. A study was undertaken to evaluate how accurately the thermocouples measured the fuel rod cladding surface temperature response and to determine whether the presence of the thermocouples may have influenced the cladding rewet and quench characteristics[5]. The findings of the study are as follows:

(1) The fuel rod cladding temperature response at the thermocouple locations was found to be consistent with the thermal-hydraulic response throughout the experiment. Analysis of the magnitude of the energy stored in the fuel rod during the experiment indicated that the thermocouples accurately reflected the total response of the fuel rod to the thermal-hydraulic conditions and that the thermocouples were not being locally rewet and quenched while the remainder of the rod was at elevated temperatures. The liquid level increase observed during reflood supports the analytical work concerning fuel rod stored energy in that the liquid level for LOCE L2-2 was similar to that of the previous nonnuclear LOCE L1-5. This similarity in behavior implies that the fuel rod stored energy at the time of reflood was the same for both experiments. For such behavior to occur, the fuel rods in LOCE L2-2 would have to lose stored energy early in the experiment, as was indicated by the fuel rod cladding surface thermocouple temperature measurements.

(2) Other experiments to evaluate the accuracy of LOFT thermocouples in measuring transient temperatures indicated that the LOFT thermocouples measured the

cladding temperatures to within 30 K during blowdown-reflood transients with cladding temperature histories similar to those predicted for LOCE L2-2.

(3) Experiments done to evaluate the influence of LOFT surface thermocouples on steady state and transient critical heat flux (CHF) characteristics of fuel rods indicate that the surface thermocouples may have a cooling effect, which appears to be a function of local thermal-hydraulic conditions.

(4) A review of experience with surface thermocouples in other loss-of-coolant experimental programs support the conclusions obtained from the LOFT thermocouple blowdown-reflood and CHF tests where such data were applicable and could reasonably be compared.

(5) The findings showed that the LOFT surface thermocouples measured fuel rod cladding temperatures within acceptable uncertainty without significant perturbation of the fuel rod rewetting characteristics during LOCE L2-2. The temperatures indicated by the thermocouples can, therefore, be used in evaluating LOFT fuel rod behavior.

On the basis of the preceding findings and an independent investigation of the LOFT experimental data, a reasonable conclusion is that the observed rewet was real, was not caused by the presence of the thermocouples, but was the result of thermal-hydraulic phenomena which were not predicted properly by the RELAP4/MOD6 computer code.

III. PREDICTED FUEL ROD CLADDING TEMPERATURE RESPONSE

Three possible reasons have been postulated as to why the RELAP4/MOD6[2] and FRAP-T4[3] computer codes did not predict the LOCE L2-2 core-wide rewet as follows: (a) the fuel rod initial stored energy may be incorrect, (b) the analytical model heat transfer surface may be in error, or (c) the core hydraulics may have been incorrectly predicted. These postulates are examined in the following sections.

1. FUEL ROD STORED ENERGY

The initial heatup rates have been shown to be a strong function of stored energy, and to be only weakly dependent upon initial heat transfer and gap conductance[5]. The initial heatup rates predicted for LOCE L2-2 are, in general, in good agreement with the LOCE L2-2 experimental data. This agreement is an indirect indication that the FRAP-T4 code adequately modeled the initial stored energy in the fuel rods.

The conclusion reached is that the disparity between predicted and measured temperatures is due to a misrepresentation of the fuel model heat transfer boundary conditions rather than to the fuel rod model itself.

Sensitivity studies concerning the effects of fuel model stored energy, gap conductance, and heat transfer boundary conditions are discussed in Appendix A.

2. THE RELAP4/MOD6 HEAT TRANSFER SURFACE

In evaluating the ability of the RELAP4/MOD6 heat transfer package to predict the heat transfer phenomena which occurred in LOCE L2-2, there are a number of areas which require attention. Some of those areas, which are described in the following sections, are delayed CHF, choice of film boiling correlation, and rewet.

2.1 Assessment of RELAP4/MOD6 Heat Transfer Calculation

The formal assessment of RELAP4/MOD6 revealed that, for the case for which delayed CHF or CHF with rewet occurred, RELAP4/MOD6 overpredicted temperatures with a 95% confidence interval by 123 to 145 K. Thus, indirect evidence exists that the code can be expected to overpredict the cladding temperature by a significant amount if either delayed CHF or rewet occurs. In LOFT LOCE L2-2, both delayed CHF and rewet occurred. The mean value of predicted minus measured peak fuel rod cladding temperature was 166 K for 24 thermocouples. A comparison between predicted and measured maximum fuel rod cladding temperatures for Semiscale Mod-1[6], Thermal-Hydraulic Test Facility (THTF)[7], and LOFT is shown in Figure 4. This comparison indicates qualitatively that the LOFT results are not significantly different from those obtained in the THTF and Semiscale Mod-1 for the rods that exhibited rewet or delayed CHF.

Thus, the comparison of predicted and measured data for LOFT LOCE L2-2 adds further evidence that the code tends to conservatively predict cladding temperature response for LOCEs when delayed CHF or rewet (or both) occur. It is not possible on the basis of either the results of LOCE L2-2 or the analysis presented in the RELAP4/MOD6 assessment report[8] to determine conclusively whether or not the problem lies with the heat transfer or the hydraulics calculations, or a combination of the two.

2.2 Heat Transfer Option Selection Sensitivity Study Results

Prior to publication of the LOCE L2-2, -3, and -4 experiment predictions, sensitivity studies were performed with the heat transfer option selection and documented in the experiment prediction report[1]. The heat transfer correlation option selection was chosen to eliminate what was considered an unrealistic near rewet for LOCE L2-3. For the LOCE L2-2 prediction, the new Groeneveld film boiling correlation was chosen, although the modified Condie-Bengston correlation was recommended by the RELAP4/MOD6 modeling guidelines[8].

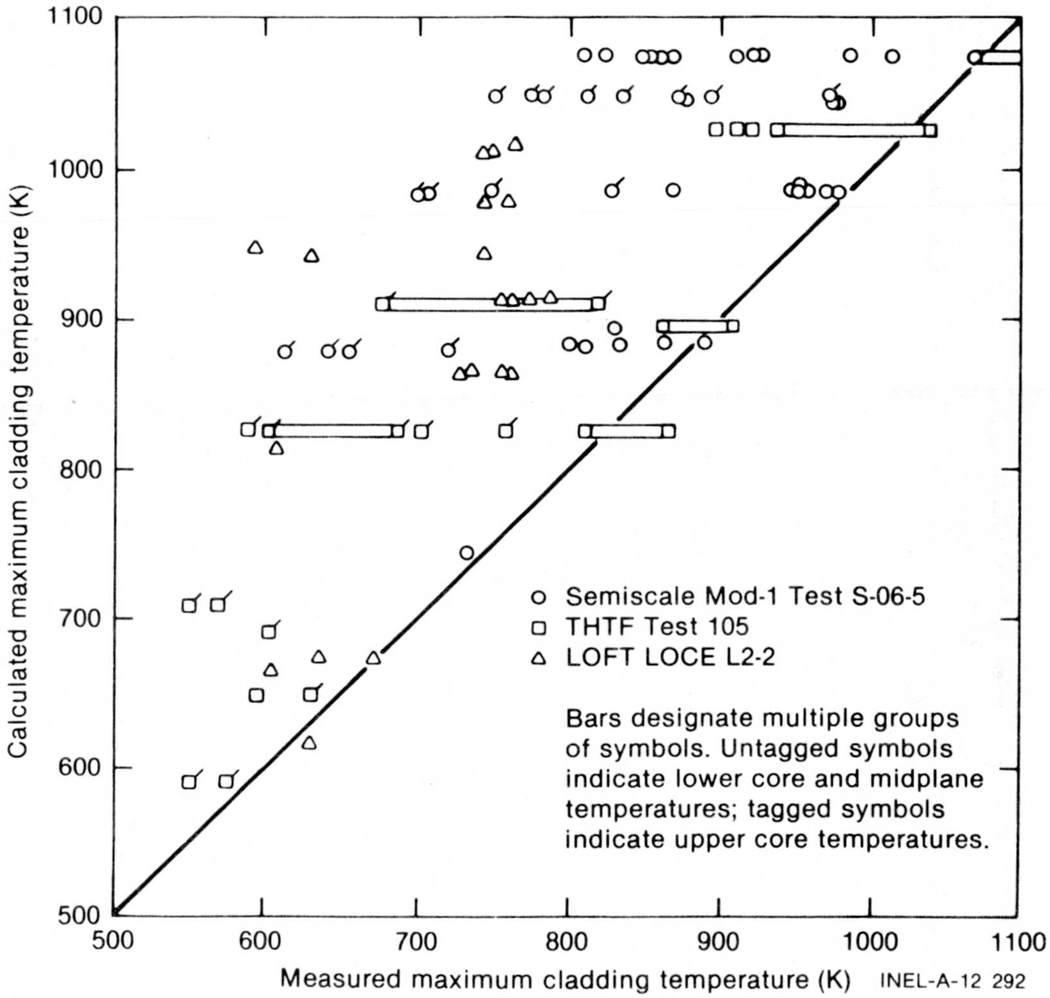

Fig. 4 Predicted versus measured local maximum fuel rod cladding temperature for the Semiscale Mod-1, THTF core base cases, and LOCE L2-2.

To determine the sensitivity of LOCE L2-2 to the heat transfer option selection, the sensitivity study was repeated, using the actual LOCE L2-2 initial conditions.

The results of the two system calculations show the effect of choice of film boiling correlation. Each of these calculations used the actual test initial conditions in the experiment prediction model. Figures 5 through 7 show the core slab surface temperature sensitivity to choice of film boiling correlation. Both the magnitude of the peak temperature and the trend of the transient were affected

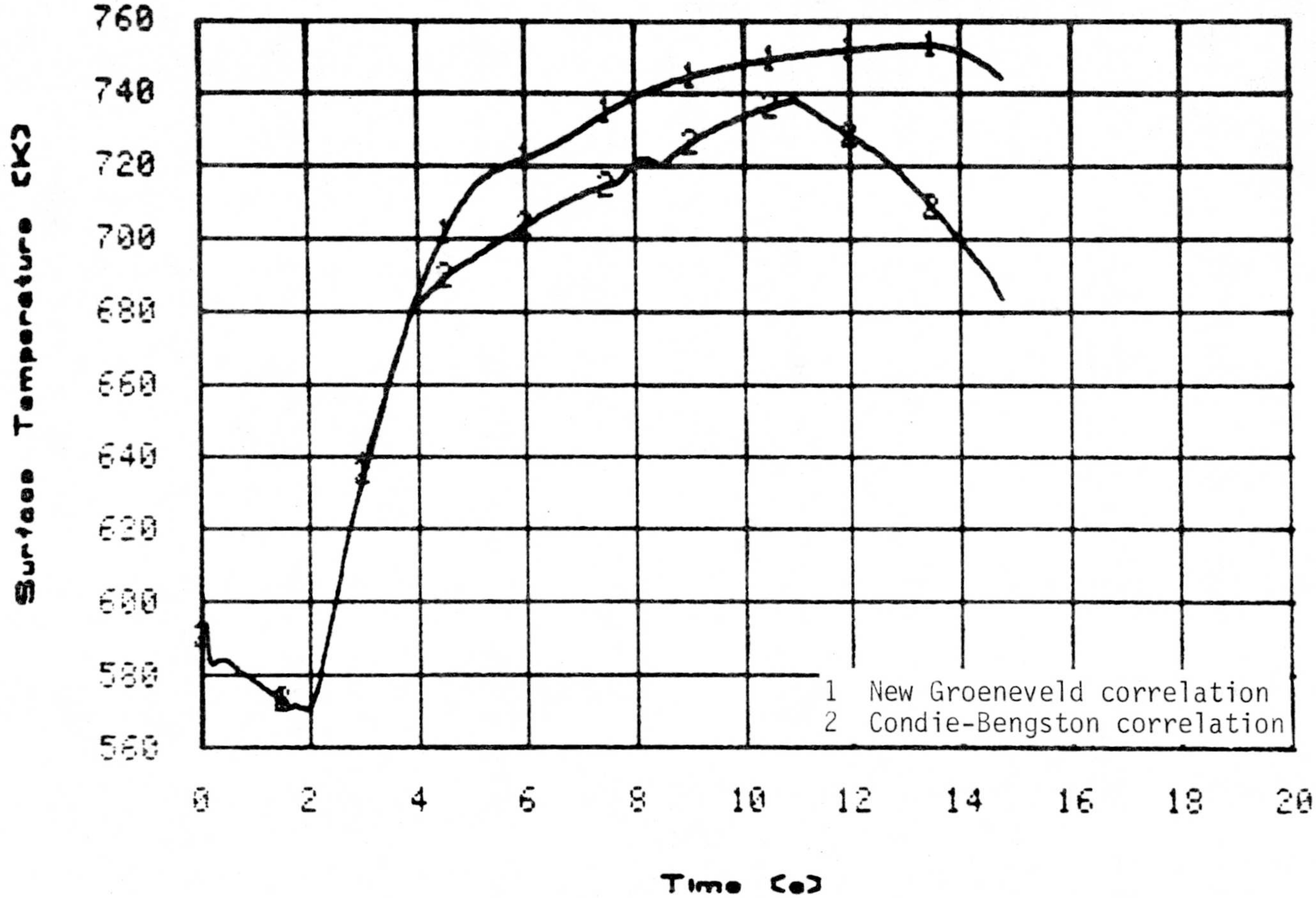

Fig. 5 Cladding temperature of average-powered fuel rod showing sensitivity due to film boiling correlation choice for lower third of core.

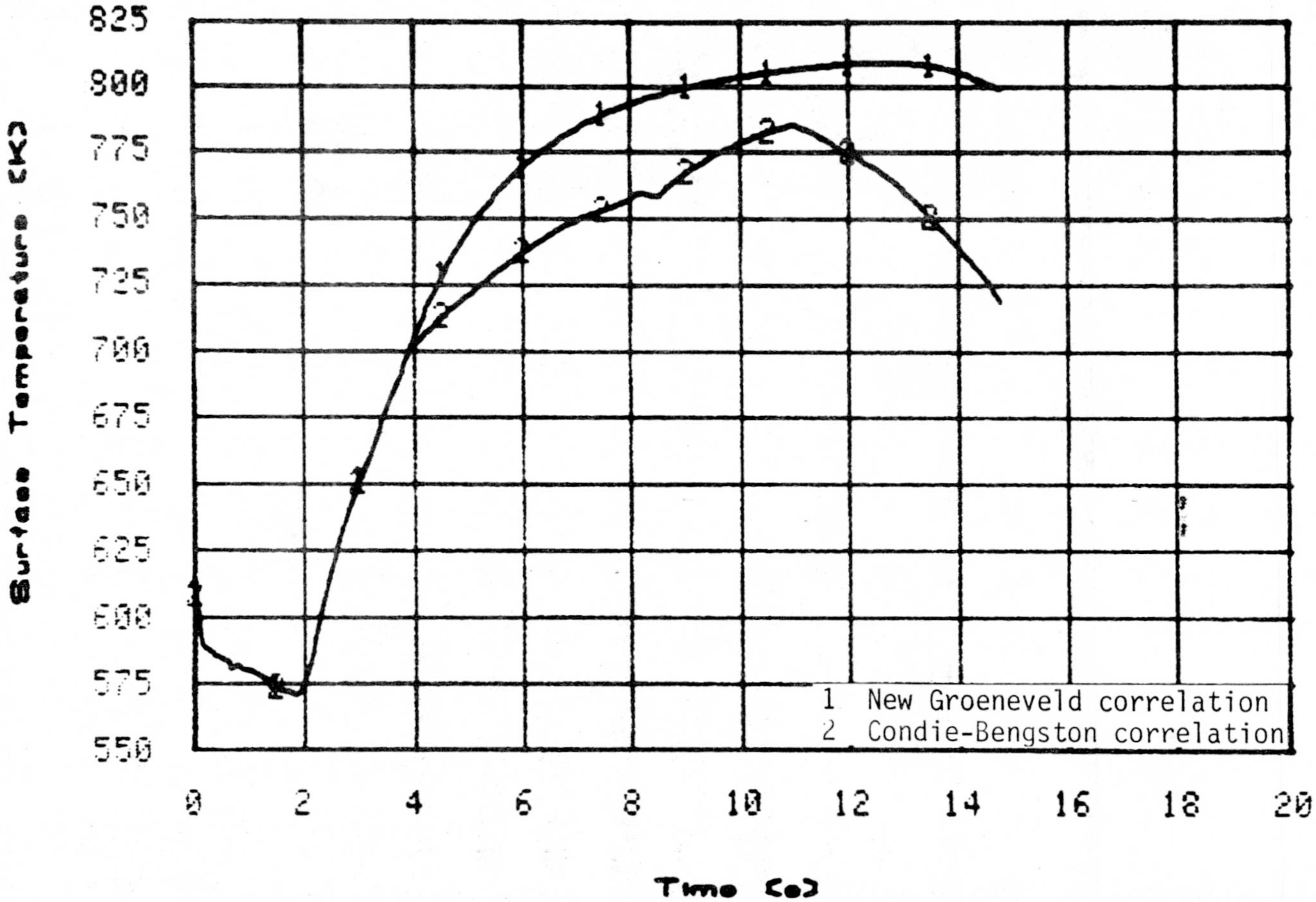

Fig. 6 Cladding temperature of average-powered fuel rod showing sensitivity due to film boiling correlation choice for middle third of core.

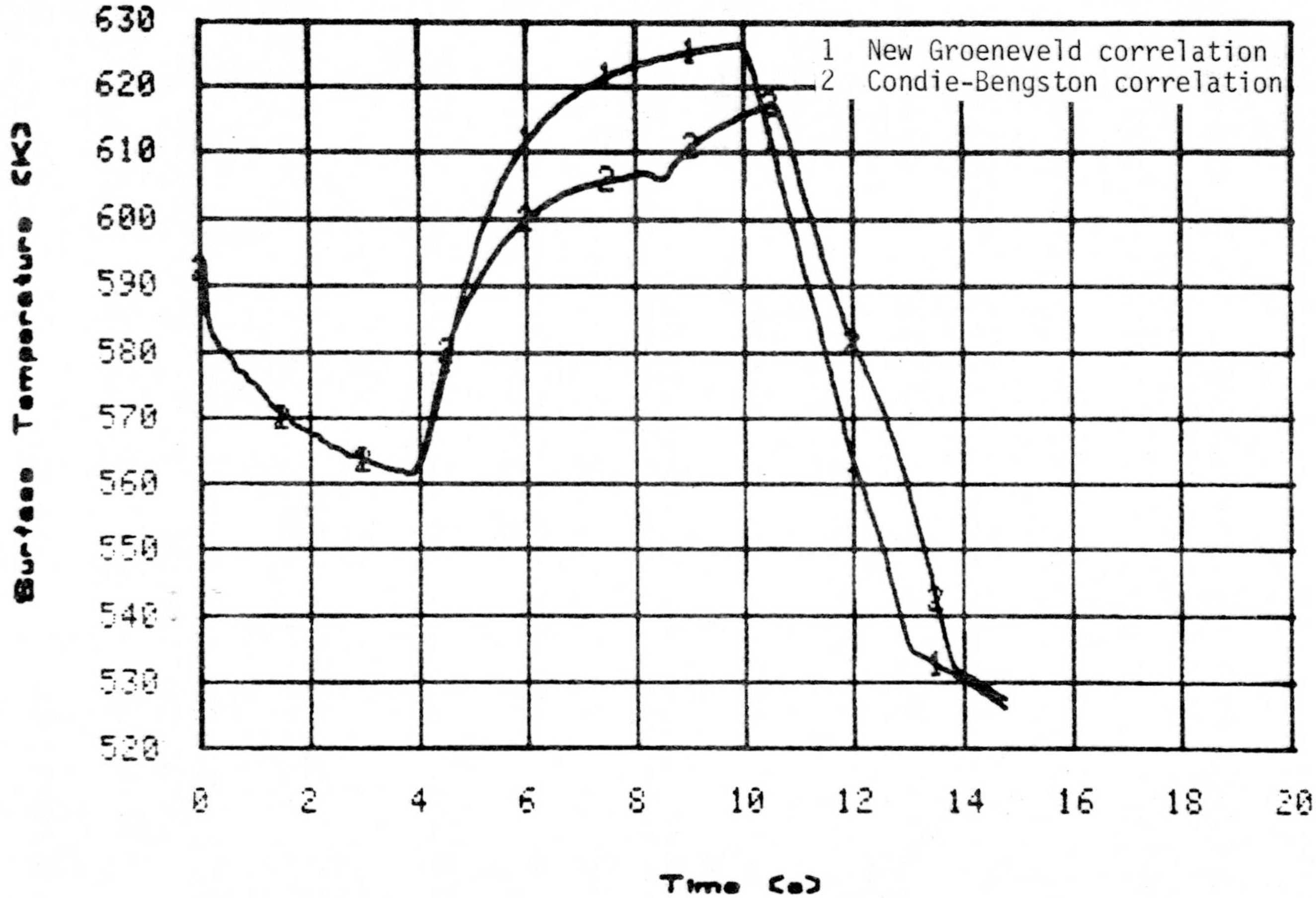

Fig. 7 Cladding temperature of average-powered fuel rod showing sensitivity due to film boiling correlation choice for upper third of core.

by this change. The decrease in the peak temperature is from 10 to 30 K for the Condie-Bengston case as compared to the new Groeneveld case. The effect on core quality is much more dramatic as shown in Figure 8. The additional heat transfer in the film boiling regime for the Condie-Bengston case causes greater vaporization of the liquid in the core and the mixture to be of higher quality. The core mass flows were not significantly affected by the choice of heat transfer correlation. The upper plenum pressure was also insensitive to this change.

A sensitivity study using the center fuel module hot rod model was also conducted from both the experiment prediction and the actual initial condition posttest system calculations as follows:

(1) The experiment prediction analysis using the new Groeneveld film boiling correlation for both the system and hot rod

(2) The experiment prediction analysis using the modified Condie-Bengston correlation for the hot rod only

(3) The posttest analysis using the new Groeneveld film boiling correlation for both the system and hot rod

(4) The posttest analysis using the modified Condie-Bengston correlation for the hot rod only.

Figure 9 shows a representative comparison of the cladding surface temperature responses for these calculations. The difference in peak cladding temperature is 100 to 130 K. Although the use of the modified Condie-Bengston correlation rather than the new Groeneveld correlation caused a significant reduction in the peak cladding temperature, no rewet occurred nor did a temperature decrease in the 5-to-10-s interval occur.

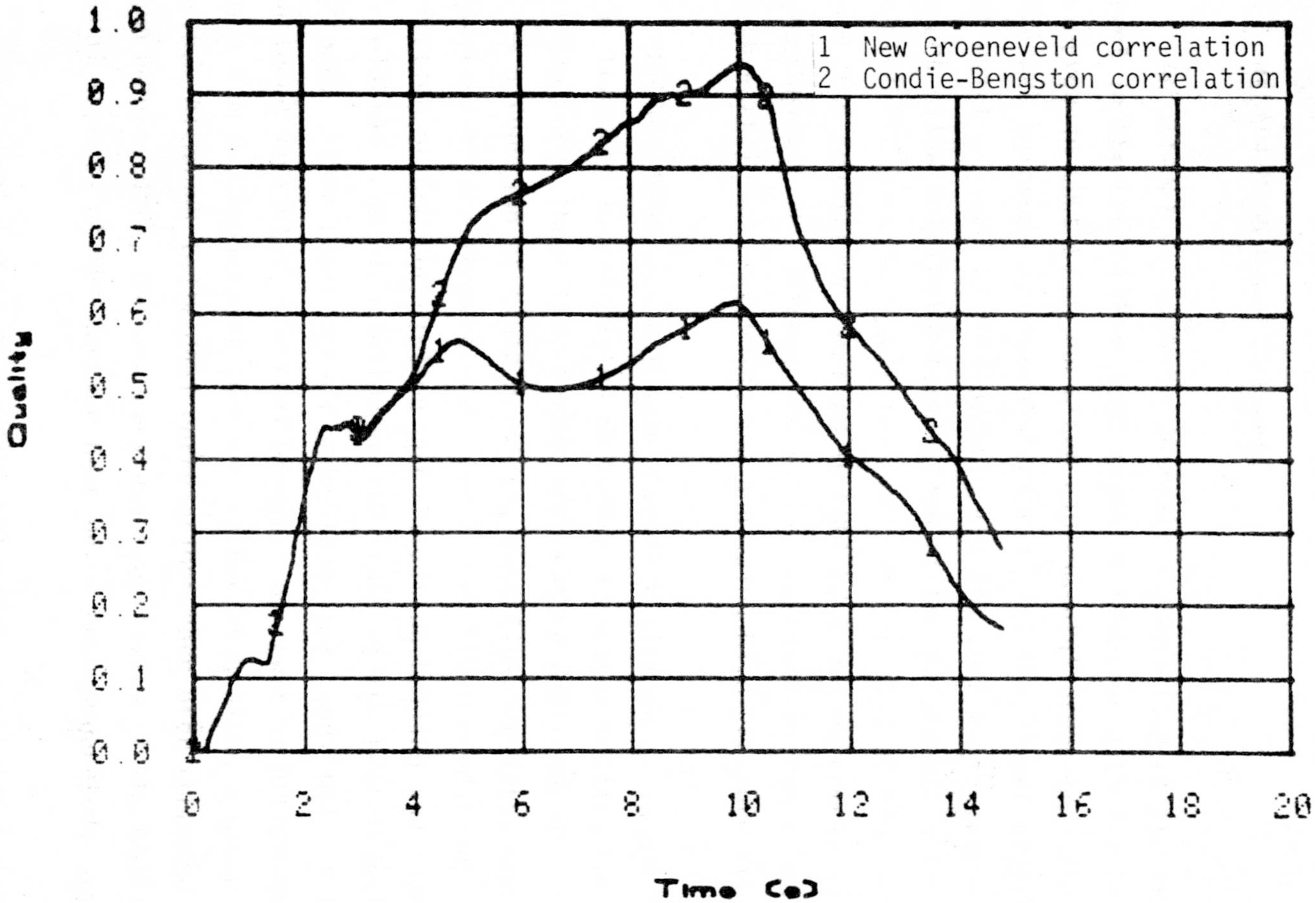

Fig. 8 Quality in center of core showing sensitivity due to film boiling correlation choice.

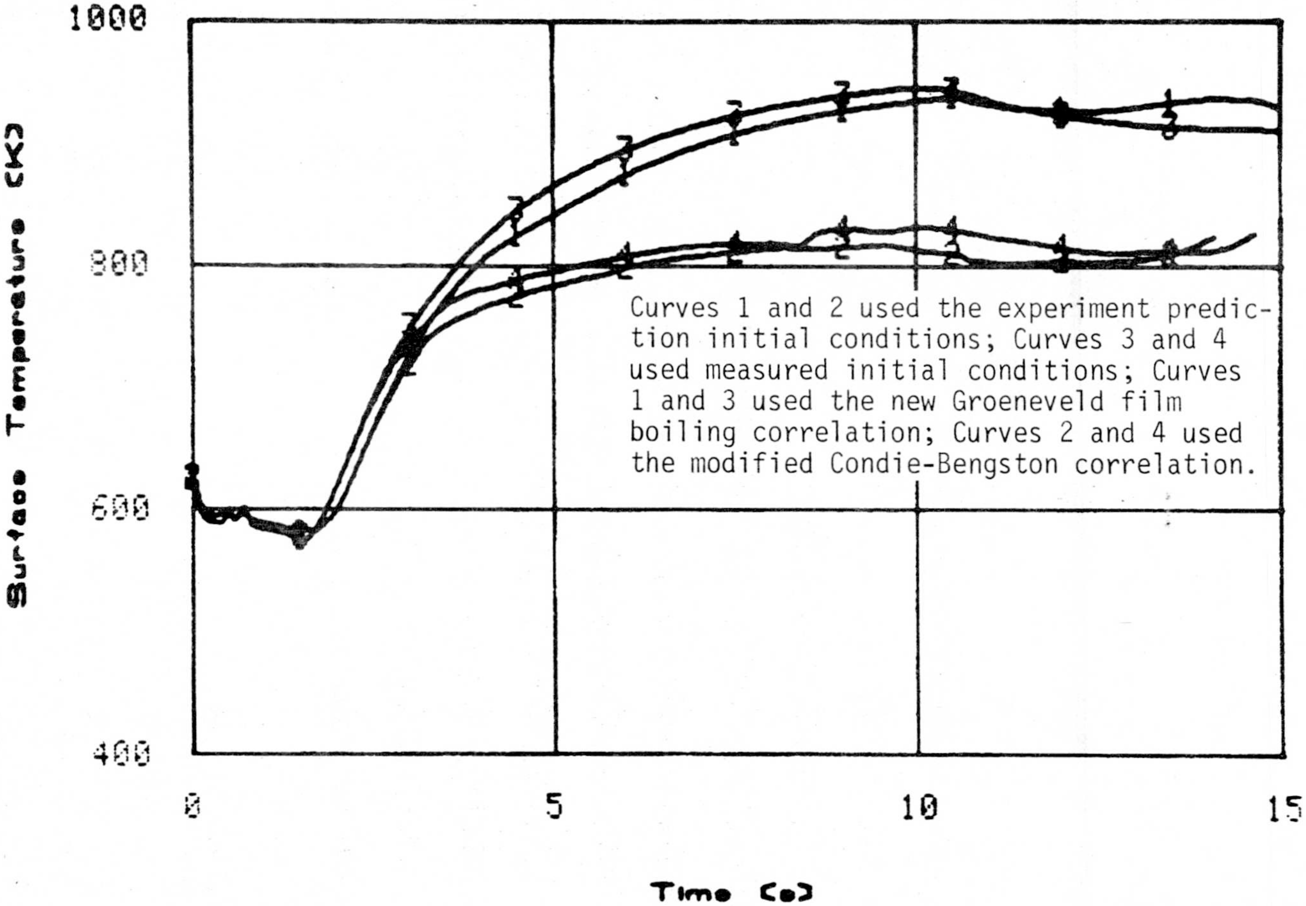

Fig. 9 Cladding temperature on highest-powered fuel rod showing sensitivity to both film boiling correlation choice and initial conditions.

From these comparisons it is evident that the use of the modified Condie-Bengston film boiling correlation will result in a lower cladding temperature, however, this change alone was not sufficient to cause the rewet observed in the test data.

2.3 RELAP4/MOD6 Rewet Criteria

An attempt was made to initiate a comparison of the criteria for rewet in the RELAP4/MOD6 heat transfer behavior with the behavior observed in LOCE L2-2 and other experimental programs. This comparison was hampered by several factors: (a) the "rewet criterion" does not exist as such in RELAP4/MOD6, (b) the LOCE L2-2 experimental data do not allow detailed determination of the parameters affecting rewet, and (c) the data available for rewet of zircaloy at high pressure under the conditions observed in LOFT L2-2 are extremely limited. Nevertheless, the attempt led to some conclusions regarding the state-of-the-art in understanding and analyzing high-pressure rewet.

RELAP4/MOD6 does not have a rewet criterion as such. Rather, the heat transfer is calculated to follow a typical boiling curve. This boiling curve (heat flux versus temperature difference) is calculated to be a function of fluid pressure, mass flux, quality, and heat transfer surface temperature. For any of these conditions, the input selection of CHF correlation and transition boiling and film boiling correlations can also influence the shape of the heat transfer surface. Since rewet occurs under transient conditions of the mentioned variables, the real progress of rewet in RELAP4/MOD6 is along a multidimensional surface, rather than along a given boiling curve. Although individual correlations have been compared to experimental data, the accuracy and sensitivity of the multidimensional aspects of the surface have never been separately assessed.

Experimental data and analytical models exist for rewet under reflood conditions (low pressure, low quench rate, top and/or bottom flooding). These data sources agree that the material properties of the surface to be rewet directly influence the quench velocity. Since zircaloy has one-half the specific heat capacity of stainless steel, yet about the same thermal conductivity, these conduction controlled models (and experiments) show that zircaloy rewets twice as fast as stainless steel. A reasonable assumption is that the dominant effect causing the rewet in LOCE L2-2 is also dependent on the fuel rod cladding material properties. Since the heat transfer data base used for developing the RELAP4/MOD6 heat transfer surface was not based on nor compared to tests with zircaloy heater elements, it is not surprising to find this package conservative when applied to zircaloy clad fuel rods.

The LOFT Instrumentation does not, at present, allow separation of the hydraulic phenomena from the heat transfer package accuracy. Therefore, separate effects tests are recommended to evaluate the high pressure rewet phenomena observed in LOCE L2-2 and the capability of the RELAP4/MOD6 heat transfer package in this regard.

3. THE RELAP4/MOD6 CALCULATED CORE HYDRAULICS

Proper prediction of core flow during blowdown is of critical importance if cladding temperature of the fuel rods is to be accurately predicted. Core flow calculations are affected by the choice of break flow model, the transition between subcooled and saturated choking models, initial conditions in the system, and other factors. The following sections describe sensitivity studies which addressed modeling problems in these general areas.

3.1 Evidence of Core Flow Underprediction

Evidence exists that the RELAP4/MOD6 calculated core flow may have been underpredicted during the period the core-wide rewet occurred. This evidence includes the data from the thermocouples which indicate a relatively rapid bottom-to-top rewet as well as the data from the drag disc in the upper plenum. Figures 10 and 11

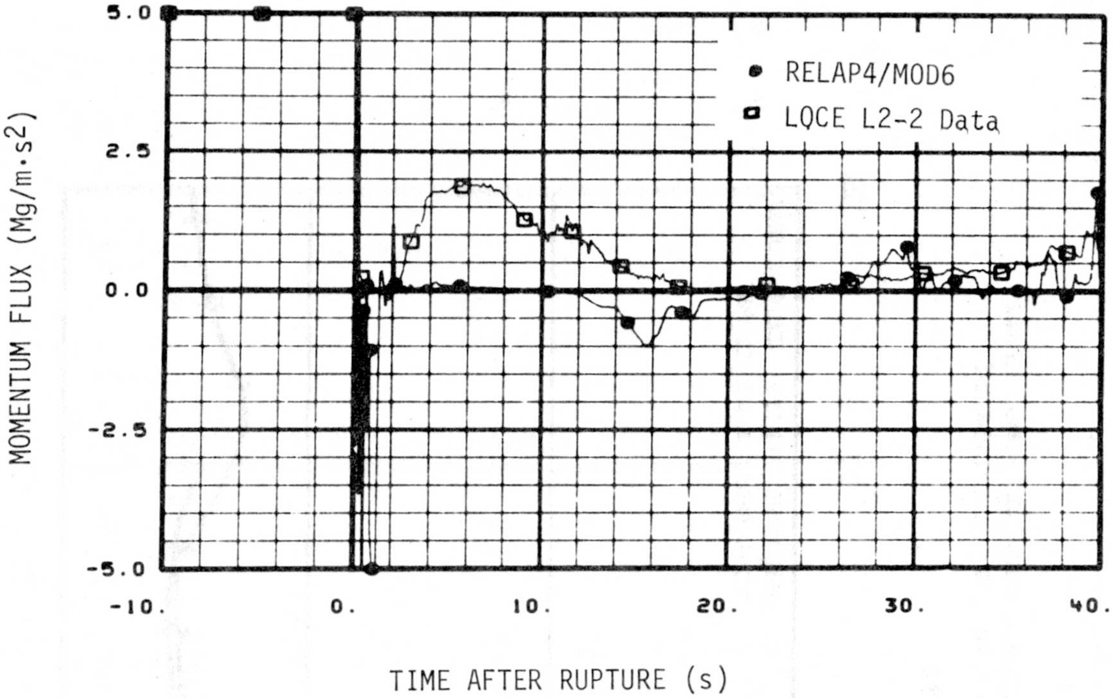

Fig. 10 Comparison of predicted and measured momentum flux above fuel Module 1.

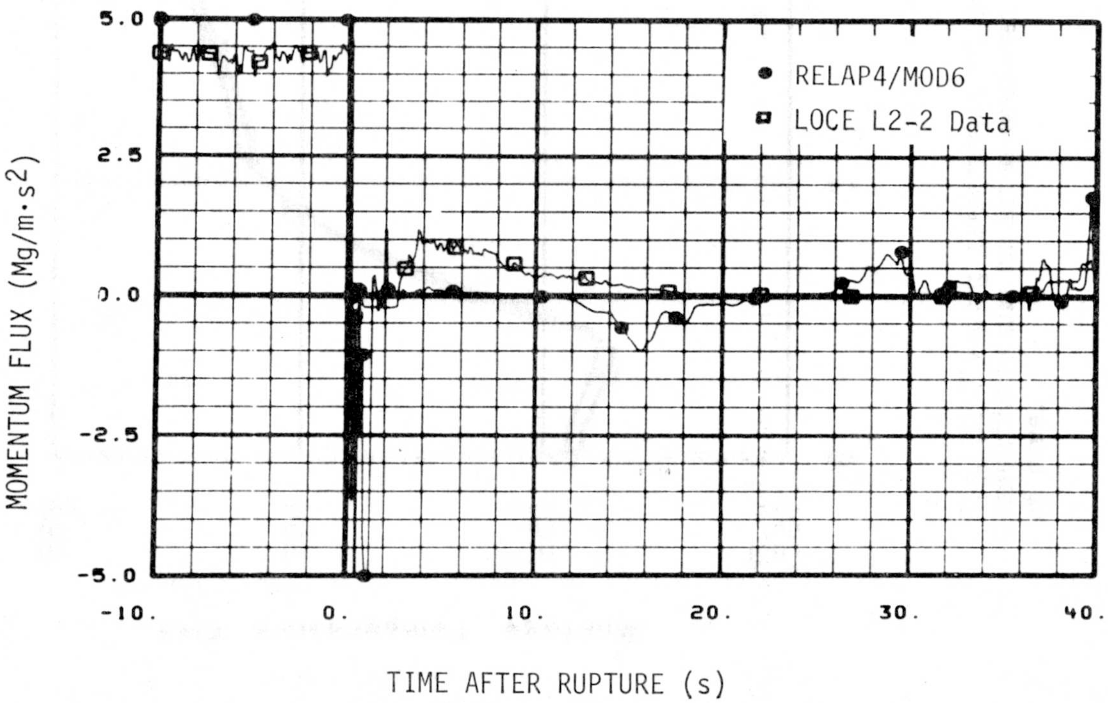

Fig. 11 Comparison of predicted and measured momentum flux above fuel Module 3.

compare the calculated and measured momentum flux in the upper plenum. The experimental data indicate that the measured momentum flux returned to approximately one-third of the initial value at 6 s after rupture; whereas the predicted momentum flux returned to less than one-tenth of the value recorded by the instruments.

Several reasons have been postulated for an underprediction of core flow at about 6 s after rupture. These include initial conditions effects, break flow effects, and problems associated with the hot rod computation scheme. Each of these potential problem areas are examined in the following sections.

3.2 Effects of Using Measured Initial Conditions

Posttest calculations using measured test initial conditions in the LOCE L2-2 experiment prediction model have been performed for both the system and center fuel module hot rod.

The core slab surface temperature response is shown in Figures 12 through 14, where Curve 1 is the experiment prediction and Curve 2 is the posttest analysis with measured LOCE L2-2 initial conditions. The peak temperature is 10 to 20 K lower for the posttest calculation than for the experiment prediction. No rewets or temperature decreases in the 3-to-10-s period are evident. A decrease in quality in the core volumes of 5 to 10% was observed. There were no significant changes in the core mass flow response. Figure 15 shows the effect of actual initial conditions on the upper plenum pressure response.

The effects of using the actual initial conditions on the center fuel module hot rod were generally small. The change in cladding temperature response shows virtually the same sensitivity as the system model. Figure 16 shows a comparison of the core qualities near the hot spot. The differences here may be attributable to the hot rod computation scheme problem to be discussed in Section 3.4. However, the quality difference in the 5-to-10-s interval is virtually unchanged.

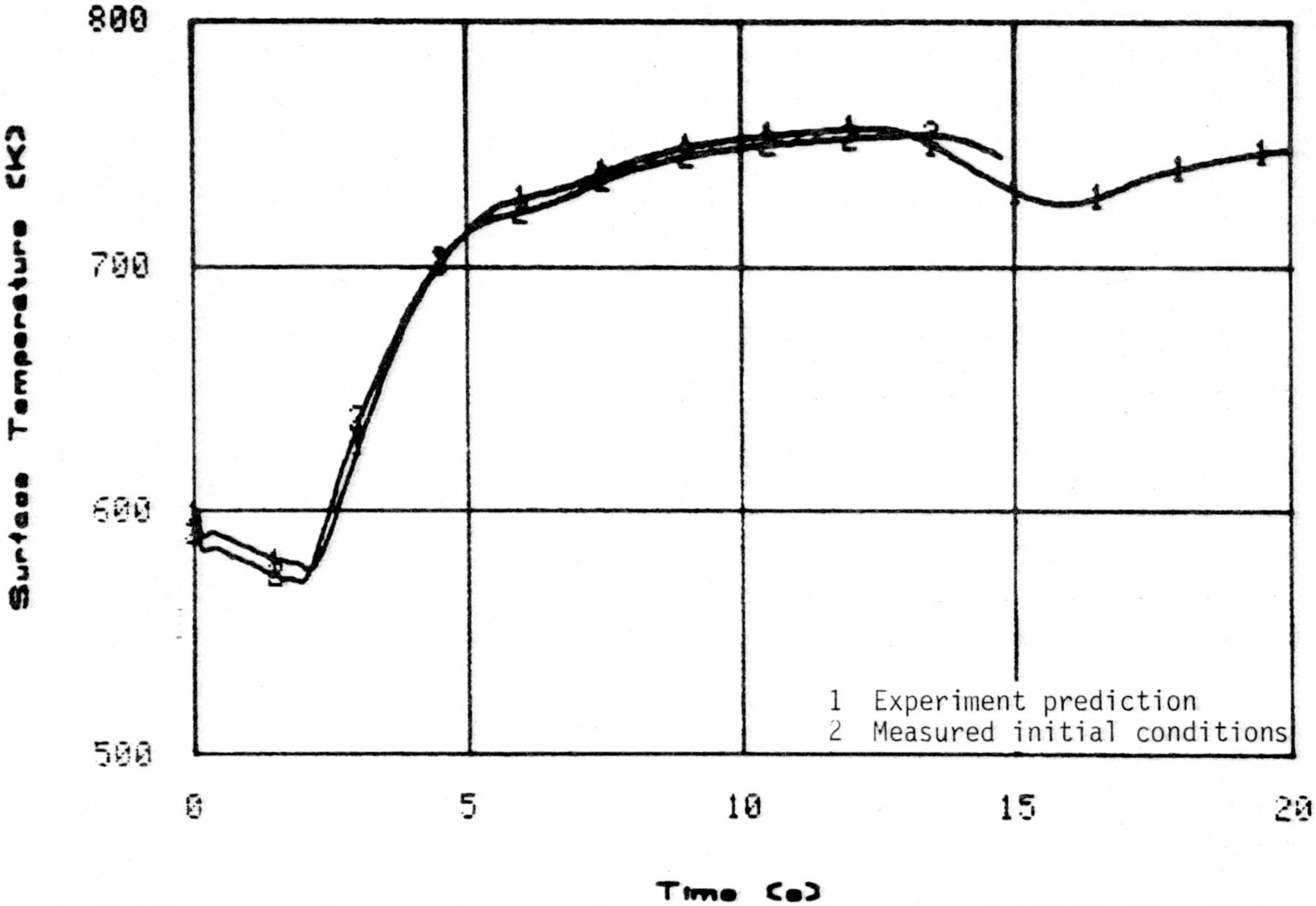

Fig. 12 Cladding temperature of average-powered fuel rod showing sensitivity due to using measured initial conditions for lower third of core.

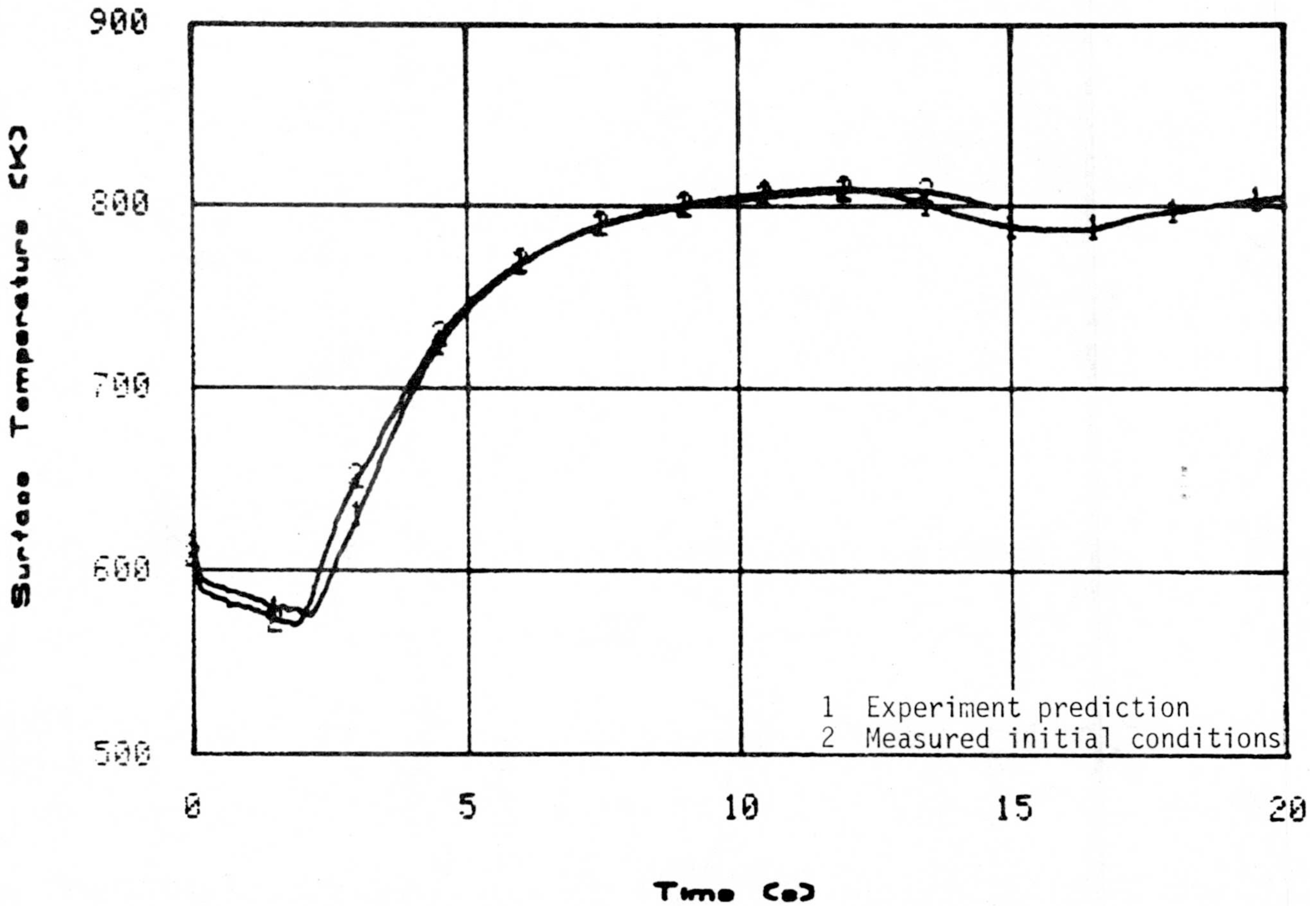

Fig. 13 Cladding temperature of average-powered fuel rod showing sensitivity due to using measured initial conditions for middle third of core.

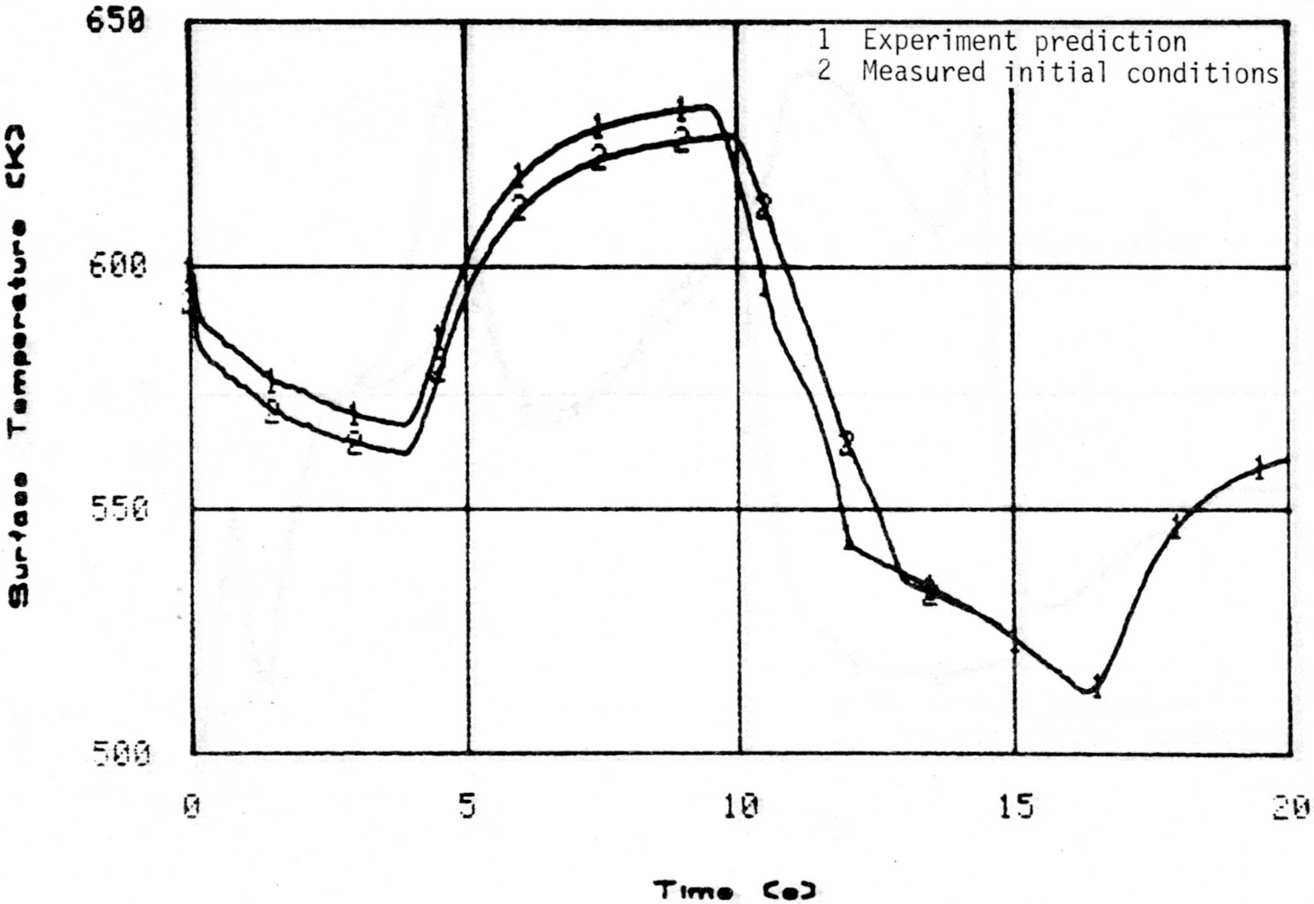

Fig. 14 Cladding temperature of average-powered fuel rod showing sensitivity due to using measured initial conditions for upper third of core.

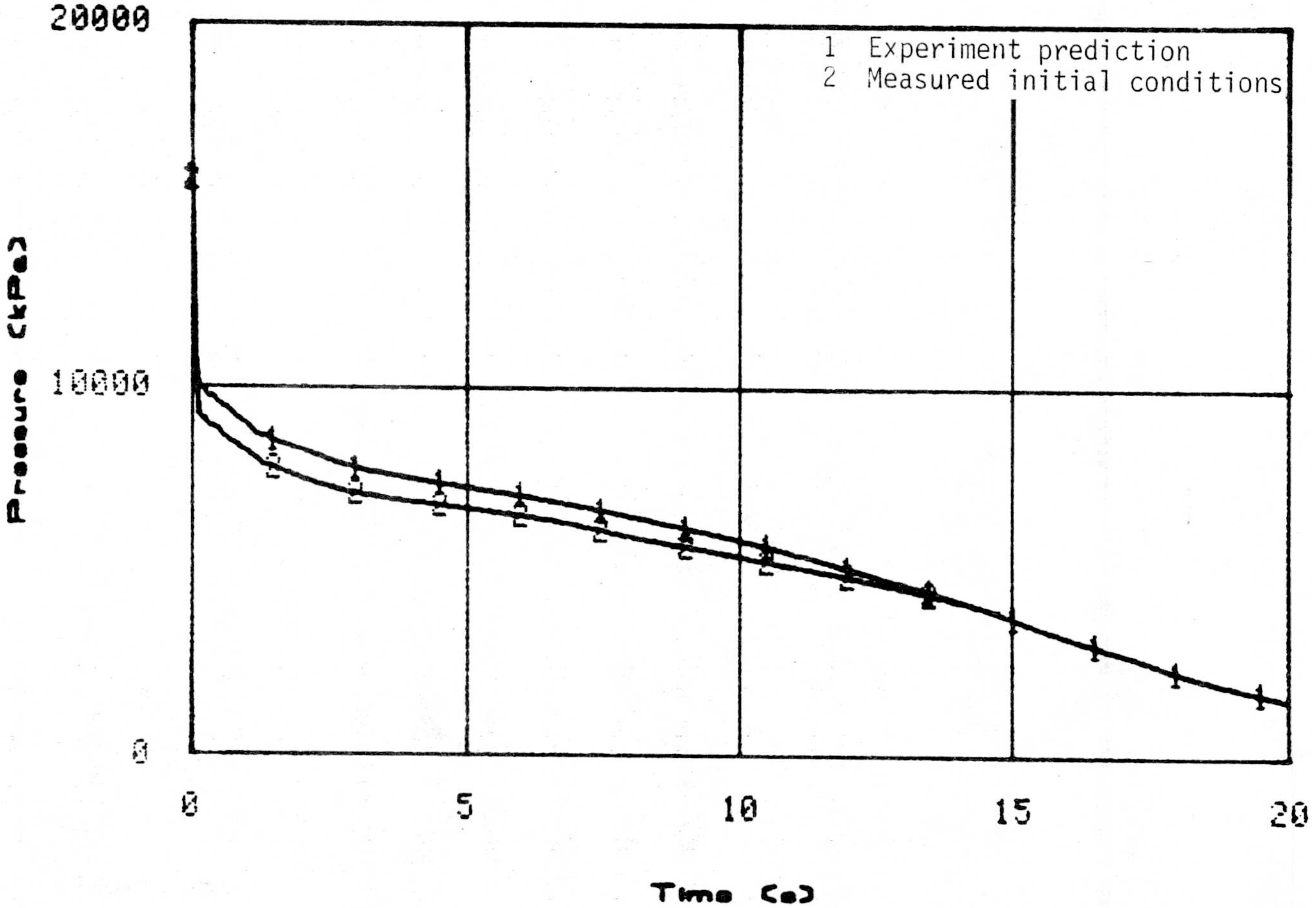

Fig. 15 Upper plenum pressure showing sensitivity due to using measured initial conditions.

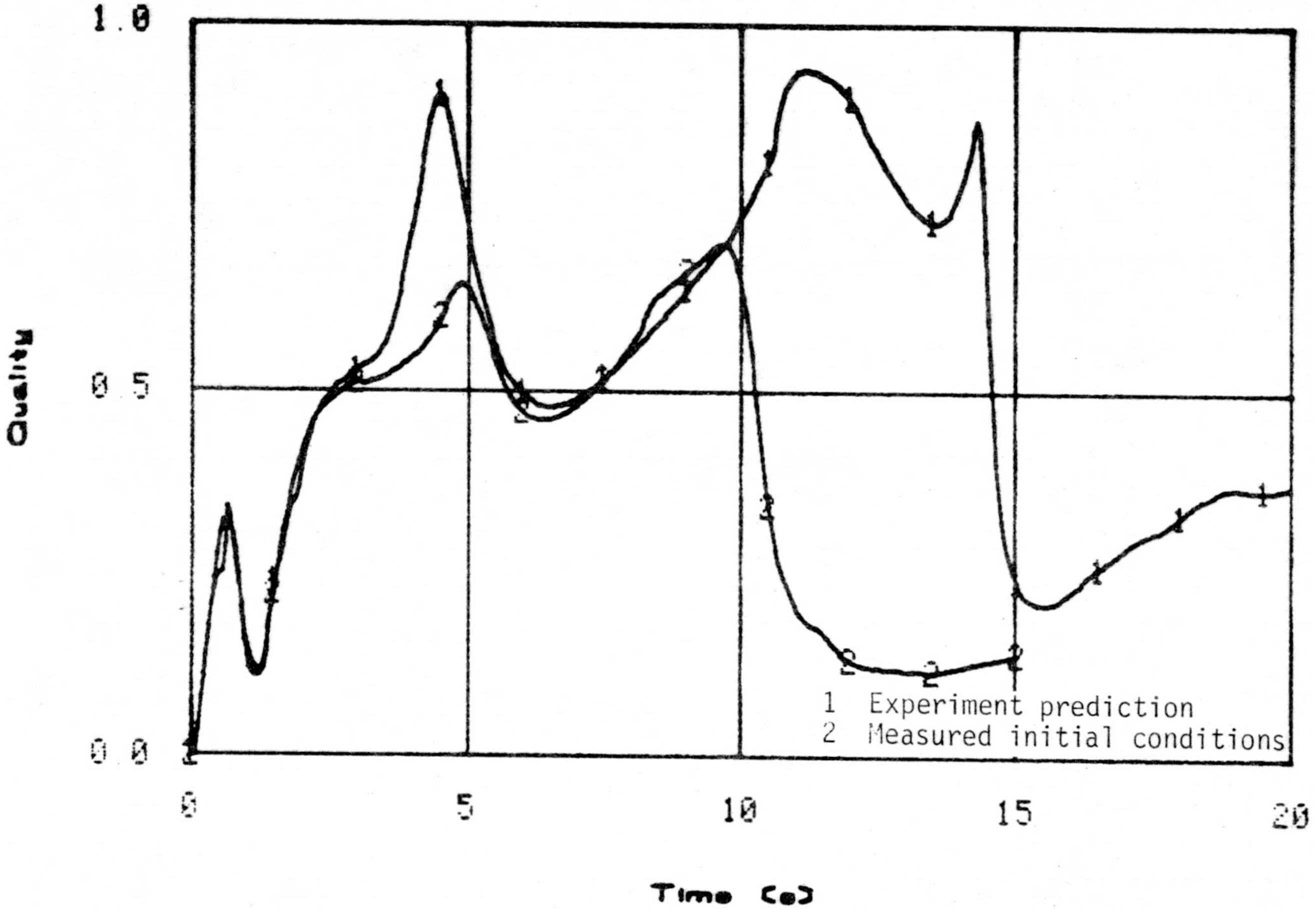

Fig. 16 Quality in middle third of core showing sensitivity due to using measured initial conditions.

From these comparisons it is apparent that the cladding surface temperature response is relatively insensitive to the difference between specified and measured test initial conditions.

3.3 Break Flow Sensitivity Study Results

To better understand the potential causes for underprediction of core flow during the time when the rewet occurred, break flow sensitivity studies were done. Two major areas were investigated: (a) effects of changing critical flow contraction coefficients and (b) effects of changing the critical flow transition quality.

3.3.1 Break Flow Contraction Coefficient Sensitivity Study Results. It was intended that a multiplier of 0.848 be applied to the saturated critical flow model at the broken loop cold leg break plane. During posttest sensitivity studies on break flow, it was discovered that, due to a subtle input error, the 0.848 multiplier, which was input, was not used. In effect, the experiment prediction was performed using the Henry-Fauske model for subcooled critical discharge, the homogeneous equilibrium model (HEM) for saturated critical flow with a transition quality of 2%, and with multipliers of 1.0 for both the subcooled and saturated models. Previous analyses have concluded that a multiplier of 0.848 should be used for the saturated discharge. LOCE L2-2 was the first experiment in which a substantial time of subcooled discharge existed in LOFT.

Evidence exists that the cold leg break flow for both the saturated as well as subcooled break discharge periods was overpredicted. Figure 17 shows a comparison between predicted and measured corrected break flow. As can be seen in the figure, both the subcooled (0 to 3 s) as well as the saturated (main difference occurs from 5 to 12 s) periods of cold leg break flow were overpredicted.

A broken loop cold leg break flow contraction coefficient sensitivity study was completed for LOCE L2-2. The base case was a posttest analysis calculation with measured initial conditions using the modified Condie-Bengston film boiling correlation. All other

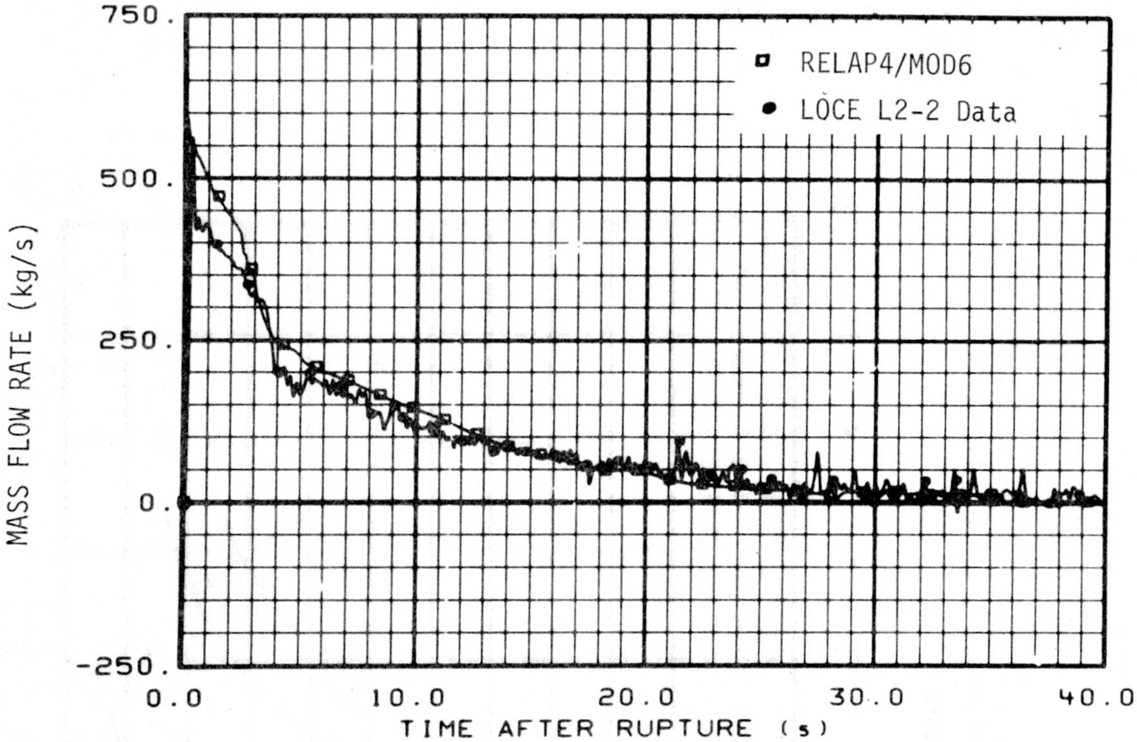

Fig. 17 Comparison of predicted and measured mass flow in the broken loop cold leg.

input options were identical to those of LOCE L2-2 experiment prediction. The broken loop cold leg break multipliers for this calculation were 1.0 for both the Henry-Fauske model and the HEM. For these sensitivity studies, the multiplier for the HEM was changed to 0.848 for one calculation, and the multipliers were both 0.848 for the Henry-Fauske model and the HEM for one calculation. The rather dramatic changes due to break flow multiplier selection are illustrated in Figures 18 through 23. The use of the multiplier on the HEM model resulted in a temperature turnover at all three core slabs at 5 to 6 s. No rewets occurred for this case. Application of the same multiplier to both the Henry-Fauske and HEM models resulted in lower cladding temperatures and a 2-s rewet of the slab, which represents the lower one-third of the core.

Application of the break flow multipliers caused sharp reductions in the quality in the core region and significant increases in the positive core mass flows during the 3.5-to-12-s interval. Higher

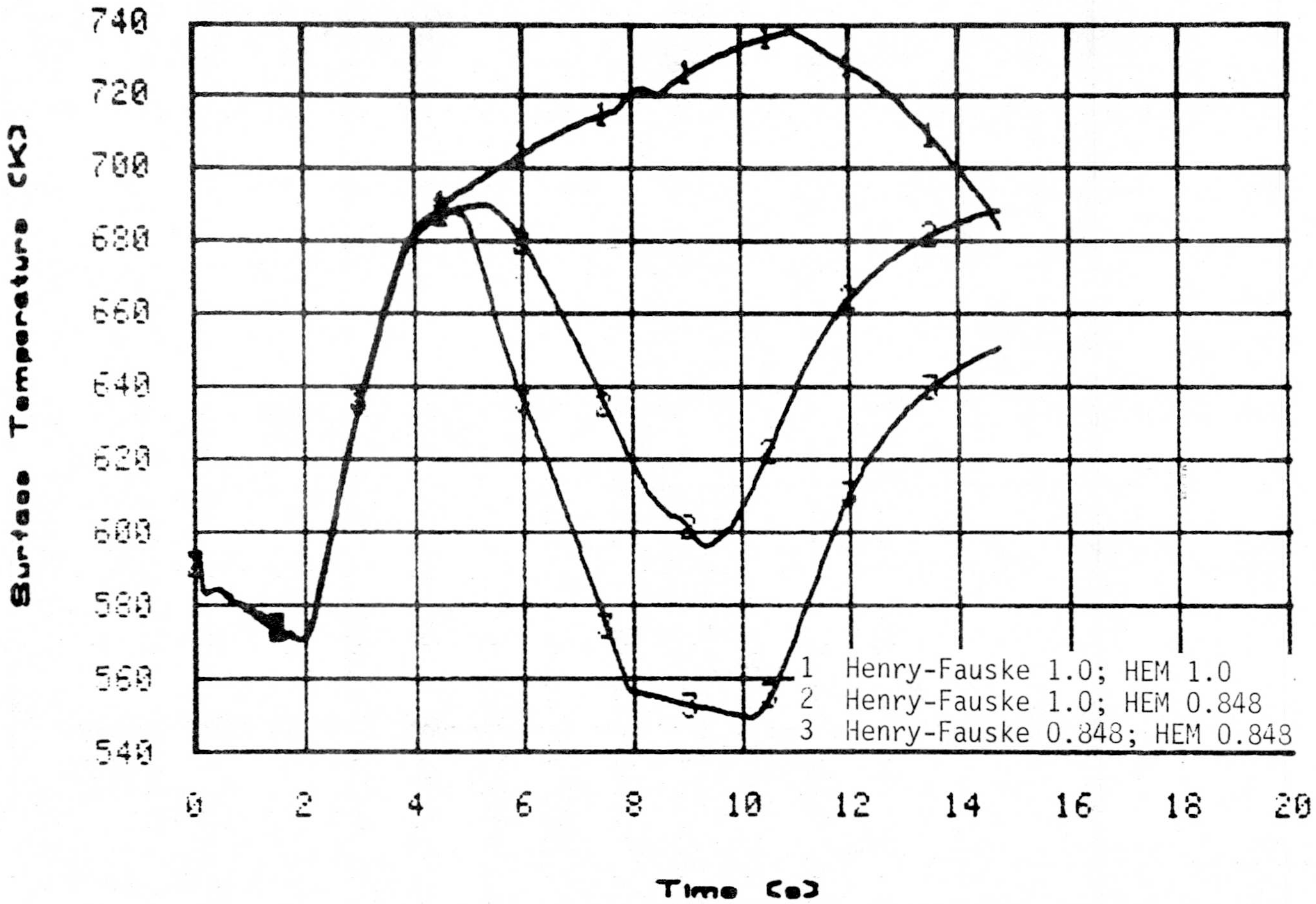

Fig. 18 Cladding temperature of average-powered fuel rod showing sensitivity due to break flow multiplier for lower third of core.

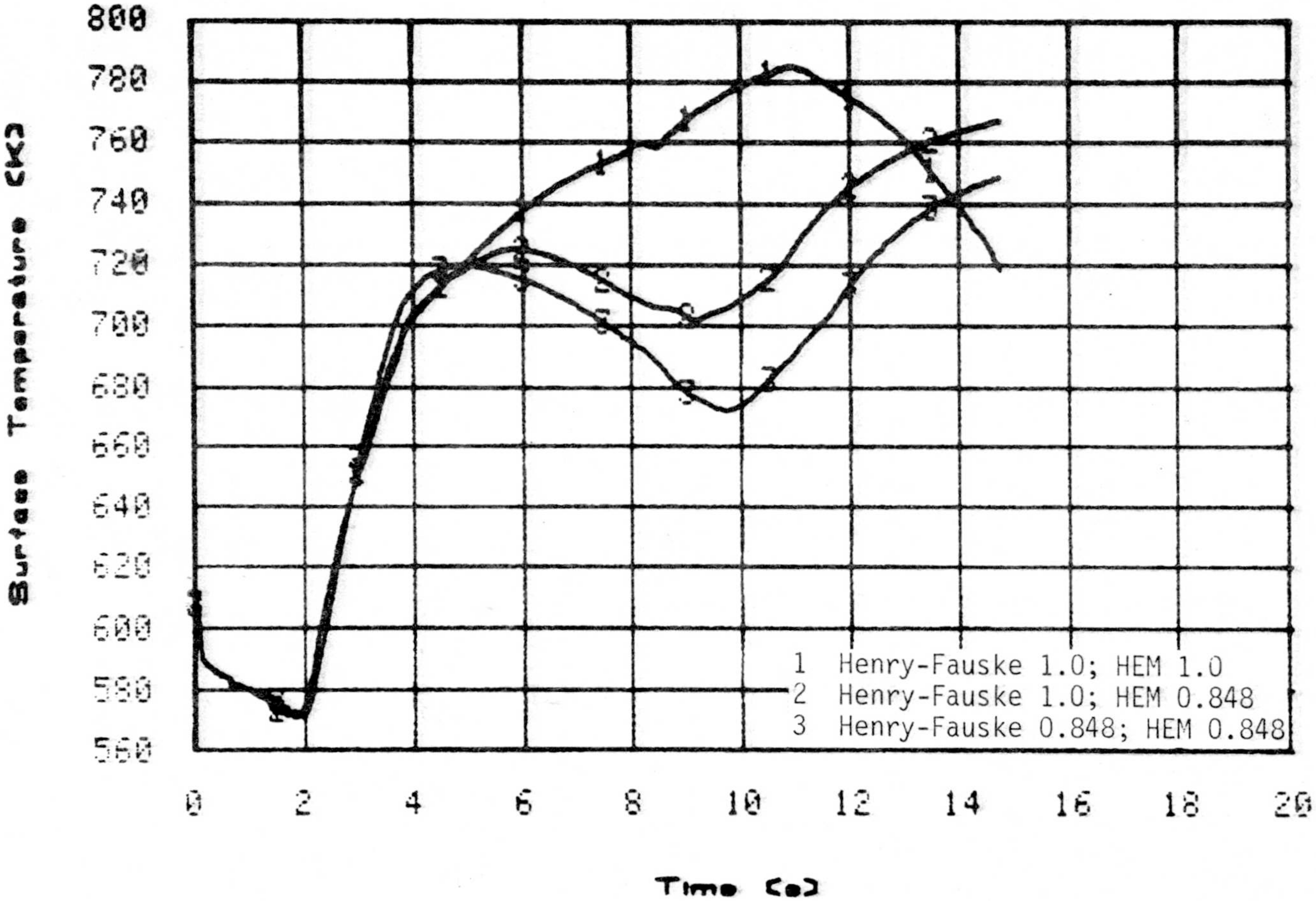

Fig. 19 Cladding temperature of average-powered fuel rod showing sensitivity due to break flow multiplier for middle third of core.

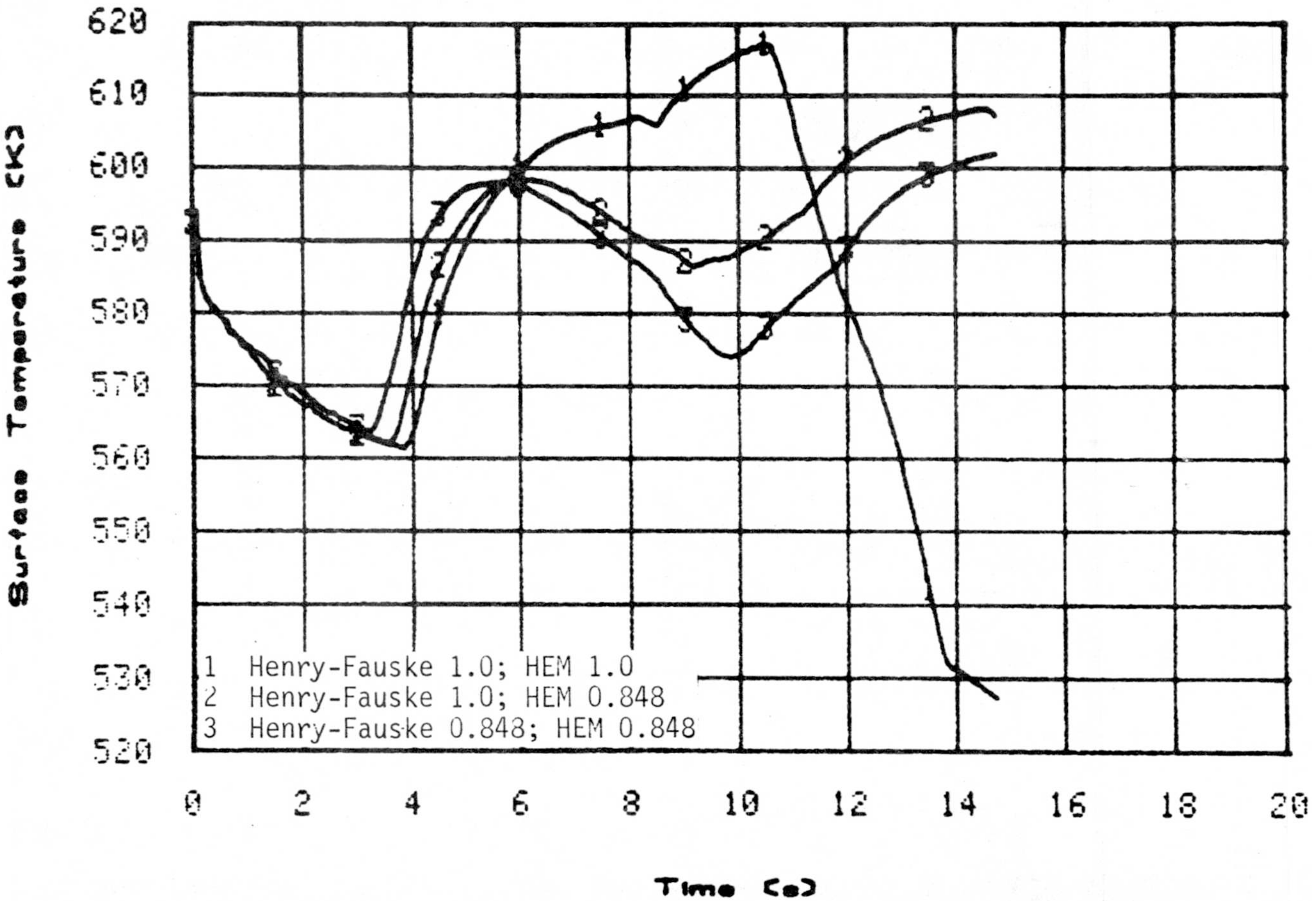

Fig. 20 Cladding temperature of average-powered fuel rod showing sensitivity due to break flow multiplier for upper third of core.

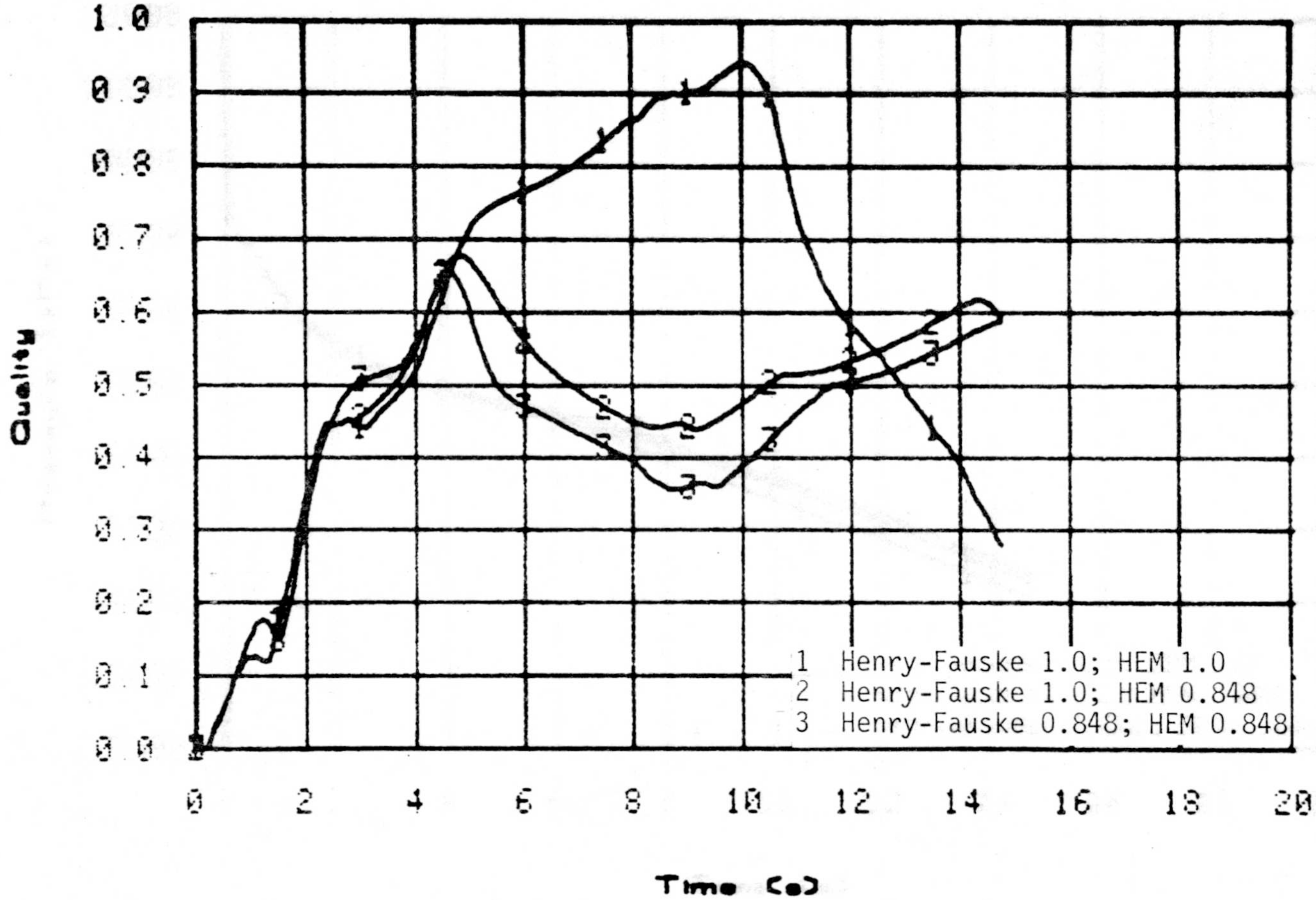

Fig. 21 Quality in middle third of core showing sensitivity due to break flow multiplier.

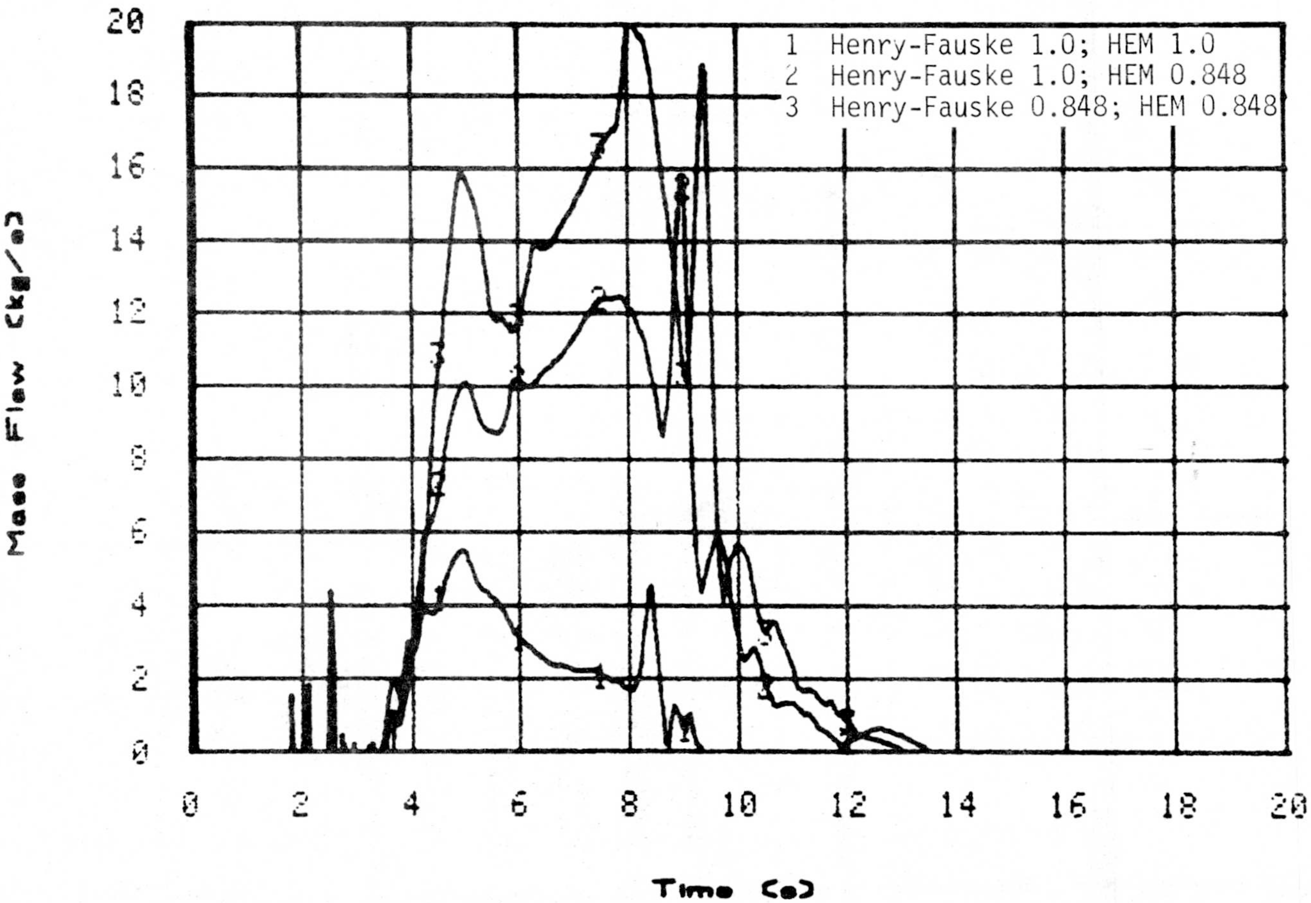

Fig. 22 Core inlet mass flow rate showing sensitivity due to break flow multiplier.

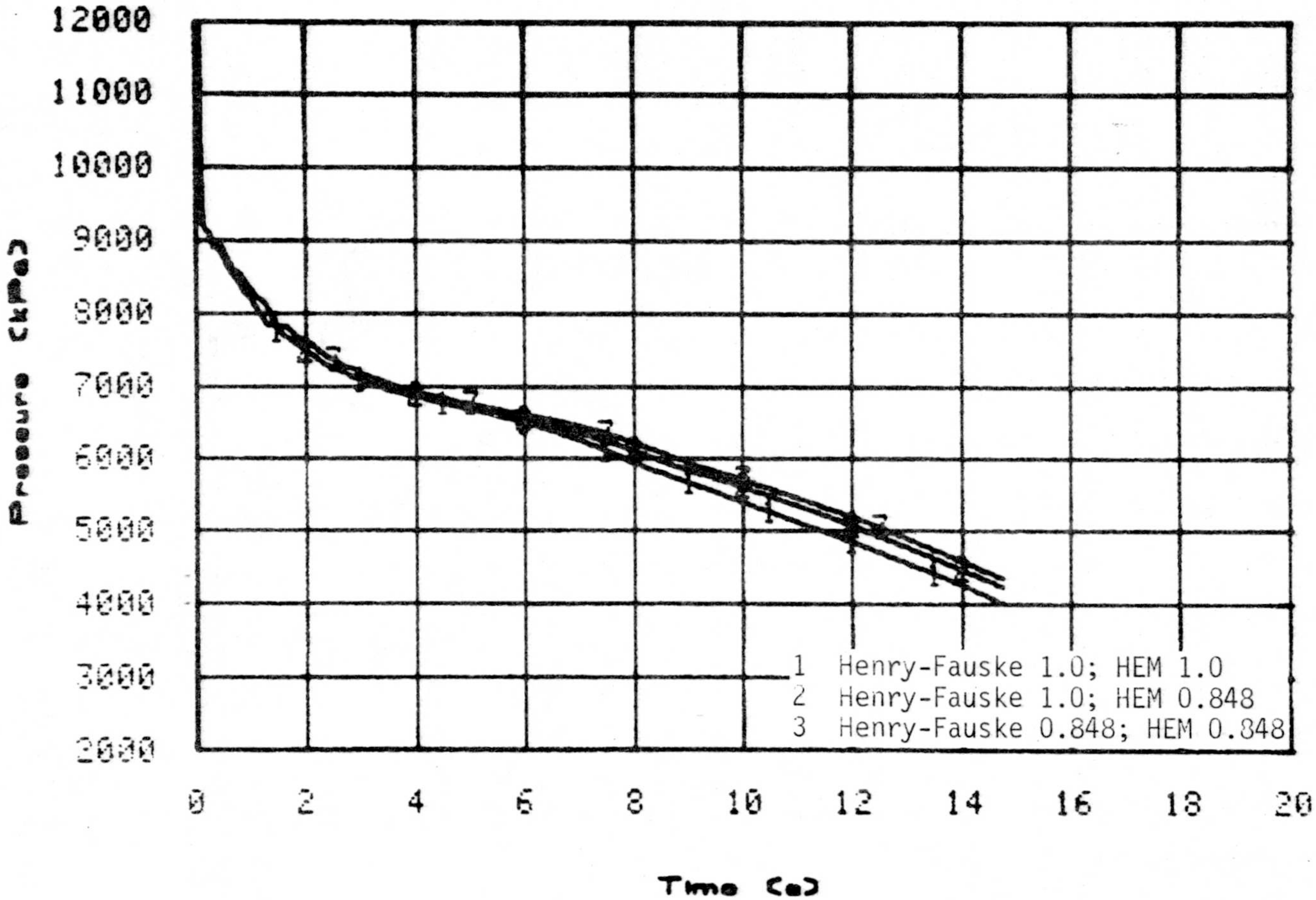

Fig. 23 Upper plenum pressure showing sensitivity due to break flow multiplier.

system pressure was also observed to accompany the successive application of break flow multipliers.

These comparisons indicate a very significant sensitivity to broken loop cold leg break flow contraction coefficient. The mechanism for this effect is quite clear. Application of the contraction coefficient reduces the cold leg break mass flow which results in a larger mass inventory in the downcomer and lower plenum. When the core flow returns to the positive direction at approximately 3.5 s, lower quality fluid is swept from the lower plenum into the core. The increase in core mass flow and decrease in core quality are responsible for the change in lower slab surface temperature response.

Application of the 0.848 multiplier to both the Henry-Fauske model and the HEM at the broken loop cold leg break cause major improvements in the break flow and cladding temperature comparisons with LOCE L2-2 data. Use of this multiplier is physically justified on the basis of vena-contracta calculations for the LOFT nozzle geometry. Other model changes, which cause an increase in the downcomer-lower plenum mass inventory, would be expected to further reduce the cladding temperatures.

3.3.2 Break Flow Transition Quality Sensitivity Study Results. The previous results have shown that the use of break flow multipliers on the Henry-Fauske (subcooled) and homogeneous equilibrium (saturated) critical flow models resulted in a calculated cold leg break flow which agreed fairly well with the measured data. In particular, the agreement was good from 0 to 3 s and very good beyond 6 s. However, between 3 and 6 s the measured mass flow dropped very sharply (in approximately 0.8 s) from subcooled to saturated choking; whereas the RELAP4/MOD6 calculation required nearly 3 s for the transition. This observation led to a sensitivity study of the critical flow transition used in RELAP4/MOD6.

Two critical flow transition options are available in RELAP4/MOD6: the first option uses the minimum of the extended

Henry-Fauske model and HEM times $\sqrt{X_t/X}$, where X is the quality and X_t is the transition quality. Figure 24 shows the form of the transition for this case. The LOCE L2-2 experiment prediction calculation used this option with X_t = 0.02; however, the variable dials for the Henry-Fauske/HEM model are not used with this option selection. Therefore, the newer transition (linear weighting transition) option has been used for the LOCE L2-2 posttest sensitivity calculations. With this option, the transition mass flow G_t is calculated as

$$G_t = G_{HF} - \left(\frac{X \cdot X_T}{X_{tu} - X_{t1}}\right)\left(G_{HF} - G_{HEM}\right)$$

where

G_{HF} = mass flow from extended Henry-Fauske correlation

G_{HEM} = mass flow from homogeneous equilibrium model

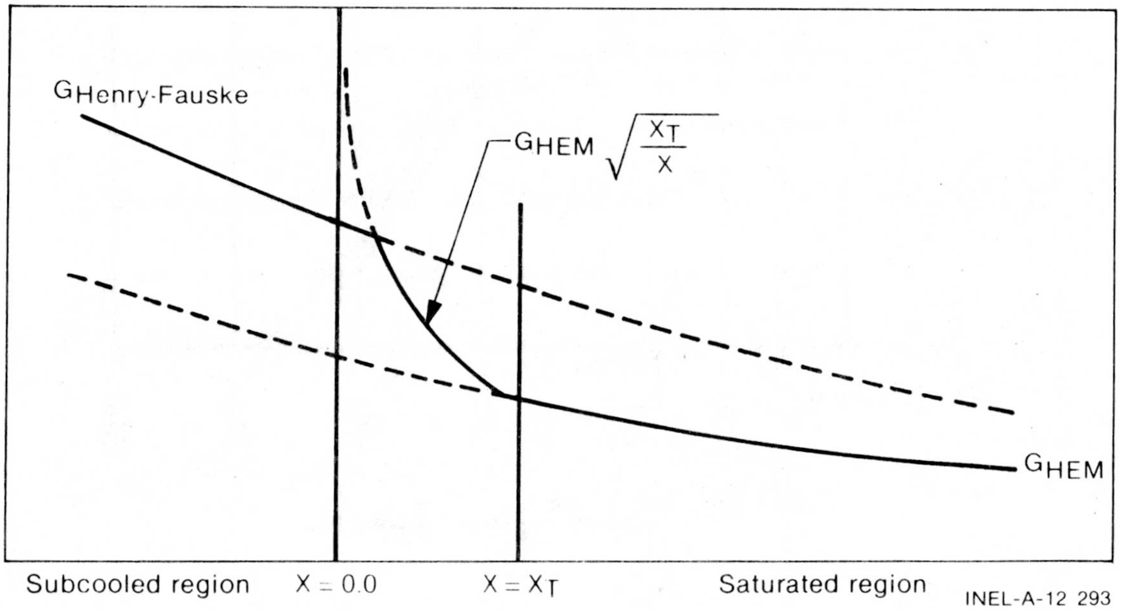

Fig. 24 Henry-Fauske/homogeneous equilibrium critical flow model.

X = quality

X_{tu} = upper transition quality

X_{t1} = lower transition quality.

The default values of X_t and X_{tu} are 0.0 and 0.02, respectively. Figure 25 shows the form of the linear weighting transition option.

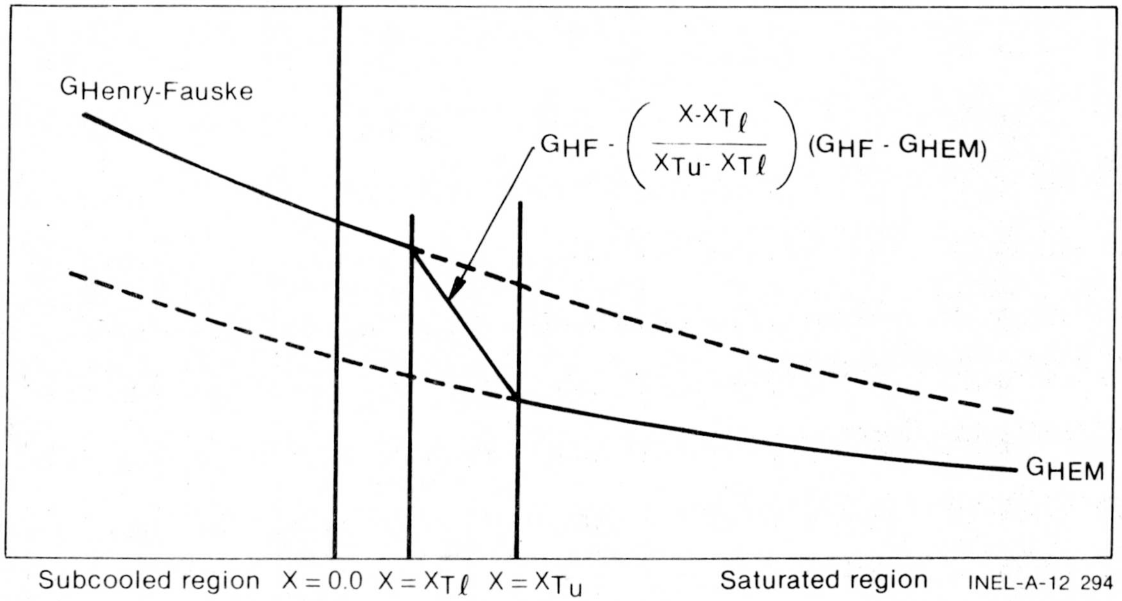

Fig. 25 Henry-Fauske/homogeneous equilibrium critical flow model with linear weighting transition.

For this sensitivity calculation, the base case (Analysis A7 in Figures 26 through 31) used break flow multipliers of 0.848 on both the Henry-Fauske and HEM correlations, Condie-Bengston transition boiling correlation, and measured LOCE L2-2 initial conditions. The default values of upper and lower transition quality were used. To test the sensitivity to transition quality, the upper transition value was changed to 0.0025, a value expected to cause the type of sharp transition observed in the LOCE L2-2 data. This calculation is referred to as Analysis A12 in Figures 26 through 31.

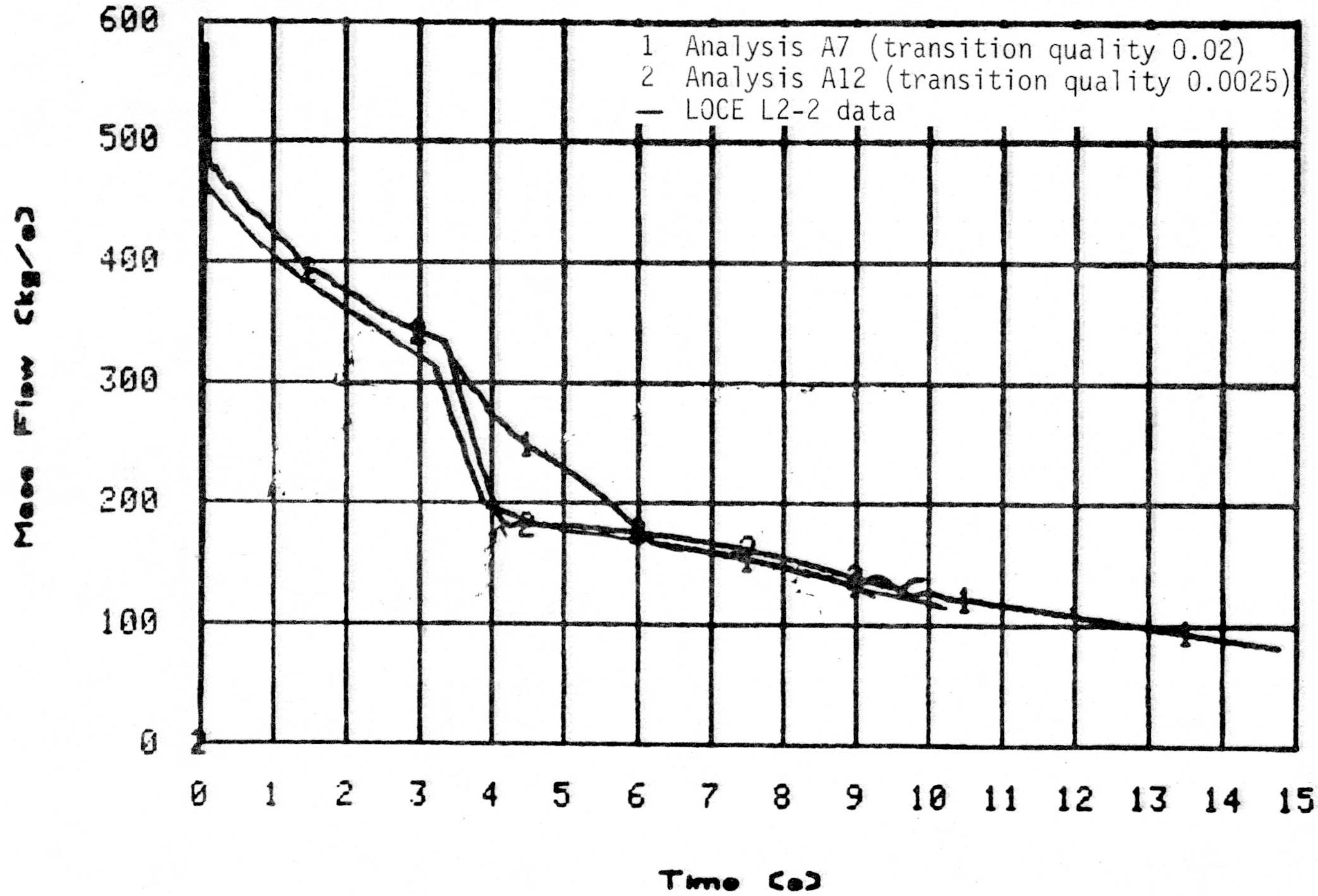

Fig. 26 Broken loop cold leg mass flow rate showing sensitivity due to critical flow transition quality.

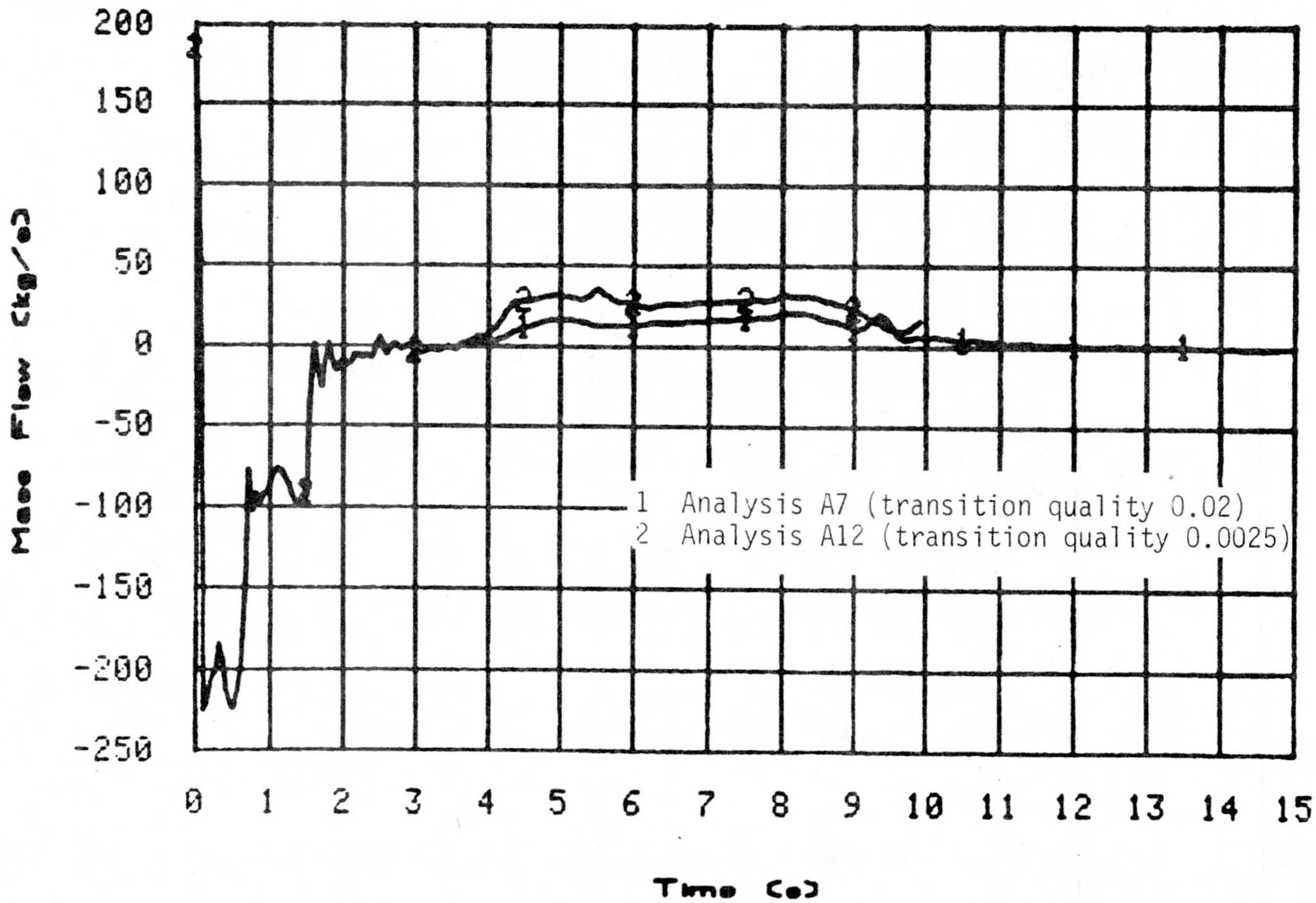

Fig. 27 Core inlet mass flow rate showing sensitivity due to critical flow transition quality.

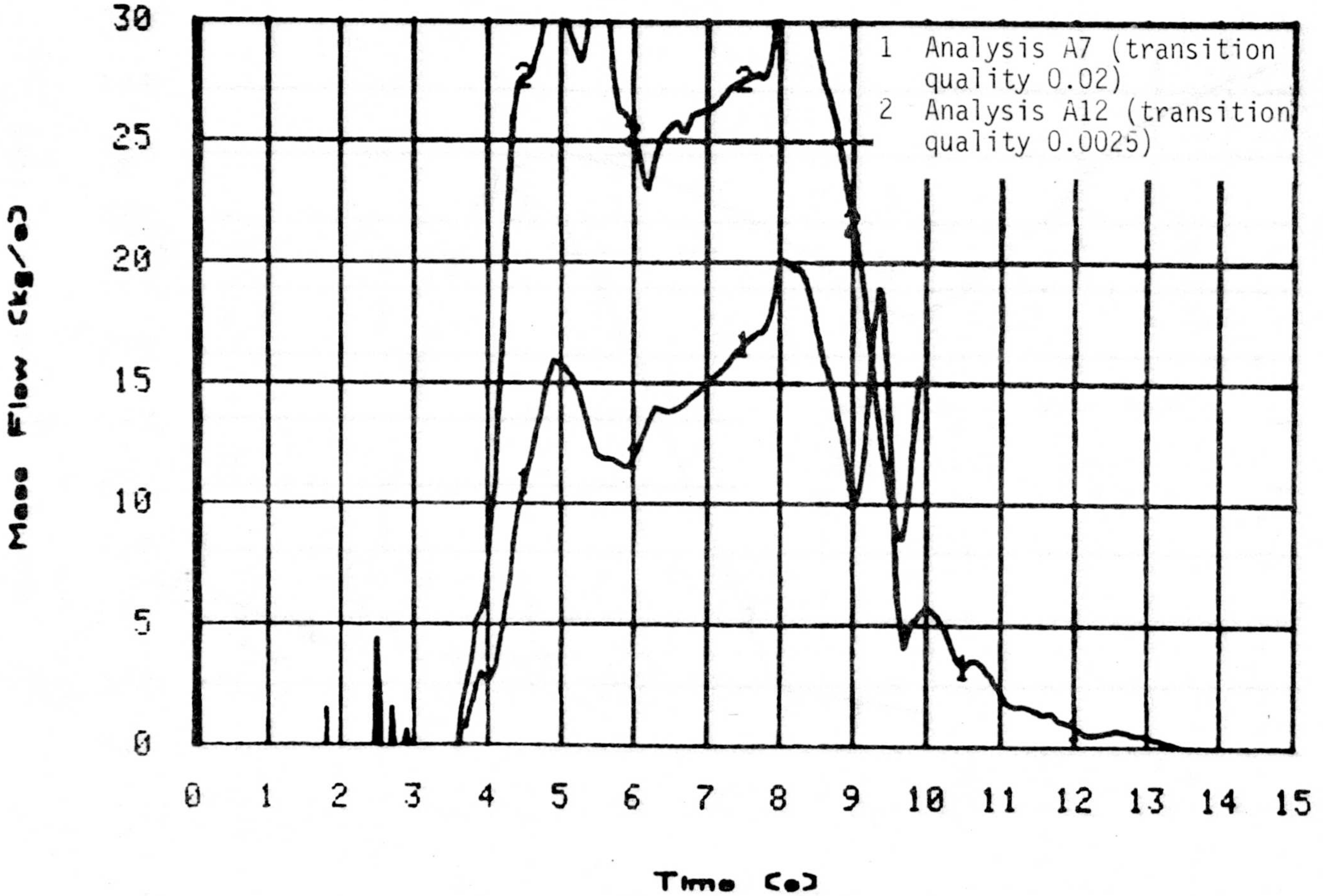

Fig. 28 Core inlet mass flow rate showing sensitivity due to critical flow transition quality (expanded scale).

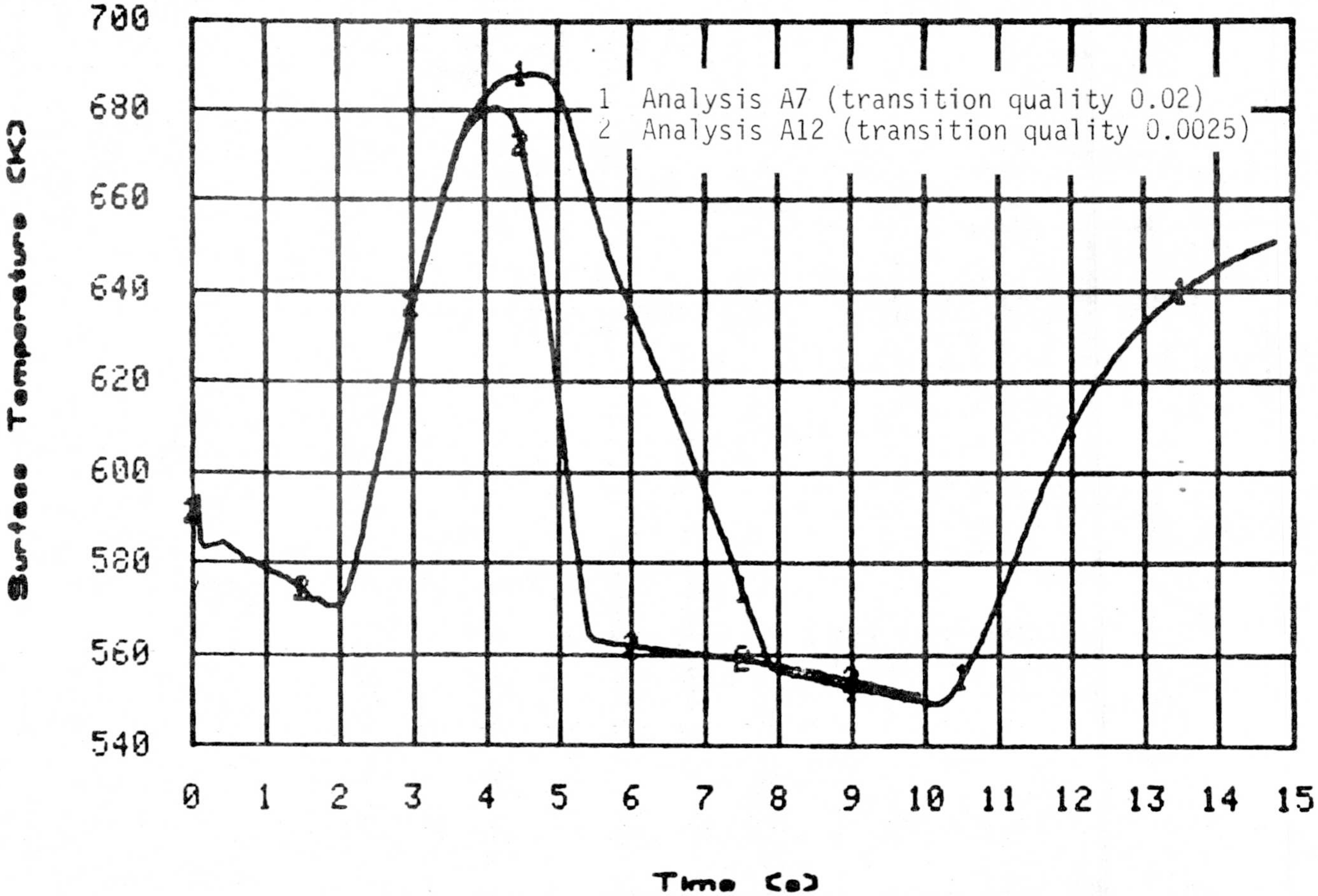

Fig. 29 Cladding temperature of average-powered fuel rod showing sensitivity due to critical flow transition quality for lower third of core.

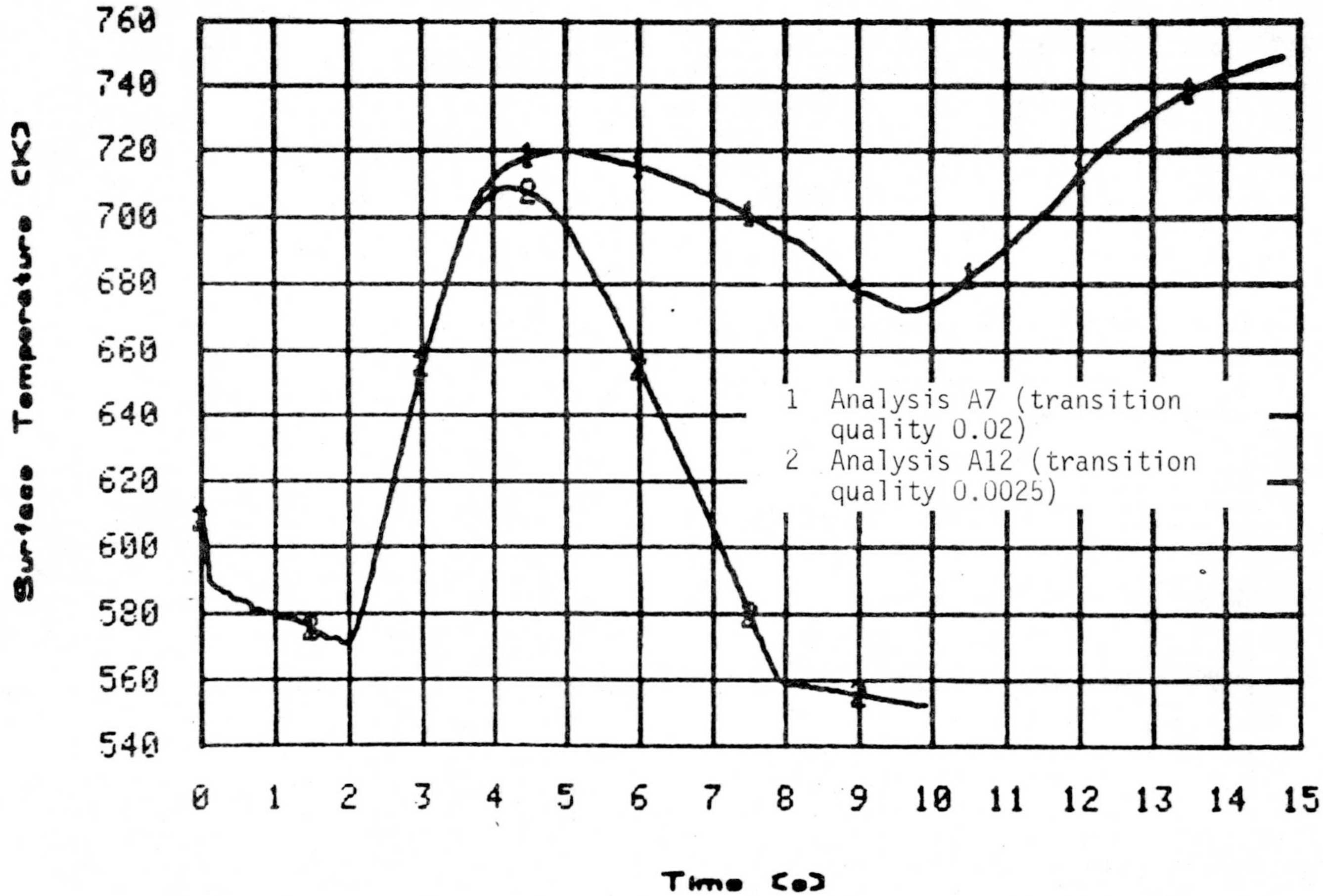

Fig. 30 Cladding temperature of average-powered fuel rod showing sensitivity due to critical flow transition quality for middle third of core.

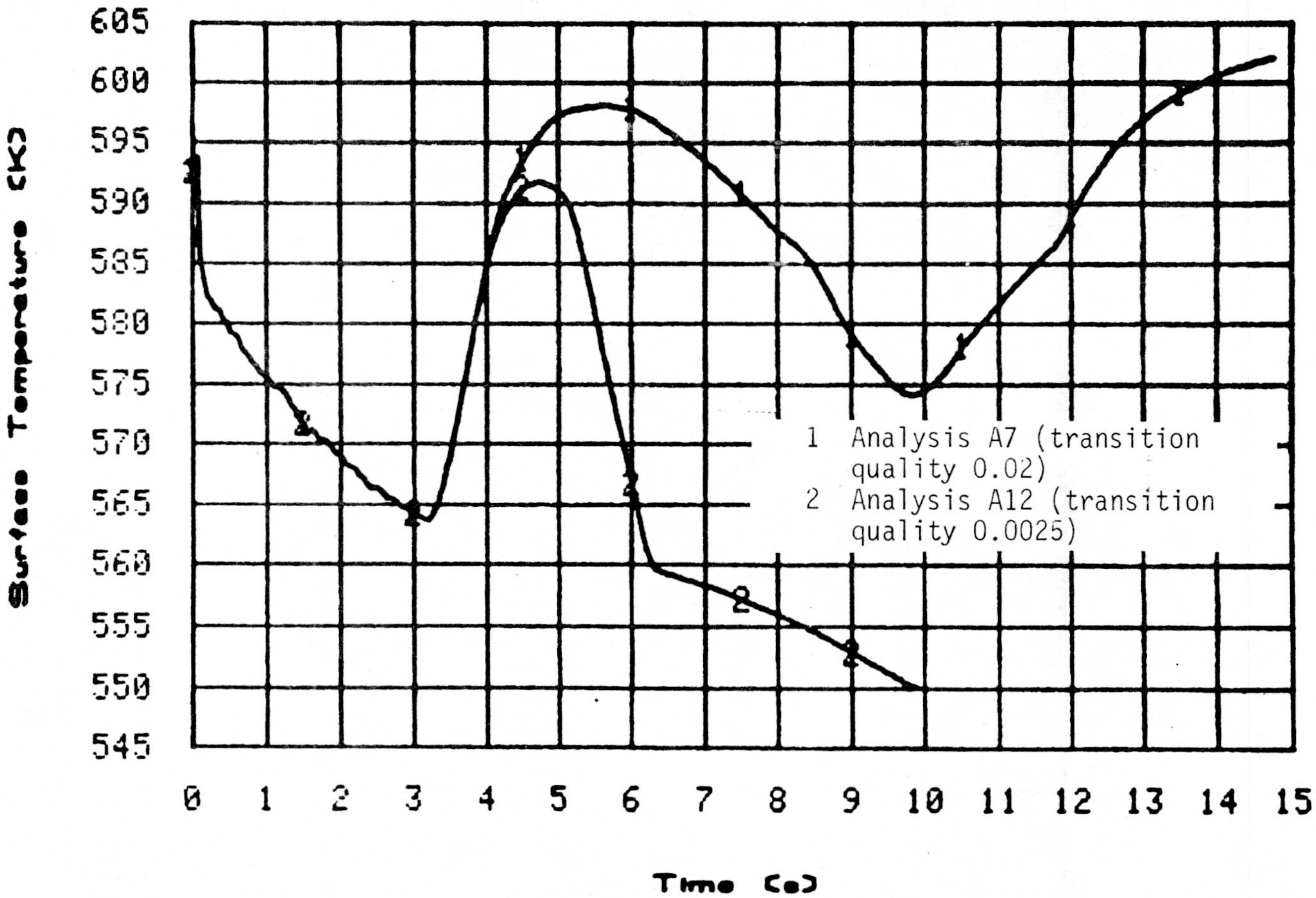

Fig. 31 Cladding temperature of average-powered fuel rod showing sensitivity due to critical flow transition quality for upper third of core.

Figure 26 shows the broken loop cold leg mass flow for the two RELAP4/MOD6 calculations and LOCE L2-2 measured data. The figure shows that the desired effect of the sensitivity was achieved. The effect of the reduced break flow on the core inlet flow is shown in Figures 27 and 28. Indeed, the positive core flow between 4 and 10 s has been doubled.

As would be expected, the stronger core flow had an effect on the core thermal response, as seen in Figures 29, 30, and 31. The bottom third of the core is calculated to reach saturation temperature at 5.4 s versus 7.8 s in the base case. The middle and upper thirds of the core, which show no rewet in the base case, now rewet at 8 and 6.3 s, respectively.

Physical justification exists for using a smaller transition quality, based on evaluation of Semiscale experimental data. Appendix B presents a discussion of the origin of the 2% transition quality and justification for using a smaller value.

3.4 Fuel Rod Computation Scheme

Comparison of the system analysis and the hot rod analysis for the LOCE L2-2 prediction caused some concern relative to the fuel rod computation scheme. This concern was based on an apparent differing in the hot channel mass flux from the system model mass flux. Figure 32 is an overlay of the core inlet mass flows for the LOCE L2-2 predicted center, control, and corner fuel module hot rods and the core inlet mass flow times 1/1300 for the system analysis in the LOCE L2-2 prediction. Since the three hot rod calculations represent a hot rod, a nearly average rod, and a cool rod, the hot rod and cool rod flows would be expected to form a narrow envelope around the average rod and system flows. As seen in Figure 32, this was not the case. In fact, the corner module hot rod (cool rod) flow remained negative; whereas the flows for the other two single rods and the system flow

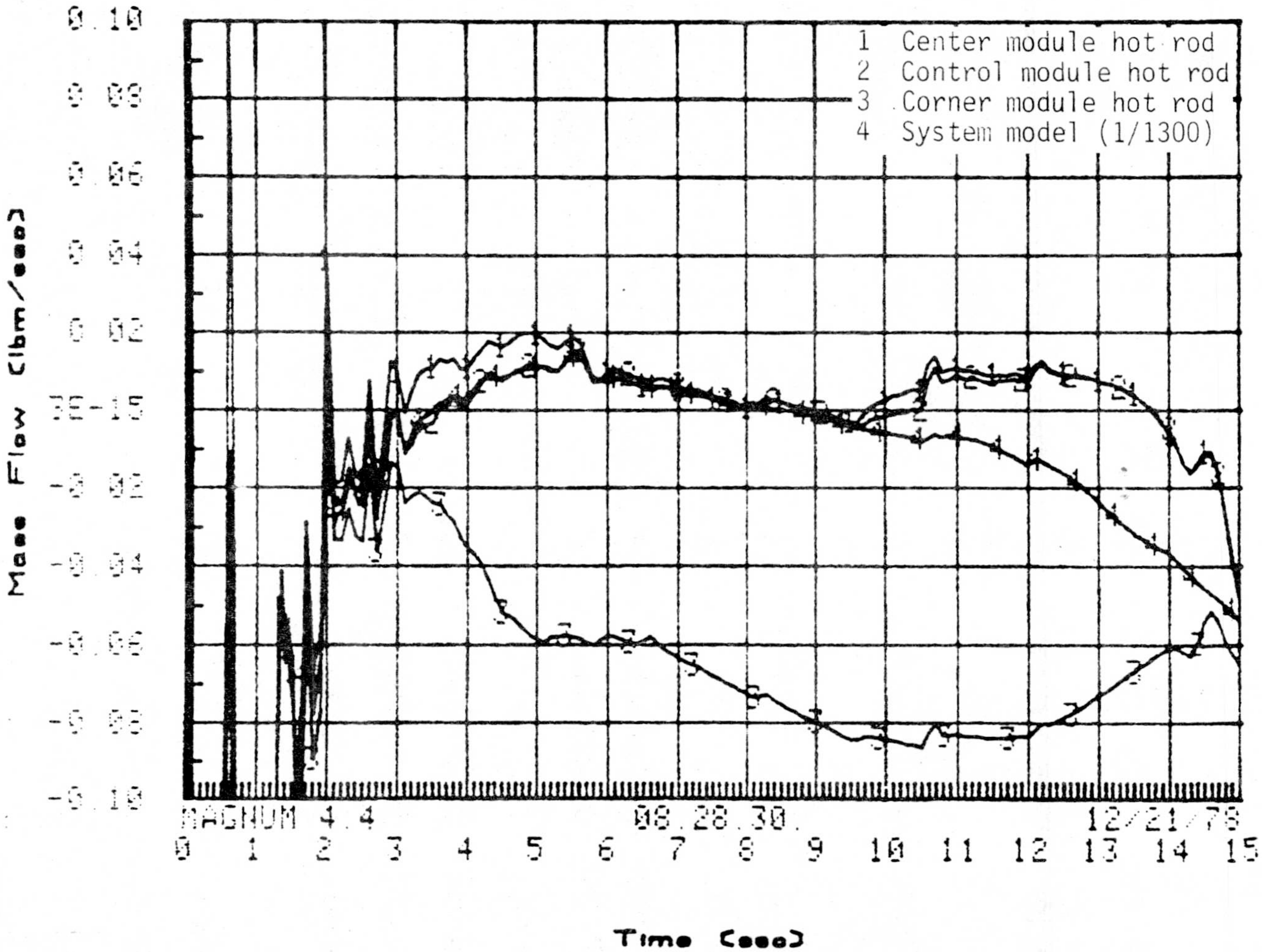

Fig. 32 Core entrance calculated mass flow rate for system model and center, control, and corner fuel module hot rods.

returned to the forward direction. A deviation of the center and control module hot rod flows from the system flow occurs at approximately 9 s after rupture.

Since the hot rod mass fluxes for the center and control fuel modules are approximately equal to the core average mass flux during the period up to 9.5 s, the conclusion reached is that the fuel rod computation problem is not a cause for the failure to predict the core-wide early rewet. As was seen in previous figures, the RELAP4/MOD6 system run did not predict a core-wide rewet.

A further discussion of the cause of the fuel rod computation scheme problem appears in Appendix C.

3.5 Effects of RELAP4/MOD6 Control Volume Corrections

After the experiment predictions reported in Reference 1 were performed, the values of the fluid volumes for several of the control volumes in the RELAP4/MOD6 system model were found to be incorrect. The value of the upper plenum volume used in the experiment prediction was 19.93 ft^3. This value should have been 31.64 ft^3. The volumes input into the experiment prediction for the reflood assist bypass piping were 8.17 and 5.87 ft^3 for the cold leg and hot leg segments, respectively. These figures should have been 6.508 and 6.389 ft^3, respectively.

A sensitivity study was performed to determine what effect using these corrected volumes would have on the LOCE L2-2 RELAP4/MOD6 analysis. In Figures 33 through 35, Analysis A7 is a posttest analysis using measured initial conditions, the Condie-Bengston film boiling correlation, and the 0.848 multiplier on the HEM and Henry-Fauske critical flow models using a 2% transition quality. Analysis A13 was identical to Analysis A7 except the volume data for the upper plenum and broken loops were corrected.

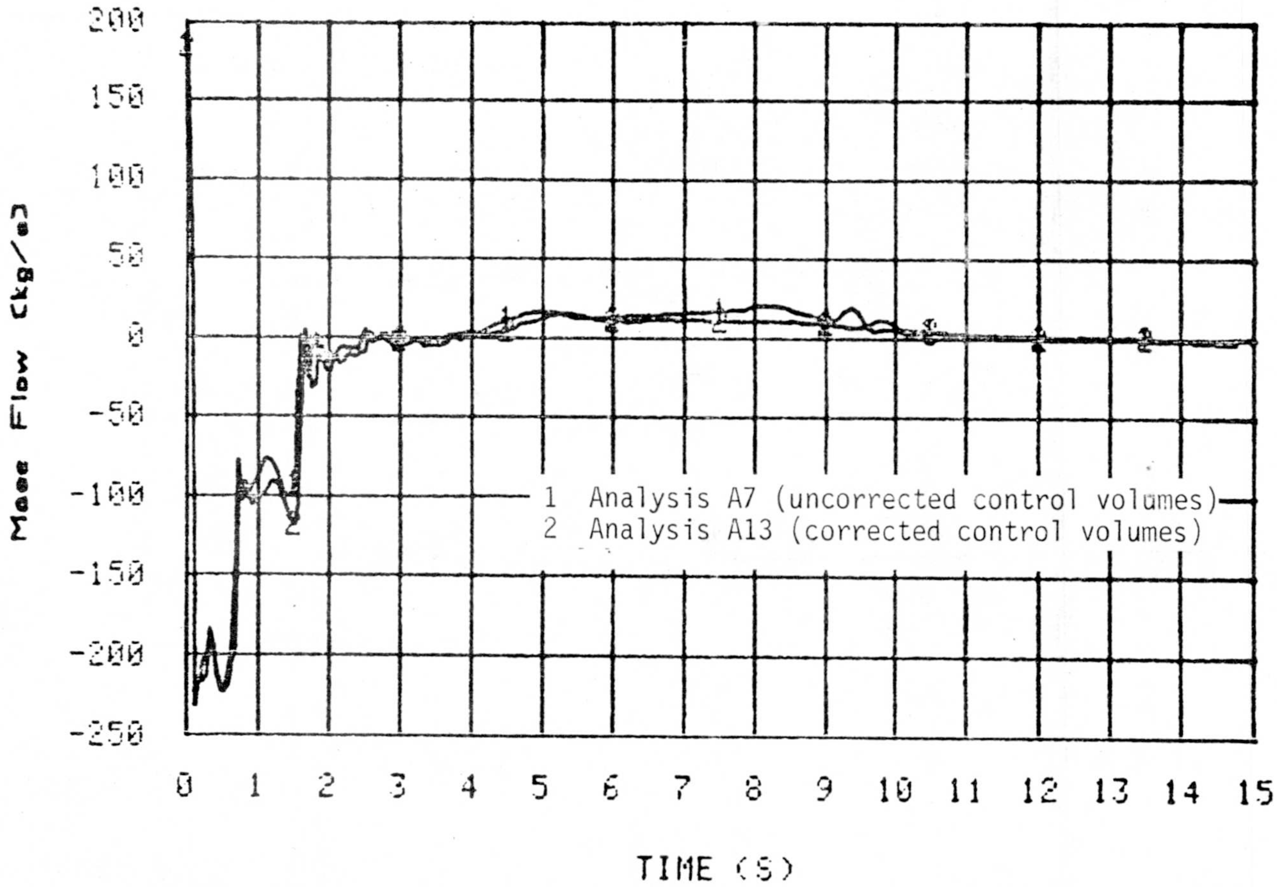

Fig. 33 Core entrance mass flow rate showing effects due to control volume corrections.

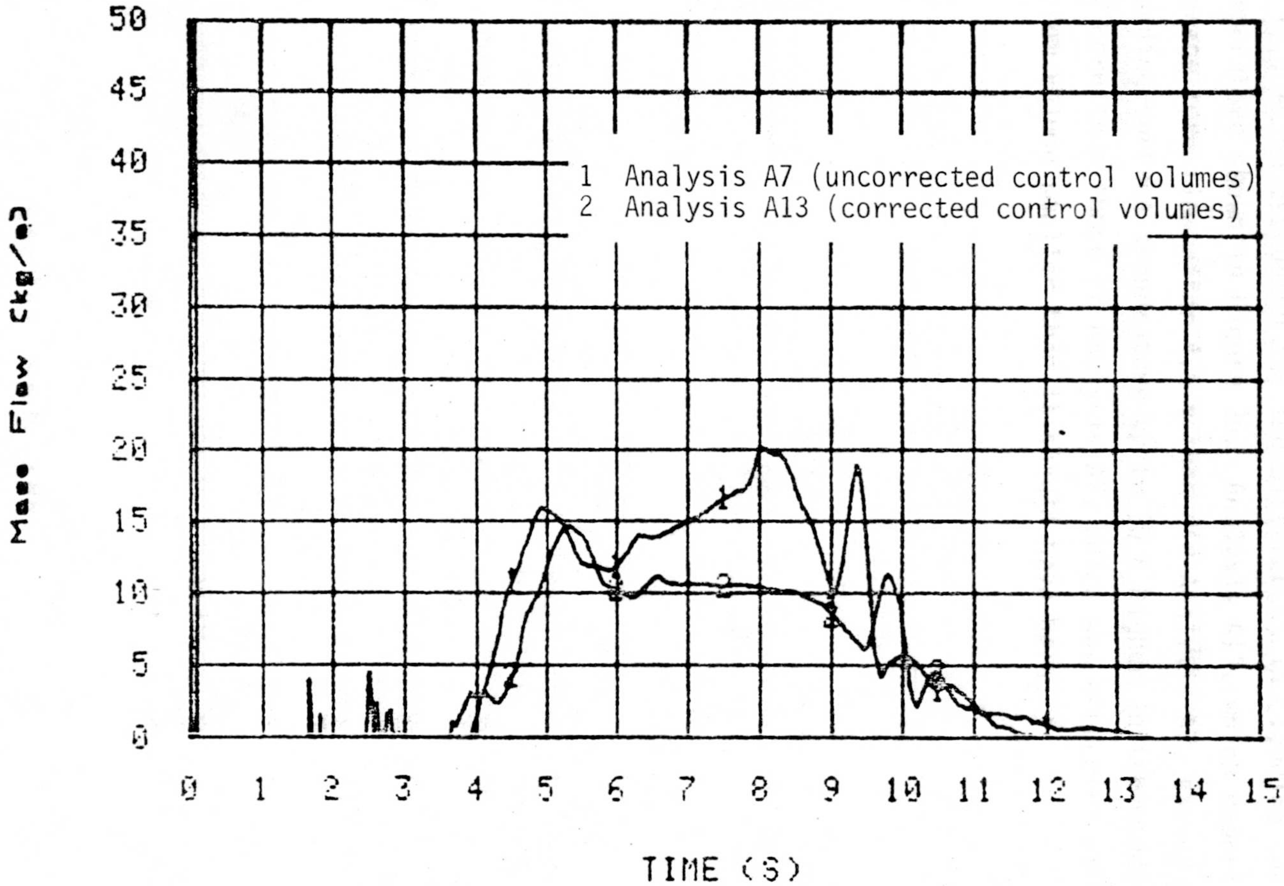

Fig. 34 Core entrance mass flow rate showing effects due to control volume corrections (expanded scale).

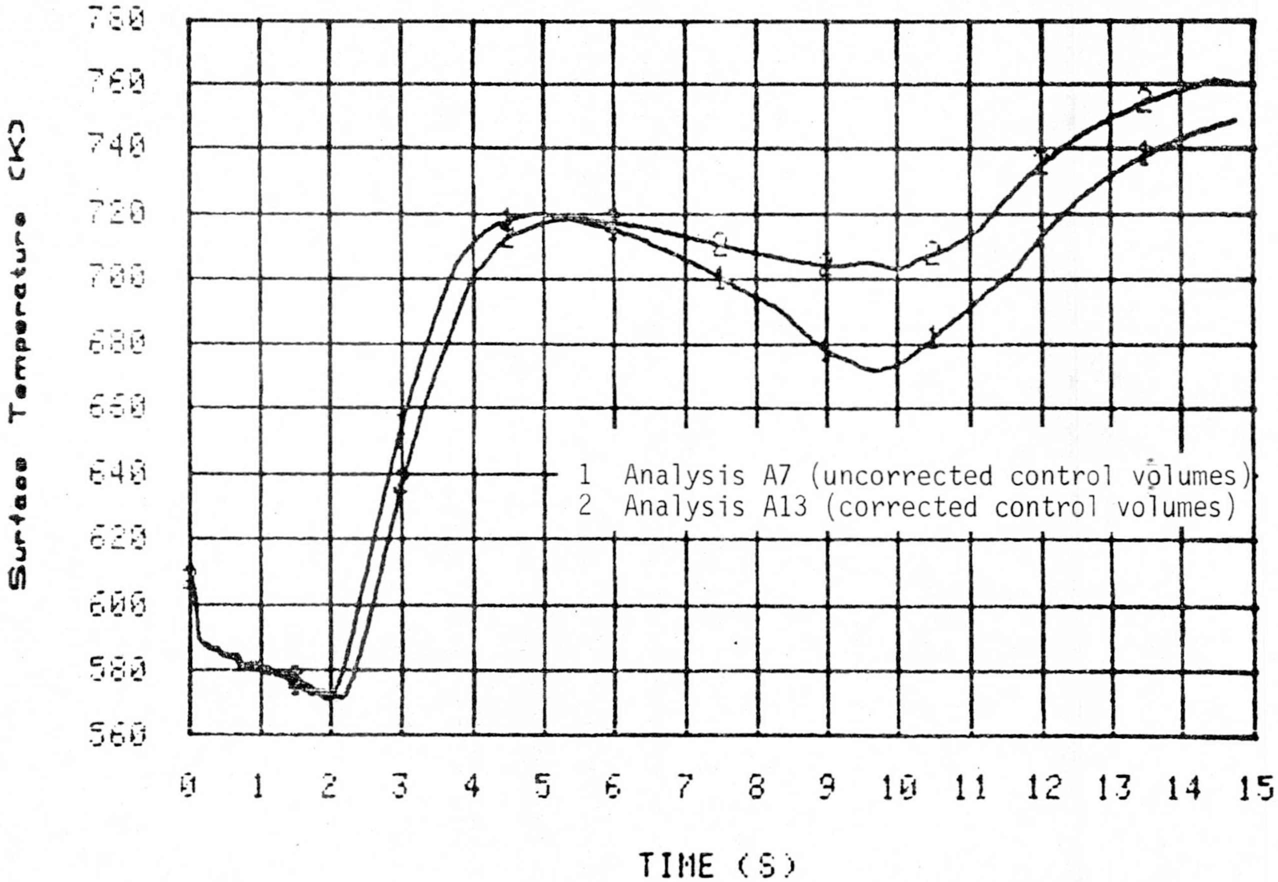

Fig. 35 Cladding temperature of average-powered fuel rod showing effects due to control volume corrections for middle third of core.

In general, the results of the two analyses were very similar. There were differences in the amount of flow through the core during several segments of the transient, as shown in Figure 33. Figure 34 shows, with an expanded scale, the differences in core flow from 4.5 to 10 s which accounted for the differences in cladding surface temperature shown in Figure 35. Analysis A13, which experienced less average core flow after 4.5 s than did Analysis A7, showed fuel rod cladding surface temperature up to 30 K higher in the middle third of the core than those of Analysis A7, which was conducted with an upper plenum volume smaller than it should have been.

IV. CONCLUSIONS

This report presents results of a preliminary analysis of LOCE L2-2 results to gain a better understanding of the disparity between predicted and measured fuel rod cladding temperature responses. Additional work needs to be done to gain a more complete understanding of how to properly predict the phenomena observed in LOCE L2-2. The conclusions based on the information presented in this report are:

(1) Fuel rod modeling of gap conductance and stored energy in the FRAP-T4 computer code appears to be appropriate and can be ruled out as a major cause of the disparity between predicted and measured fuel rod cladding temperature response. FRAP-T4 has been demonstrated to adequately predict the early fuel rod cladding temperature rise rate, which is sensitive to the fuel rod stored energy.

(2) The difference of LOCE L2-2 initial conditions from the initial conditions used in the experiment prediction had no significant effect on the fuel rod cladding temperature prediction.

(3) The selection of the film boiling correlation used in the LOCE L2-2 prediction analysis can cause a significant effect on the fuel rod cladding temperature prediction. However, posttest sensitivity studies reveal that failure to predict the core-wide early rewet cannot be attributed to the choice of the film boiling correlation alone. The disparity between predicted and measured fuel rod cladding temperatures is not due entirely to the choice of the film boiling correlation used in the prediction analysis.

(4) A problem in the method of using RELAP4/MOD6 system model plenum conditions to drive hot rod models was discovered. This problem did not appear to affect the prediction of center and control bundle fuel rod response substantially at the time at which rewet occurred, but would affect the long-term prediction of fuel rod cladding temperature response.

(5) The most likely major cause of the disparity between predicted and measured fuel rod cladding temperature responses for LOCE L2-2 is a combination of inappropriate prediction of core hydraulic behavior, due to inappropriate break flow modeling, and core heat transfer rates, due to an inappropriate choice of film boiling correlations.

The conclusion was also reached that additional work needs to be done in the following areas:

(1) A complete analysis of LOCE L2-2 needs to be done to demonstrate how the code calculations would have compared to experimental data had the experiment prediction analysis been run without input errors.

(2) A complete analysis of LOCE L2-2 needs to be done to demonstrate how the code calculations would have compared to experimental data had the experiment prediction analysis been run with the additional insight into critical flow modeling that has been gained since LOCE L2-2.

(3) Separate effects tests are necessary to better understand high pressure rewet on zircaloy clad heater rods and to assess the capability of analytical model heat transfer packages.

(4) The experiment predictions for LOFT LOCEs L2-3 and L2-4 should be repeated due to problems which have been identified in the prediction methods, including (a) an inappropriate choice in heat transfer option selection, (b) an inappropriate choice of break discharge multipliers, and (c) errors associated with driving fuel rod models with system boundary conditions.

(5) In spite of an input check and a modeling approach review by the prediction consistency committee, a significant input error (break discharge) occurred in the prediction analysis for the L2 series experiments. Other errors of less significance were discovered in the plant geometric description. The quality assurance system needs to be reviewed and possibly revised to reduce the probability of such errors occurring in the future.

V. REFERENCES

1. W. H. Grush et al, Best Estimate Experiment Predictions for LOFT Nuclear Experiments L2-2, L2-3, and L2-4, LOFT-TR-101 (November 1978).

2. S. R. Fisher et al, RELAP4/MOD6 - A Computer Program for Transient Thermal-Hydraulic Analysis of Nuclear Reactors and Related Systems - User's Manual, CDAP-TR-003 (January 1978).

3. L. J. Siefken et al, FRAP-T4 - A Computer Code for the Transient Analysis of Oxide Fuel Rods, CDAP-TR-78-027 (July 1978).

4. M. McCormick-Barger, Experiment Data Report for LOFT Power Ascension Test L2-2, NUREG/CR-0492, TREE-1322 (February 1979).

5. E. L. Tolman et al, Fuel Rod Response for LOFT Test L2-2 (MLHGR = 26.3 kW/m) LTR 20-97 (January 1979).

6. E. M. Feldman and D. J. Olson, Semiscale Mod-1 Program and System Description for the Blowdown Heat Transfer Tests (Series 2), ANCR-1230 (August 1975).

7. Oak Ridge National Laboratory, Project Description, ORNL-PWR Blowdown Heat Transfer Separate-Effects Program - Thermal-Hydraulic Test Facility (THTF), ORNL/NUREG-23, R2 (February 1976).

8. Code Assessment Branch, Assessment of the RELAP4/MOD6 Thermal-Hydraulic Transient Code for PWR Experimental Applications, CAAP-TR-78-035 (December 1978).

APPENDIX A

FUEL ROD STORED ENERGY, GAP CONDUCTANCE, AND HEAT TRANSFER SENSITIVITY STUDIES

BLANK

APPENDIX A

FUEL ROD STORED ENERGY, GAP CONDUCTANCE, AND HEAT TRANSFER SENSITIVITY STUDIES

For short times after a fuel rod experiences departure from nucleate boiling (DNB), the fuel rod stored energy, fuel cladding gap conductance, and surface heat transfer control the cladding heatup. A study was undertaken to evaluate the relative influences each of these parameters has on the initial fuel rod cladding temperature slope to determine if a correlation between steady state stored energy and initial cladding temperature increase after critical heat flux (CHF) could be used to evaluate fuel rod stored energy.

Figure A-1 shows the calculated peak cladding temperatures for Loss-of-Coolant Experiments (LOCE) L2-2, L2-3, and L2-4 and shows significant differences in initial fuel rod cladding temperature slope as the steady state fuel rod power (and stored energy) increases. The initial cladding temperature slope and fuel rod stored energy for LOCEs L2-2, L2-3, and L2-4 are tabulated and correlated graphically in Figure A-2 (dashed curve) and suggest that stored energy can be correlated to the initial temperature slope.

The effect of heat transfer from the fuel rod on initial cladding temperature rise was evaluated by comparing the fuel rod cladding temperature history for an adiabatic and best estimate LOCE L2-2 prediction together with actual LOCE L2-2 data, as shown in Figure A-3. These comparisons suggest that heat transfer does not significantly affect the initial temperature rise.

Calculations were also performed to determine if differences in transient gap conductance would affect the initial cladding temperature slope. The results show the changes in gap conductance do not strongly affect the initial temperature slope, as shown in Figure A-4.

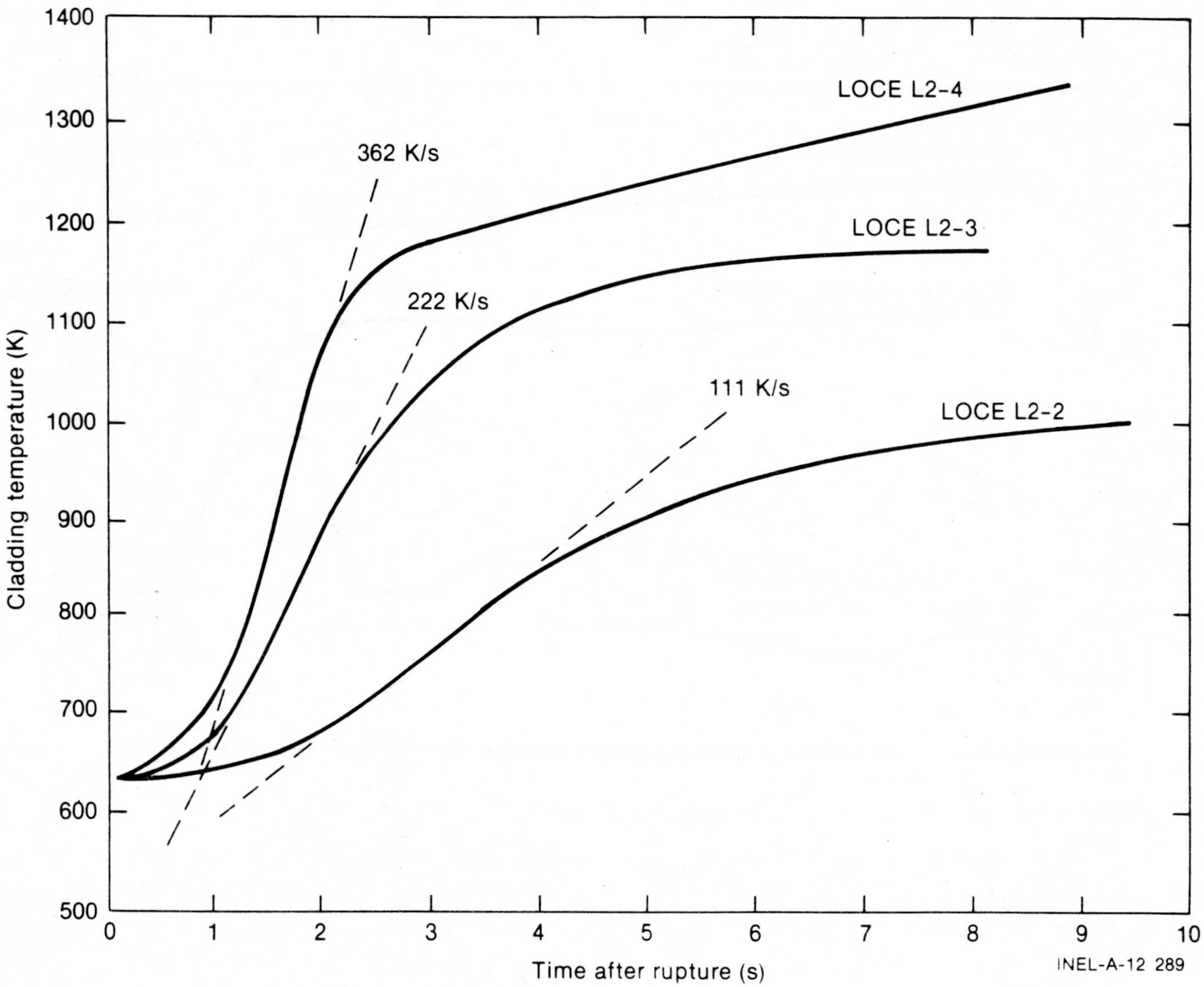

Fig. A-1 Calculated fuel rod cladding temperature response for LOCEs L2-2, L2-3, and L2-4.

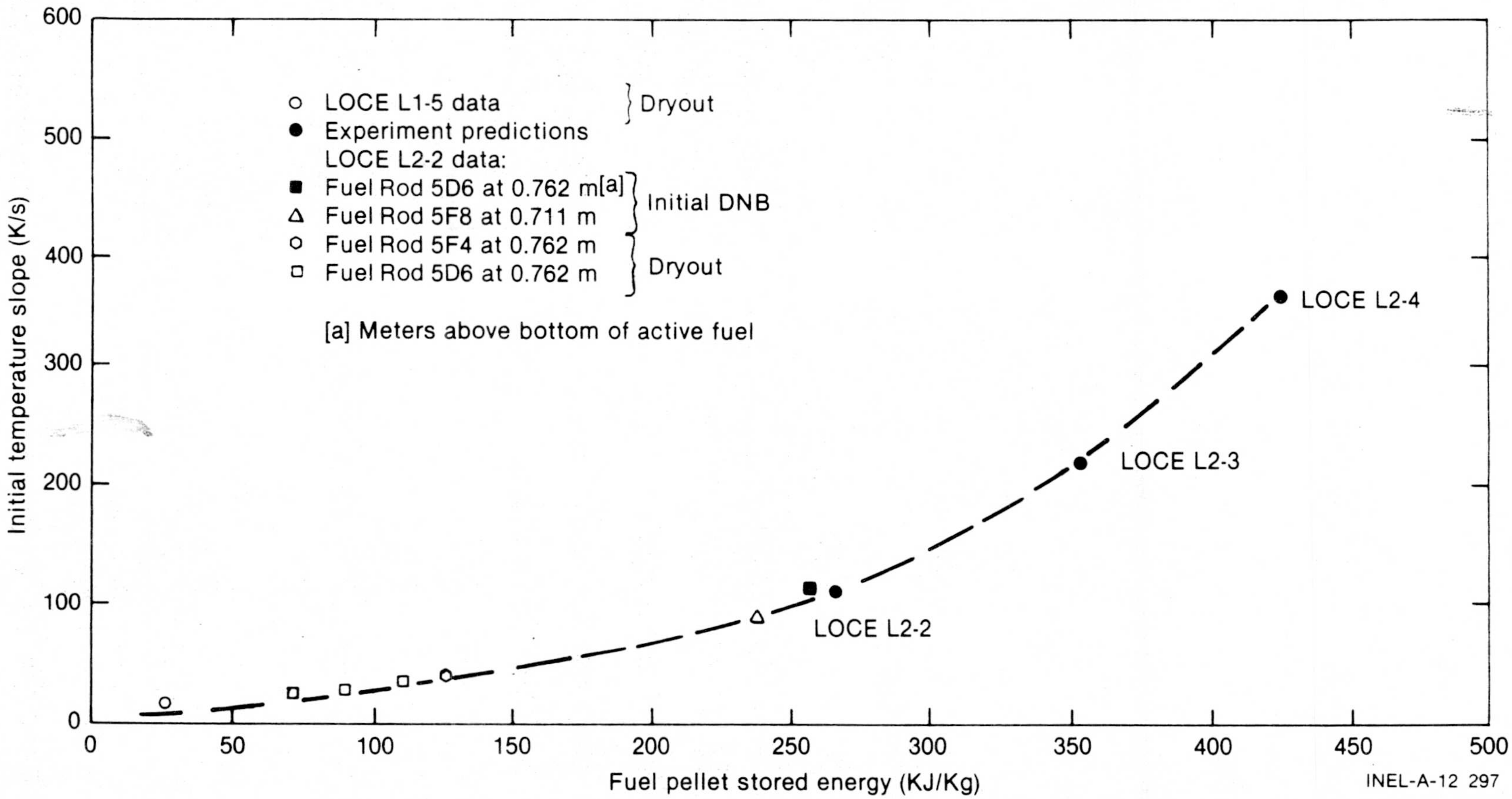

Fig. A-2 Initial fuel rod cladding temperature slope as a function of fuel rod stored energy.

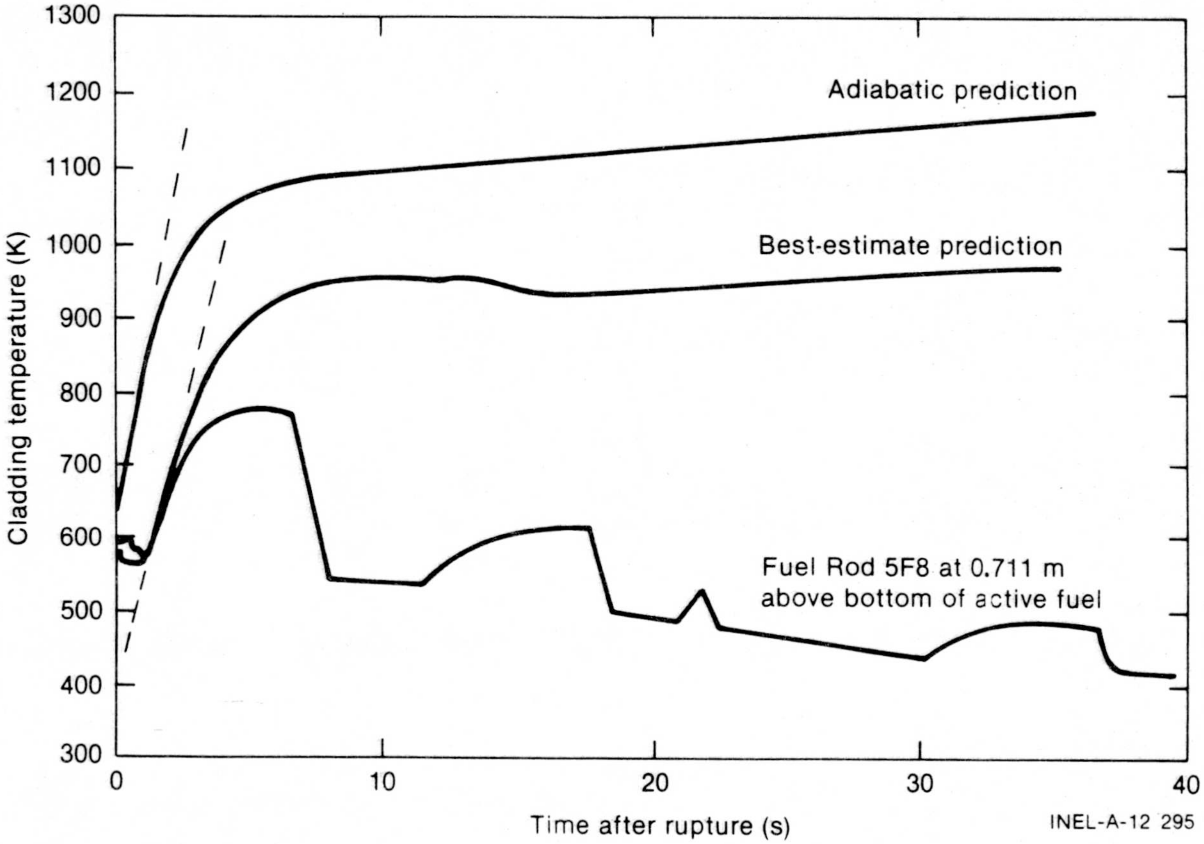

Fig. A-3 Fuel rod cladding temperature history for adiabatic and best-estimate LOCE L2-2 prediction compared with LOCE L2-2 measured data.

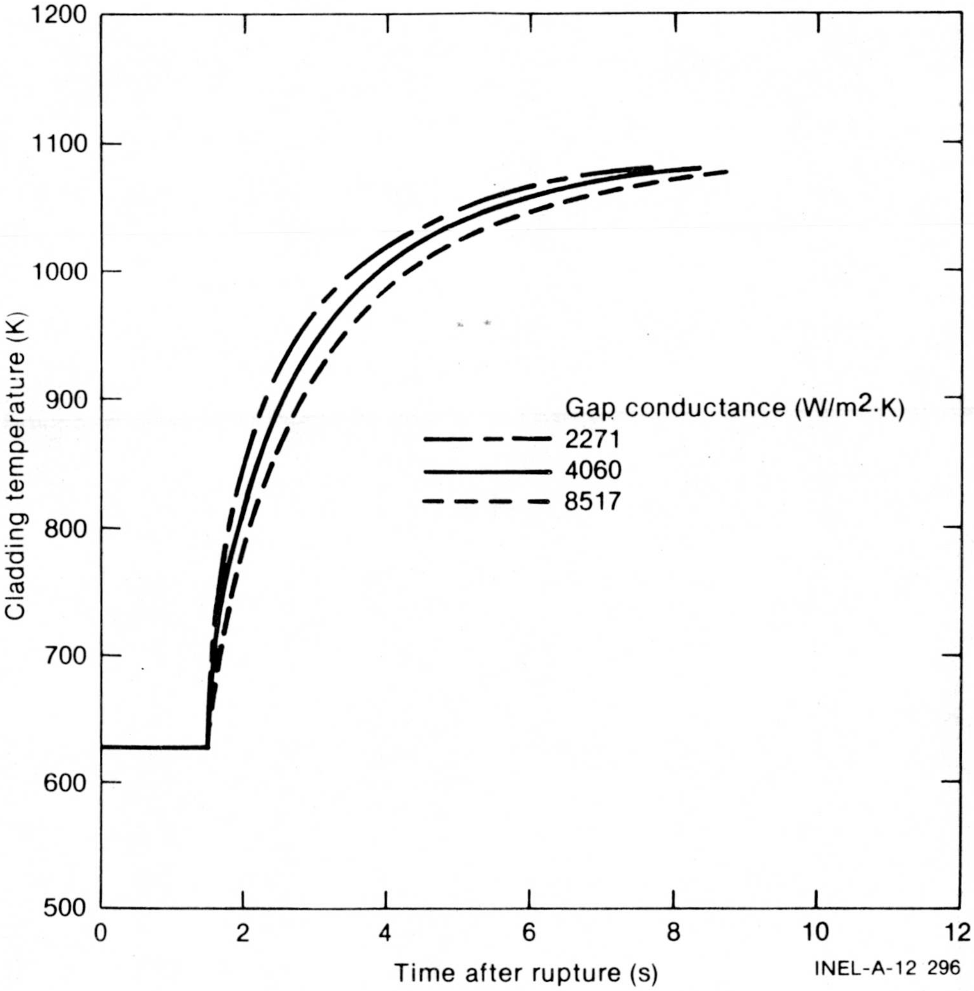

Fig. A-4 Fuel rod cladding surface temperature response as a function of fuel-cladding gap conductance for simulated LOCE L2-2 conditions.

The fuel rod cladding temperature increase indicated by several thermocouples that experienced secondary DNB were also compared to the correlation shown in Figure A-2. The stored energy at these locations was obtained from FRAP-T4 calculations using heat transfer coefficients calculated by the INVERT computer code[a]. Data points for these cases indicate the correlation between fuel stored energy and initial temperature rise after CHF is consistent over a large range of fuel stored energy.

---

a. INVERT, Idaho National Engineering Laboratory Configuration Control Number H00086IB.

The conclusions, based on this study, indicate that stored energy and initial cladding temperature rise can be closely correlated. Surface heat transfer and transient gap conductance effects on initial cladding temperature increase are second-order compared to the influence of stored energy.

APPENDIX B

CRITICAL FLOW TRANSITION QUALITY

BLANK

APPENDIX B

CRITICAL FLOW TRANSITION QUALITY

The purpose of this appendix is to present and discuss a recommendation for using a critical flow transition quality of 0.25% rather than the 2% default value.

In D. G. Hall's analyses (References B-1 and B-2) of Test S-02-4, which was conducted in the Semiscale Mod-1 facility with Henry nozzles, Hall noted that as the upstream stagnation quality approaches 2%, the ratio of measured-to-calculated flow rate using the homogeneous equilibrium model (HEM) critical flow model becomes relatively constant. Figure B-1 shows the mass flow ratio while Figures B-2 and B-3 show the upstream quality. This approach allows use of a break flow multiplier, which can be applied to the HEM and would be applicable over a wide range of qualities that must be greater than 2%.

Figures B-4 and B-5 show the mass flow ratios for five different critical flow models plotted as a function of time for Test S-02-4.

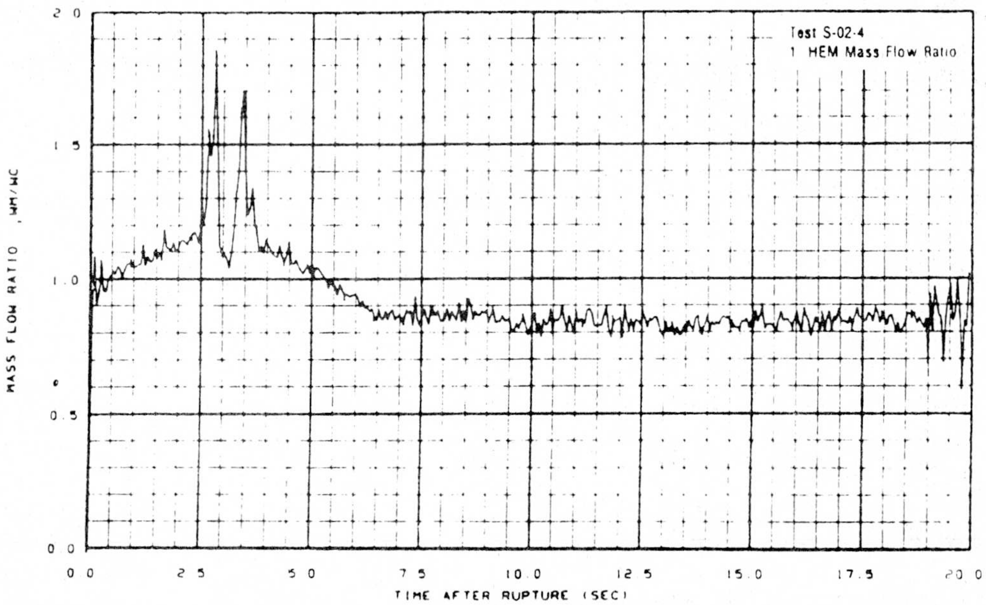

Fig. B-1 Ratios of measured break mass flow rates to HEM calculated critical mass flow rates.

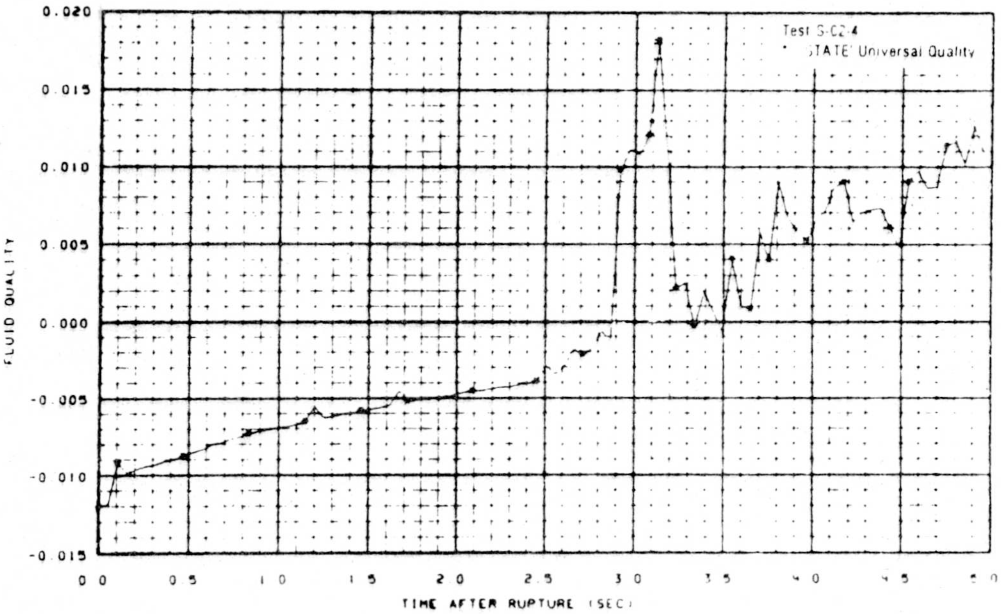

Fig. B-2 Stagnation universal quality calculated by MASFLO program.

Ignoring the spikes in the data between 2.5 and 3.5 s, it can be seen that the HEM multiplier changes relatively little while the Henry-Fauske multiplier changes nearly 35% between 2 and 5 s. Thus, by using a 2% quality for the transition quality instead of a smaller value, better agreement with the experimental data is sacrificed in the low quality region. Since the Henry-Fauske ratio takes such a sharp change as quality becomes greater than zero, this suggests that the Henry-Fauske model should not be used for qualities greater than zero.

Semiscale Mod-1 Test S-06-5 was conducted with a nozzle which was L/D scaled to the Loss-of-Fluid Test (LOFT) nozzle. The same trends discussed above may be seen in Test S-06-5. Figure B-6 shows the upstream stagnation quality for Test S-06-5, while Figures B-7 and B-8 show mass flow rates and mass flow ratios for Test S-06-5. Figures B-9 and B-10 show the mass flow ratios for HEM and Henry-Fauske models plotted as a function of universal quality. It should be noted that in the 0 to 2% quality range, the multiplier for HEM changes from 1.12 to 1.03 (a change of approximately 9%), while the Henry-Fauske multiplier changes from 0.75 to 0.65 (a change of approximately 15%).

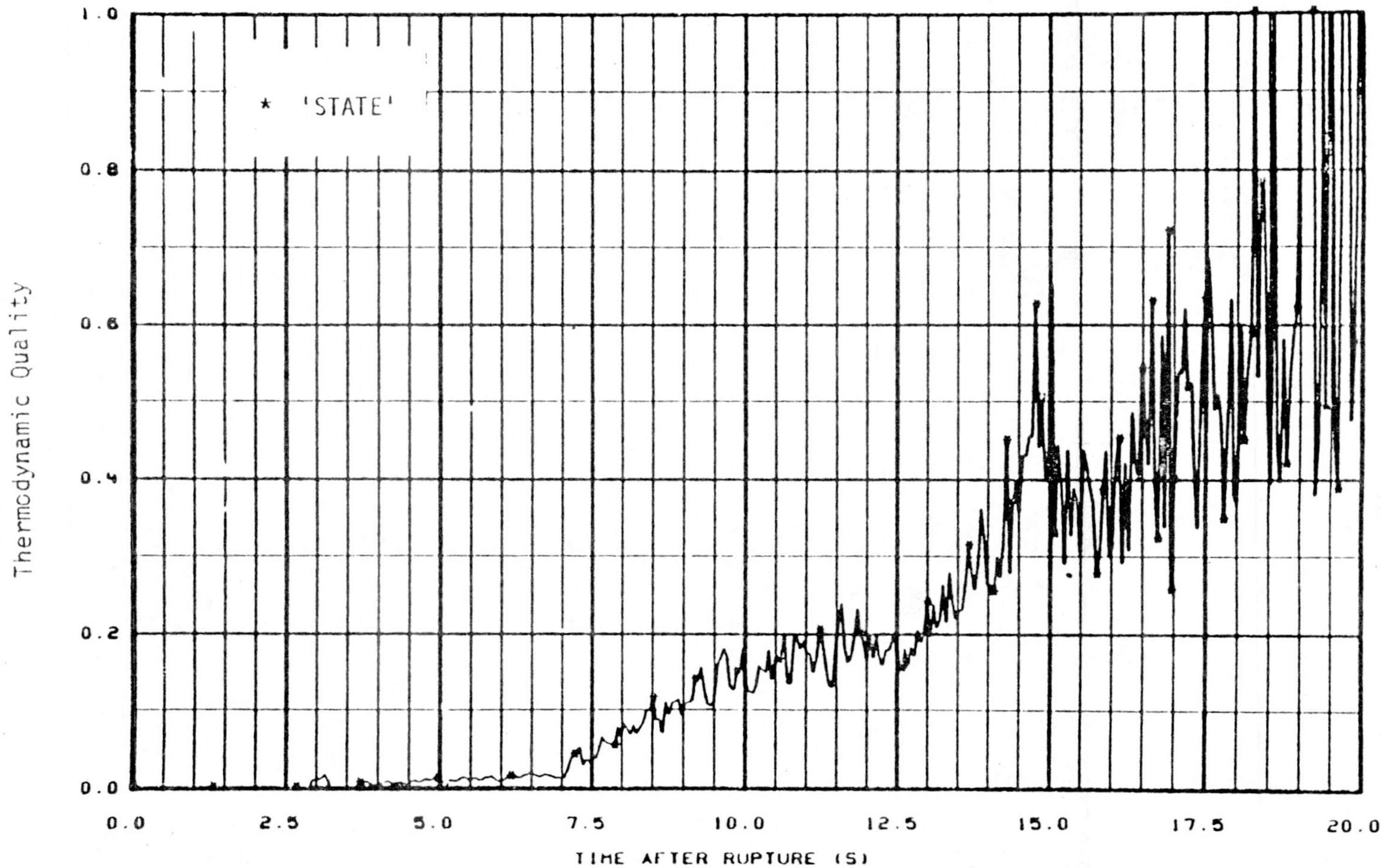

Fig. B-3 Stagnation quality history for Semiscale Mod-1 Test S-02-4.

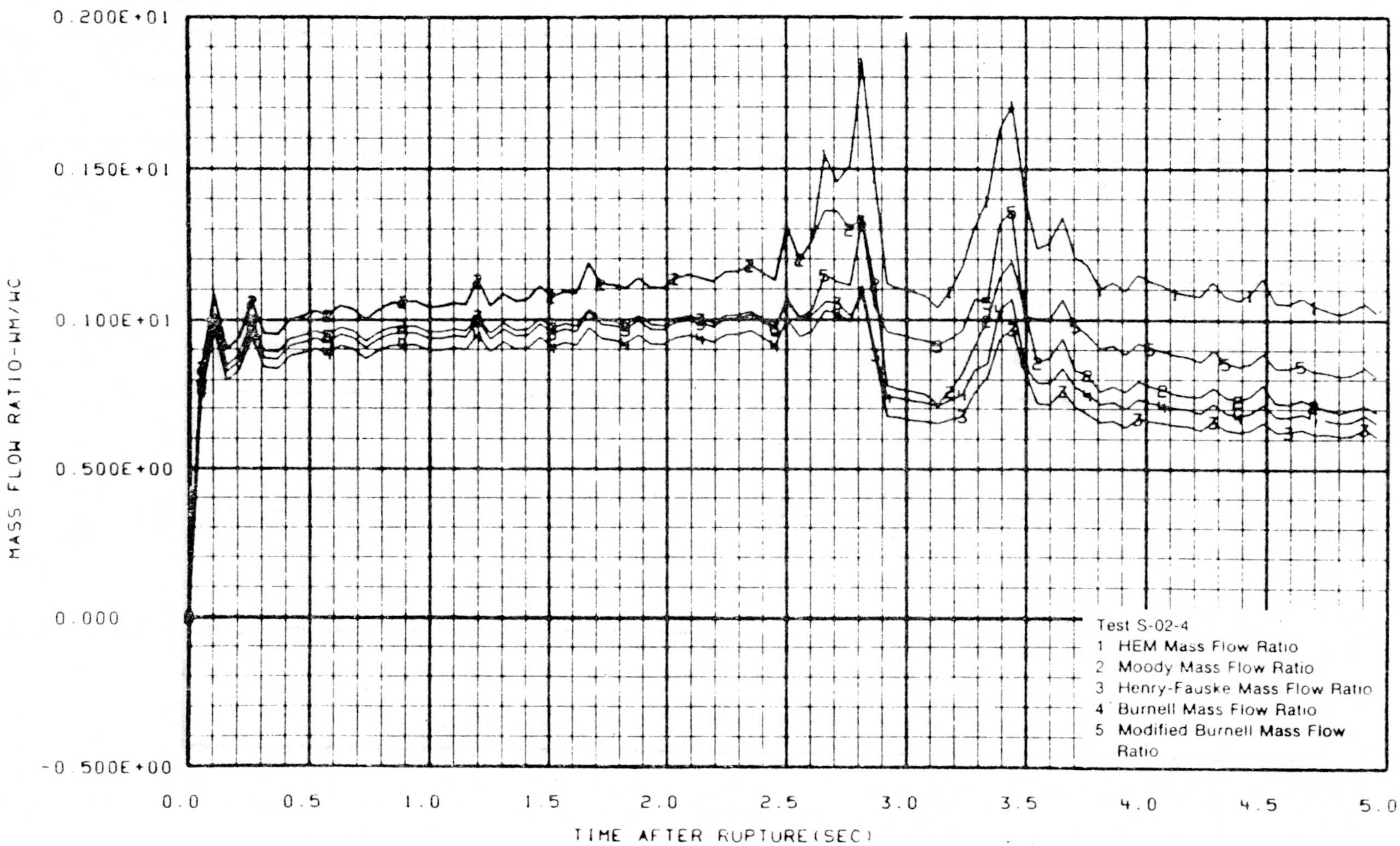

Fig. B-4 Ratios of measured break mass flow rates to critical mass flow rates calculated using five critical flow models (t = 0 to 5 s).

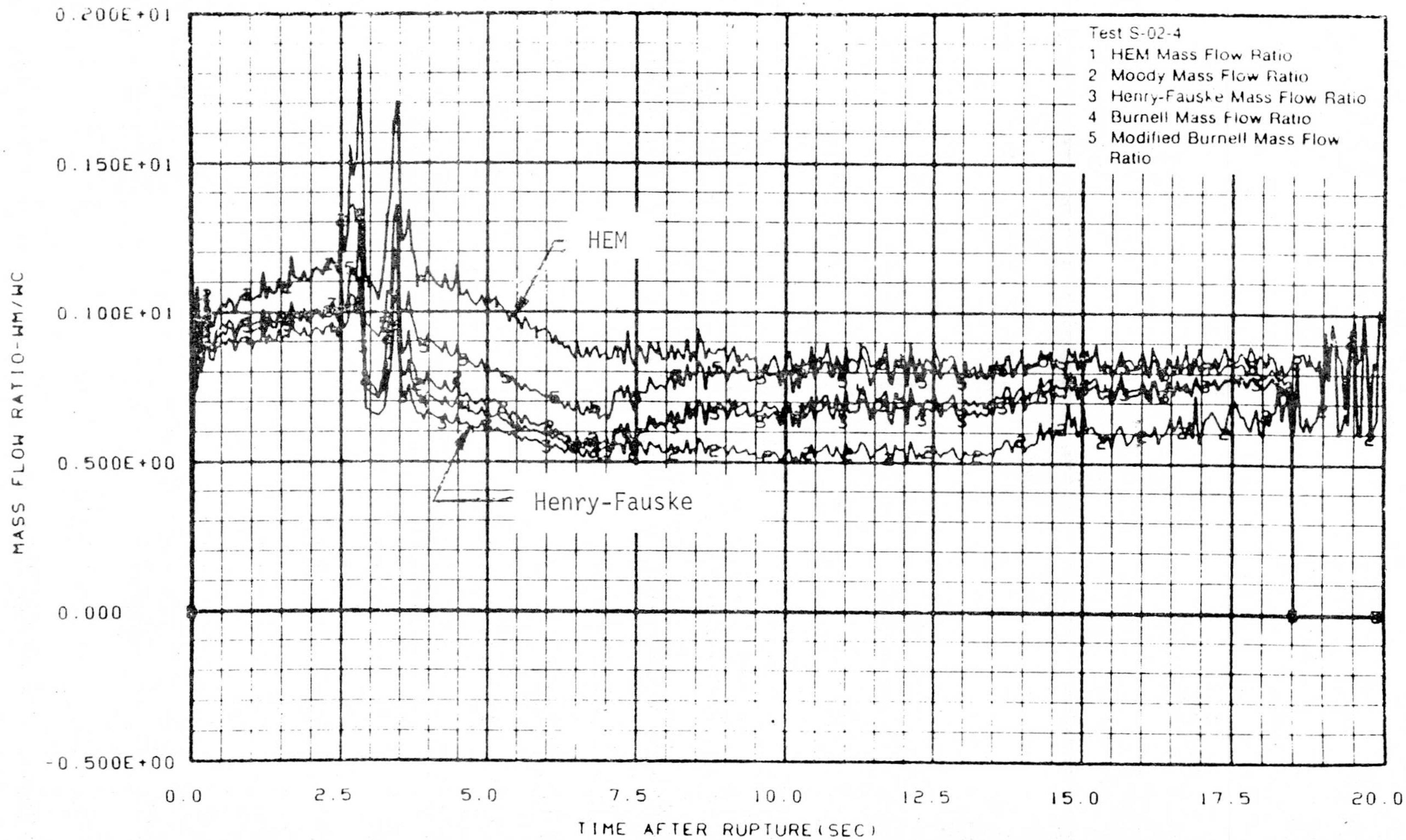

Fig. B-5 Ratios of measured break mass flow rates to critical mass flow rates calculated using five critical flow models (t = 0 to 20 s).

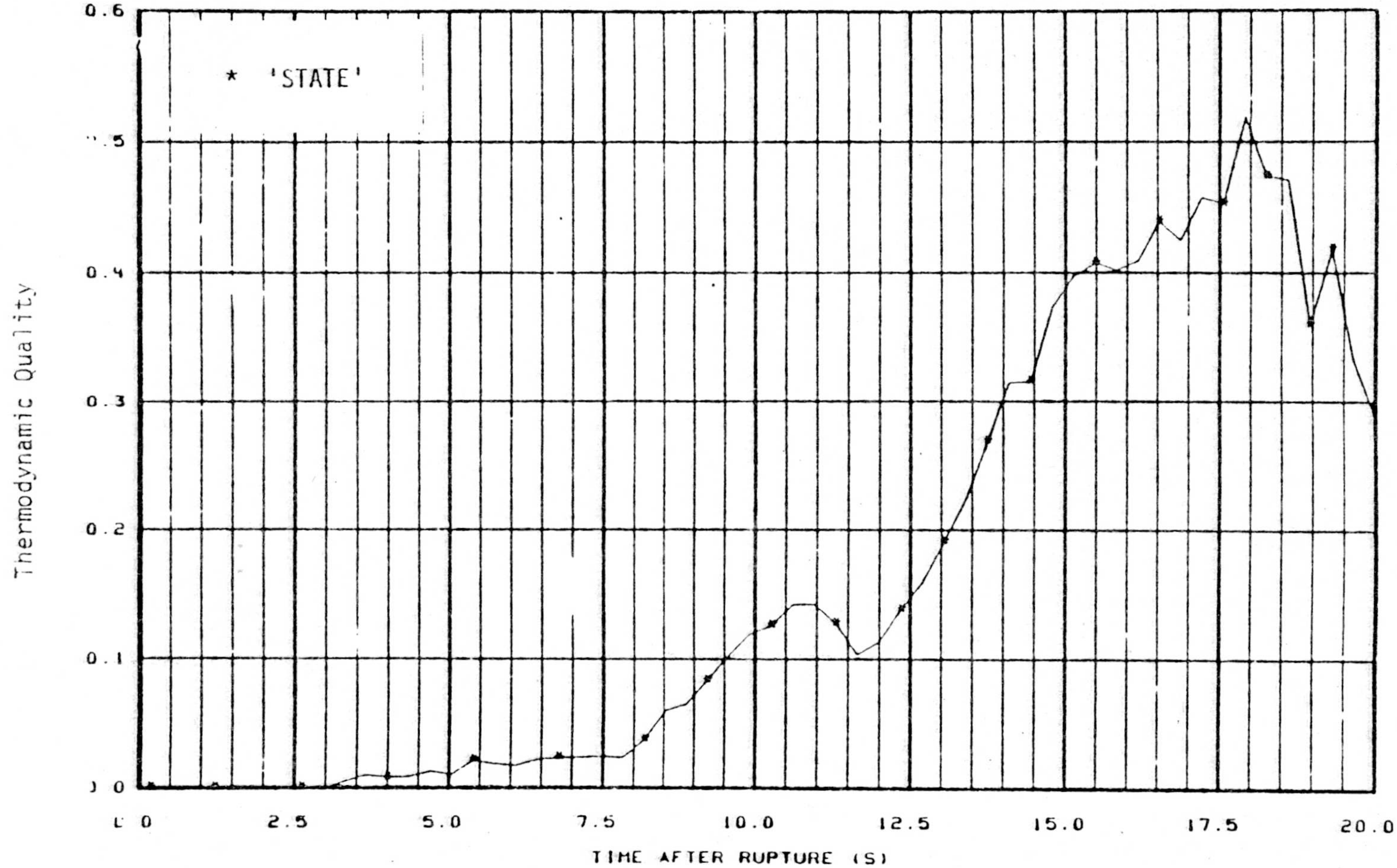

Fig. B-6 Stagnation quality history for Semiscale Mod-1 Test S-06-5.

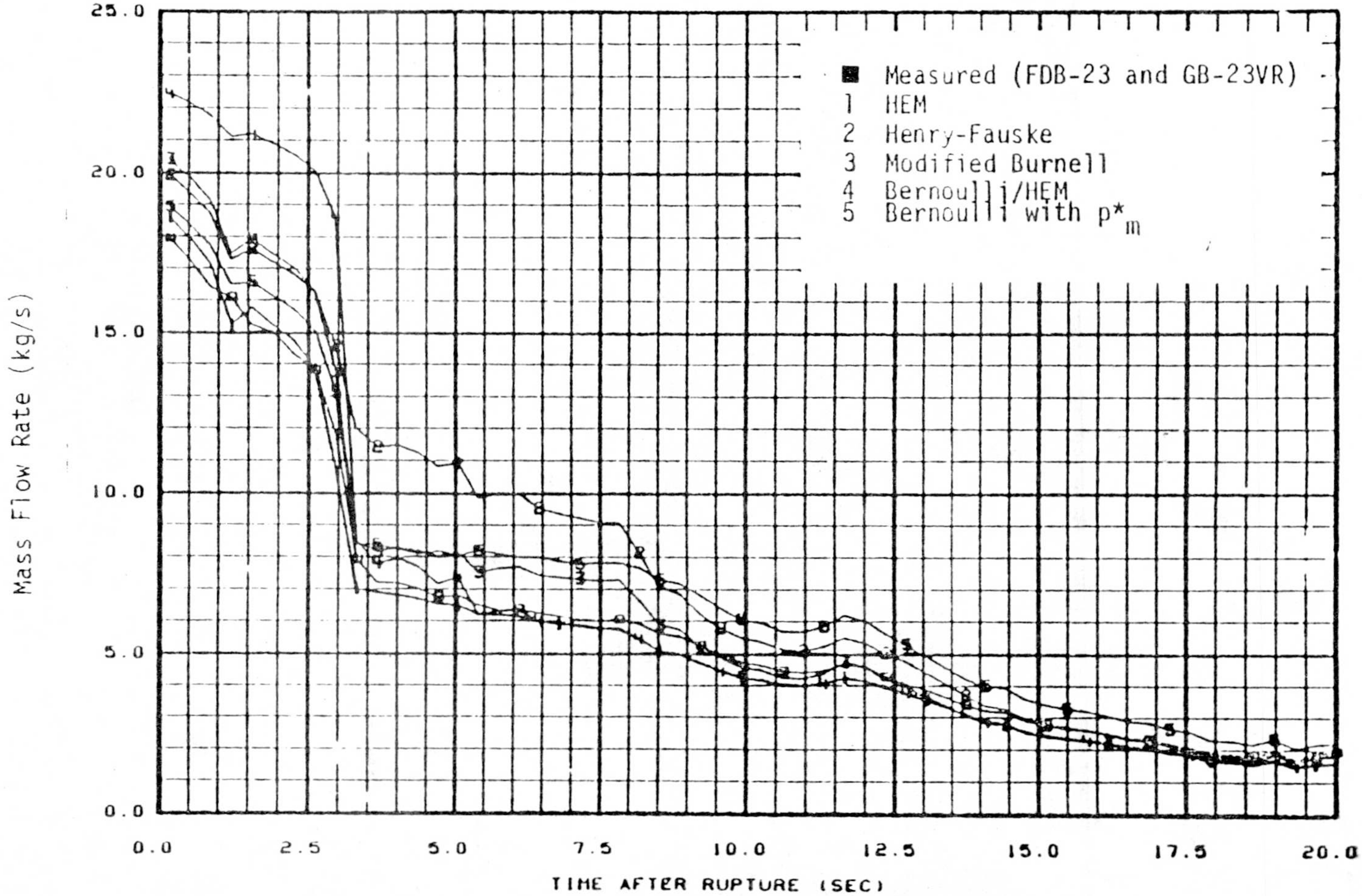

Fig. B-7 Comparison of measured break flow rates and calculated critical flow rates for Semiscale Mod-1 Test S-06-5.

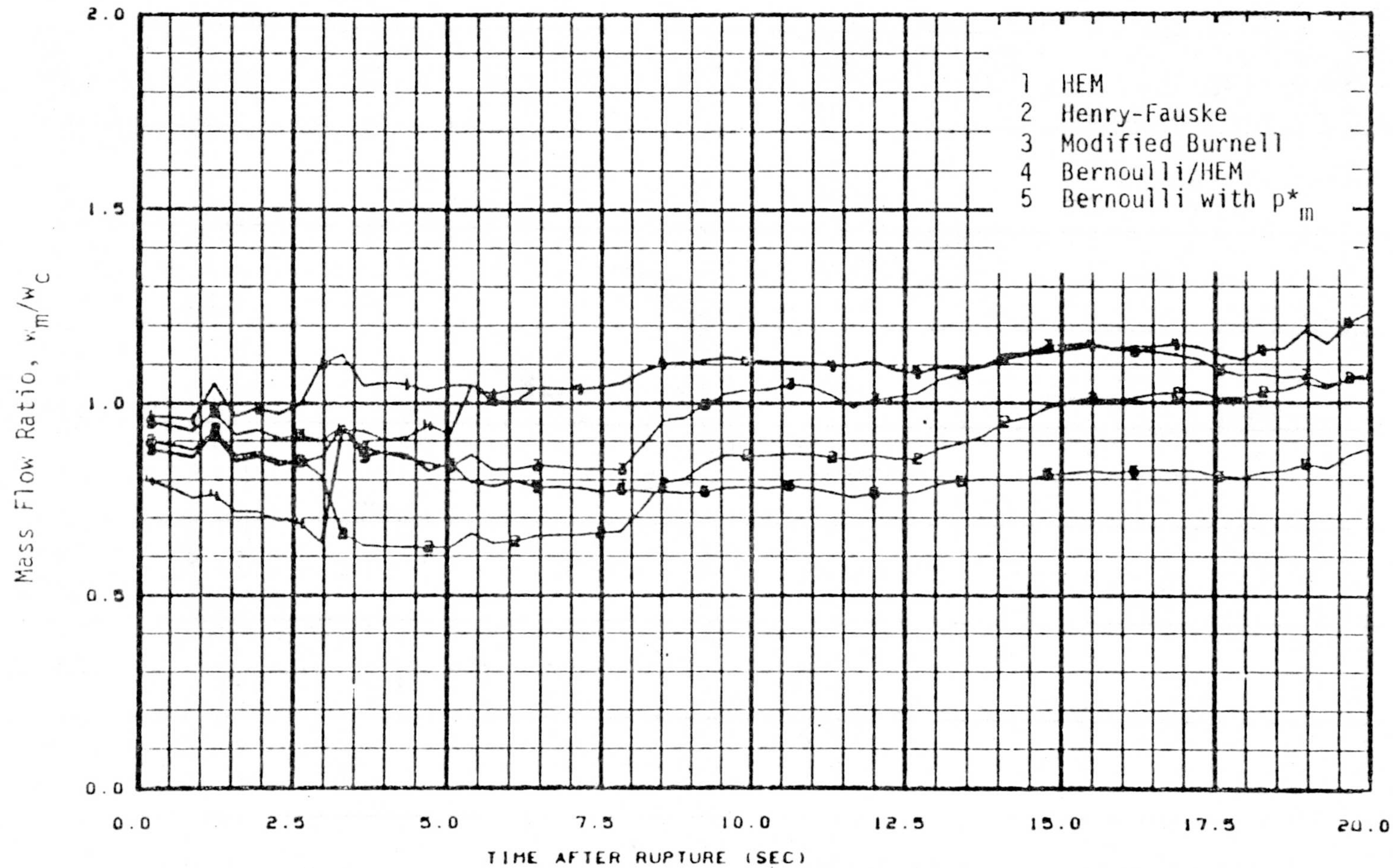

Fig. B-8 Ratios of measured to calculated break flow rates for Semiscale Mod-1 Test S-06-5.

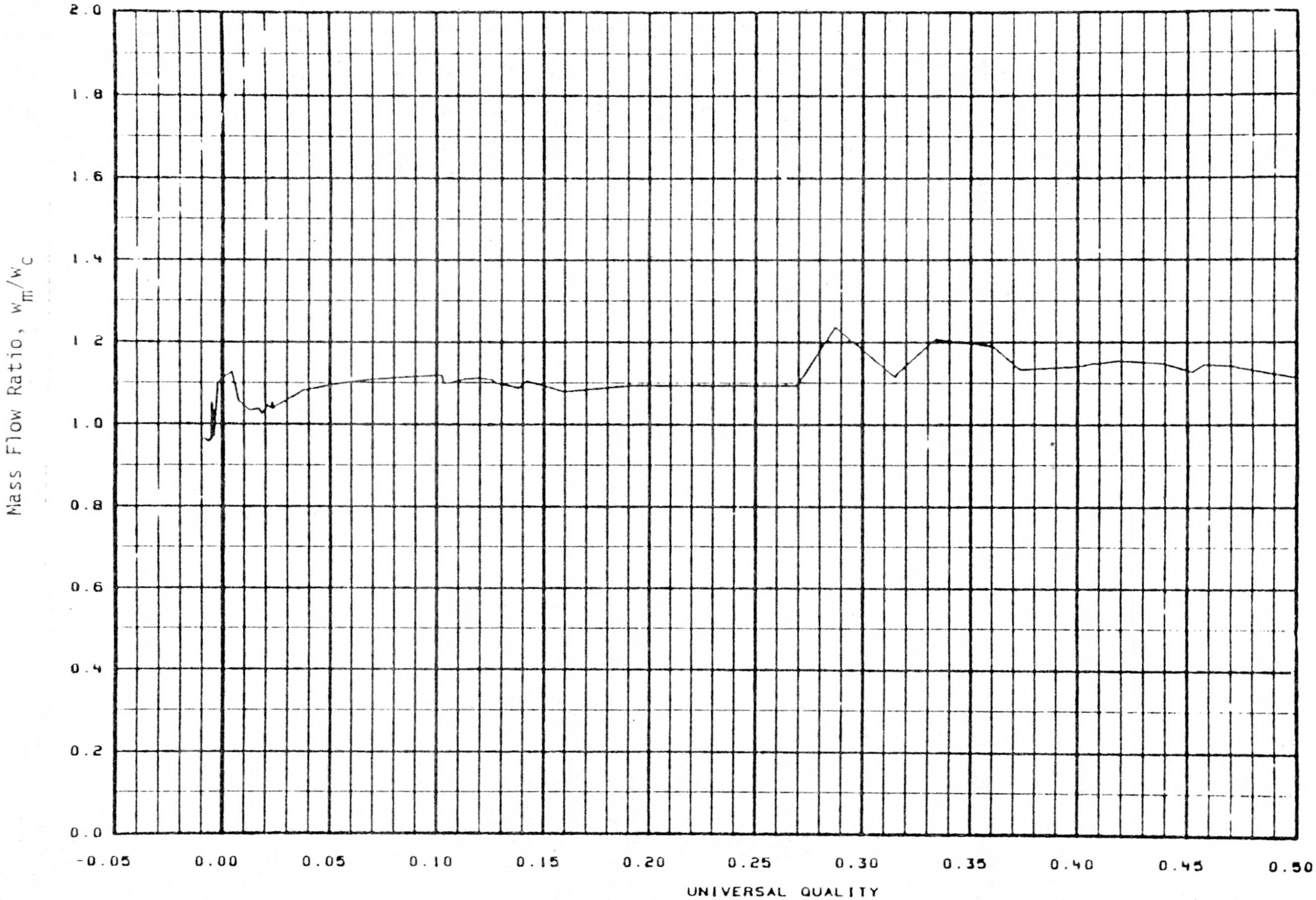

Fig. B-9 HEM mass flow ratio as a function of stagnation universal quality for Semiscale Mod-1 Test S-06-5.

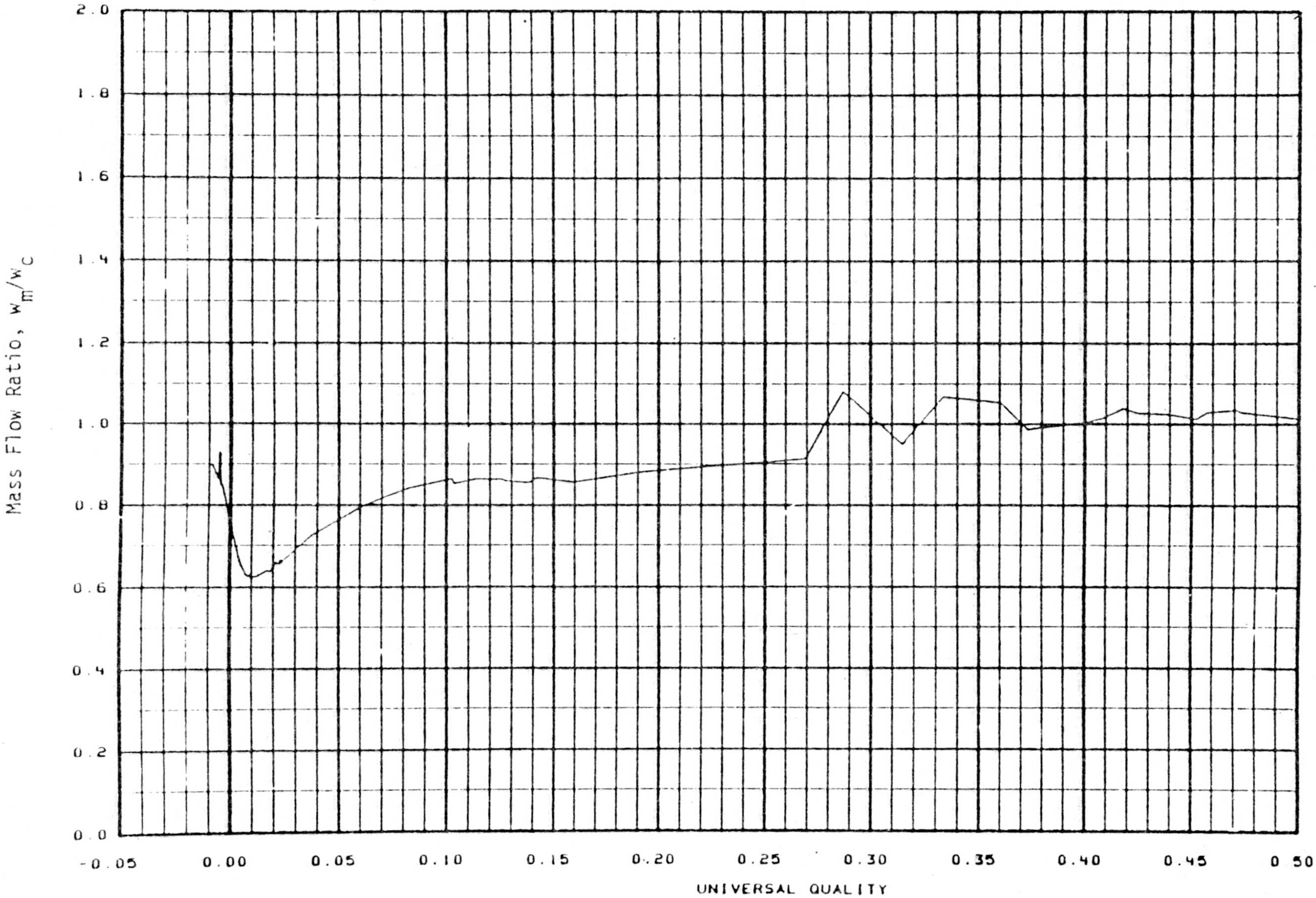

Fig. B-10 Henry-Fauske mass flow ratio as a function of stagnation universal quality for Semiscale Mod-1 Test S-06-5.

To minimize the variation in break flow multiplier, the data suggest that the transition quality should be set to a smaller value than 2%.

As seen in the previous analysis, it is important to properly predict break flow during the time at which the broken loop cold leg fluid is at low qualities. To properly predict core flow in LOFT Loss-of-Coolant Experiment L2-2, it is necesasary to predict break flow during the critical flow transition period. To accomplish this, it is recommended that the transition quality be set at 0.25%. The transition quality value is somewhat arbitrarily selected to be a small number. Zero would be ideal, but a small positive value is chosen to prevent the possibility of the model causing numerical problems due to a step changed in critical flow.

REFERENCES

B-1. D. G. Hall, A Study of Critical Flow Prediction for Semiscale Mod-1 Loss-of-Coolant Accident (LOCA) Experiments, TREE-NUREG-1006 (December 1976).

B-2. D. G. Hall, Empirically Based Modeling Techniques for Predicting Critical Flow Rates in Nozzles, Tubes, and Orifices, CVAP-TR-78-010 (May 1978).

BLANK

APPENDIX C

DETERMINATION OF THE CAUSE OF THE FUEL ROD COMPUTATION SCHEME PROBLEM

BLANK

APPENDIX C

DETERMINATION OF THE CAUSE OF THE FUEL ROD COMPUTATION SCHEME PROBLEM

A simple problem was developed to test the hot rod computational scheme for closure. The three core volumes and the adjacent volumes at each end were extracted from the system model and run as a whole-core hot rod with the end volumes as time dependent. Figure C-1 shows the five volumes (Volumes 1, 55, 54, 53, and 29) which were used. Since the input parameters for the whole-core hot rod were identical to the corresponding values for the system run, the results of the two calculations should be nearly identical. Any significant differences would indicate that the fundamental problem exists with the hot rod calculation scheme.

Comparison of the time zero edit information for these calculations revealed differences in the steady state solution of the momentum equation at the junctions connected to the time-dependent volumes. Further investigation revealed that the volume-averaged velocity, WVBAR, for a time-dependent volume is calculated in the new problem rather than being passed from the old problem data tape. Since WVBAR is calculated based on the inlet and outlet junction flow rates, different values will be calculated by the system and hot rod runs. As illustrated in Figure C-2, the system run has both inlet and outlet junctions, while in a hot rod calculation, one or the other is missing. WVBAR is used in the momentum equation to calculate friction losses in the volume and form losses at the junction. Depending on the nodalization and option selection of the system and hot rod calculations, the differences in WVBAR could be significant.

A new method of applying time-dependent volumes to hot rod calculations was devised. This method replaces each of the time-dependent volumes of the old method with a pair of time-dependent volumes. As illustrated in Figure C-3, the first and last time-dependent volumes will have only one junction and, as before, have an incorrect WVBAR calculated. Therefore, the momentum equation solution

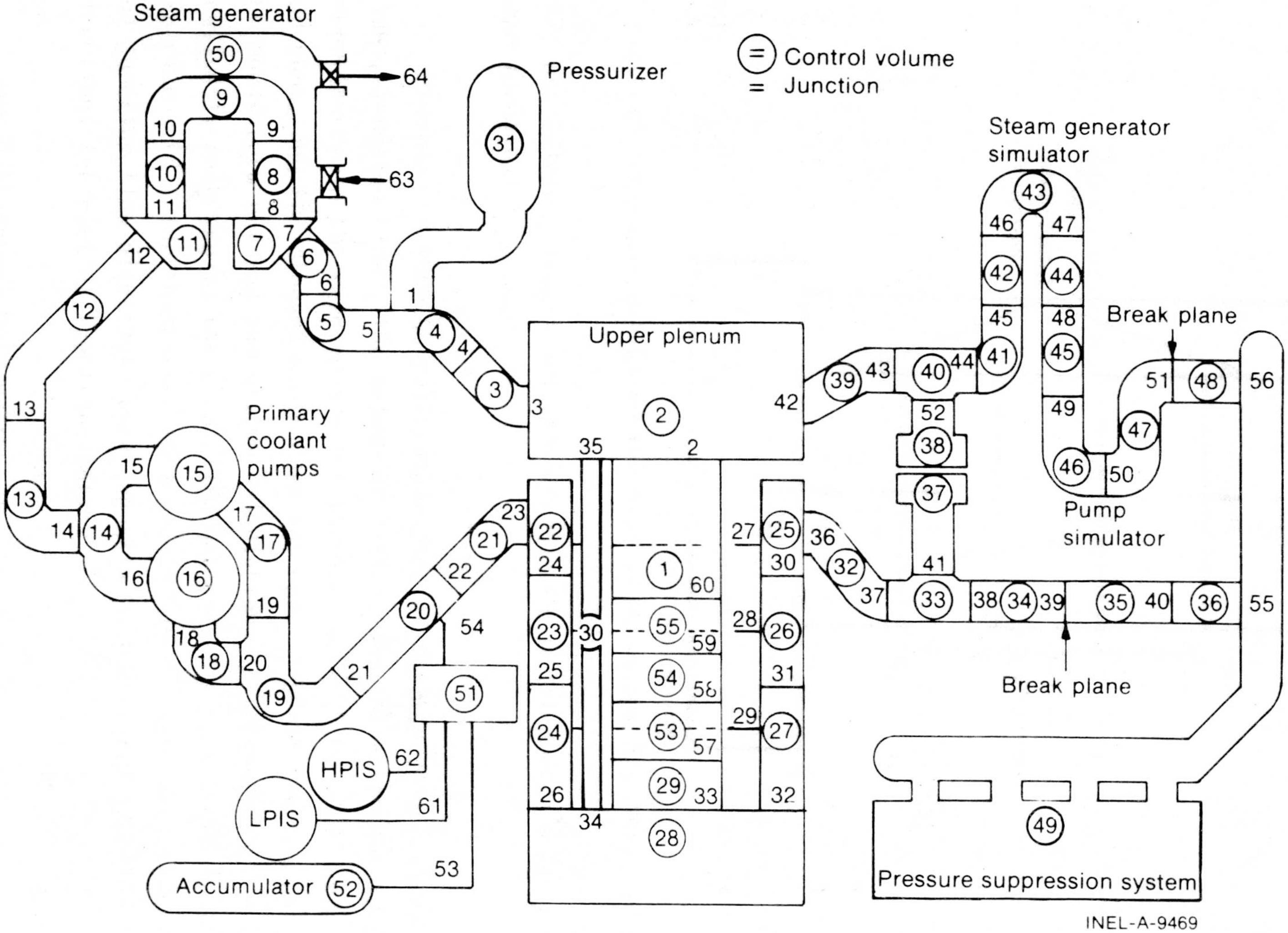

Fig. C-1 Model schematic of LOFT system showing volumes used to test the hot rod computational scheme.

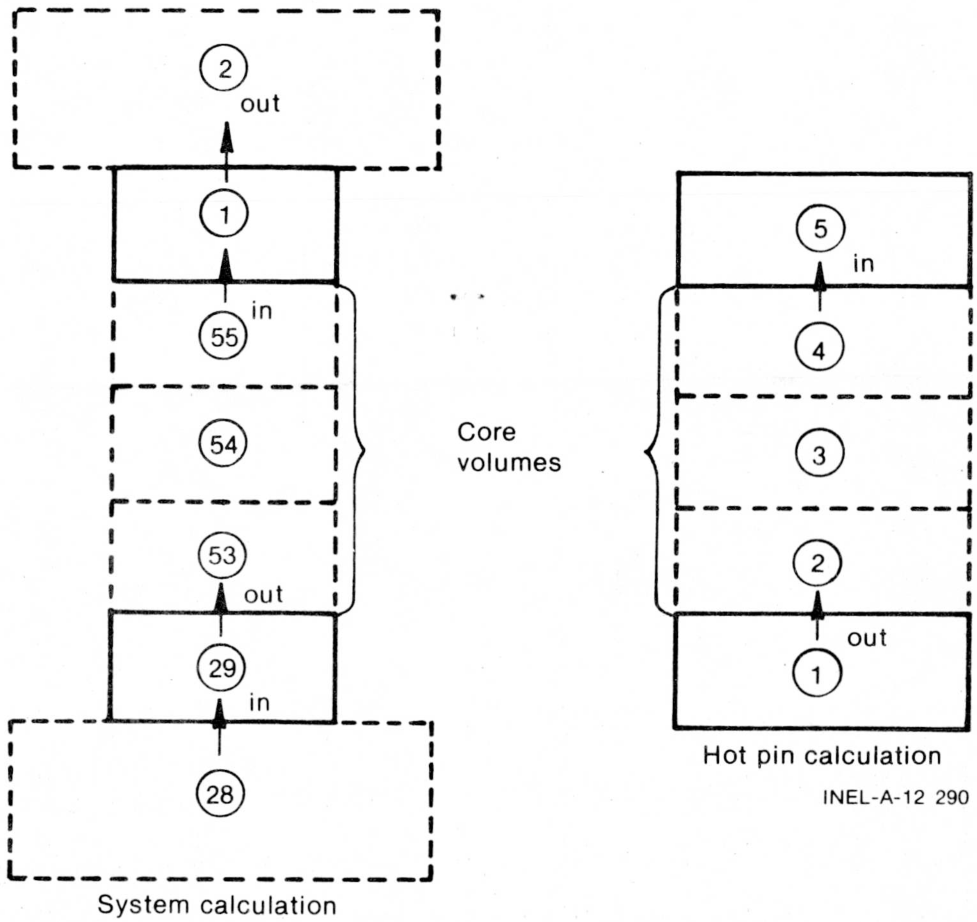

Fig. C-2 Schematic of junction connected to plenum volumes for system and hot rod calculations.

at Junctions A and D will be in error. However, the interior time-dependent volumes have both inlet and outlet junctions, and the correct WVBAR will be calculated. Therefore, the momentum equation solution at Junctions B and C should be the same as in the system calculations.

The computation scheme, dubbed the elegant hot rod, was tested by adding Volumes 2 and 28 to the five volume whole-core hot rod model shown in Figure C-1. Comparison of the time zero edit junction data for these elegant whole-core hot rod and system calculations indicated the expected discrepancy at the junctions connecting the time-dependent volume pairs. However, for the four junctions connected to

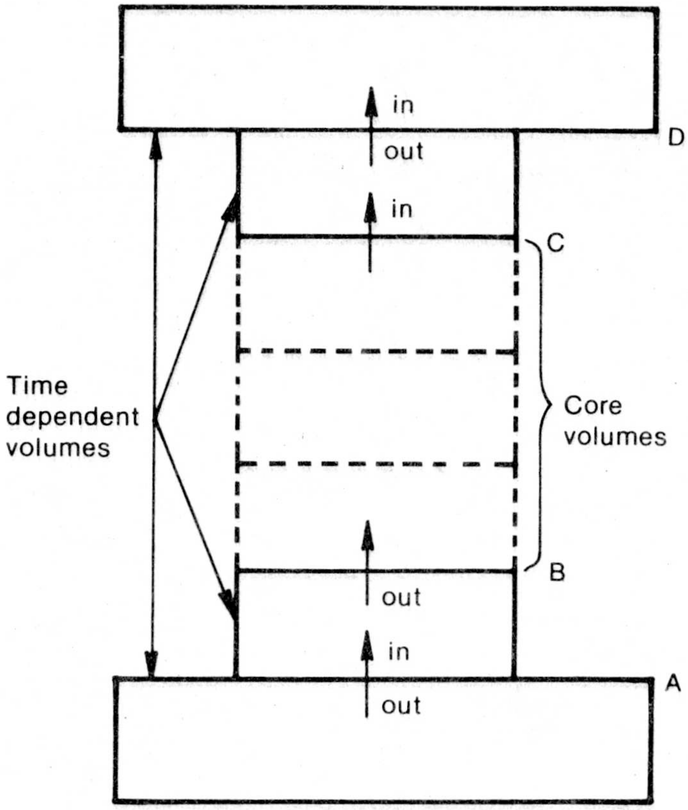

Fig. C-3 Schematic depicting the dual time-dependent volume method.

the core volumes, the steady state solutions of the momentum equation were identical.

Figures C-4 through C-11 compare the calculated volume average flows, junction flows, the volume qualities, and the heat slab surface temperatures in the core region for the system run, the whole-core hot rod runs, and the elegant whole-core hot rod. The differences between the whole-core hot rod and system calculations is substantial. As previously observed in the prediction analysis for Loss-of-Coolant Experiment L2-2 for the corner fuel module hot rod, the whole-core hot rod junction flow directions were opposite to the system junction flow directions for part of the transient.

Some differences between the elegant whole-core hot rod and the system calculations are evident in these figures. They are thought to

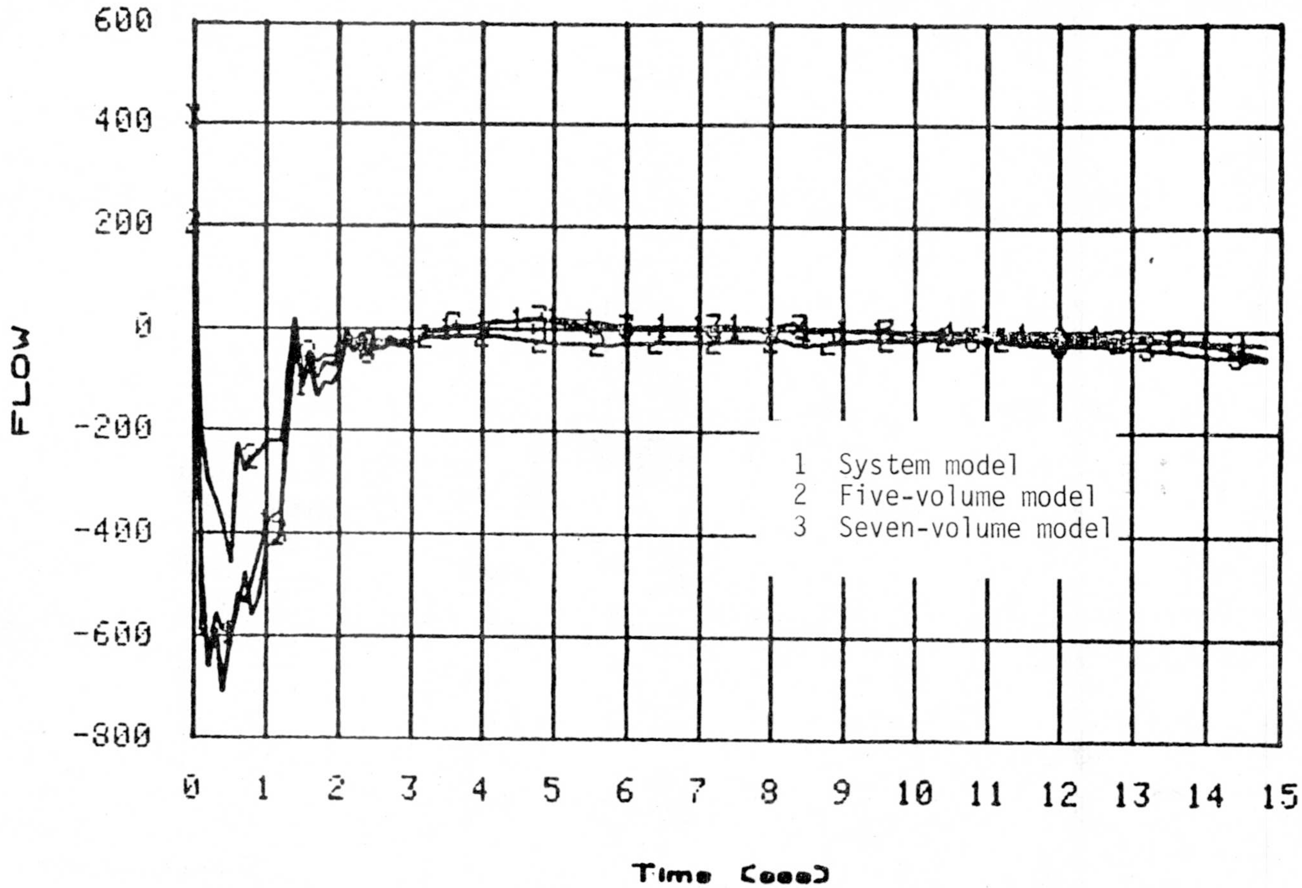

Fig. C-4 Volume-averaged velocity for volume below the core.

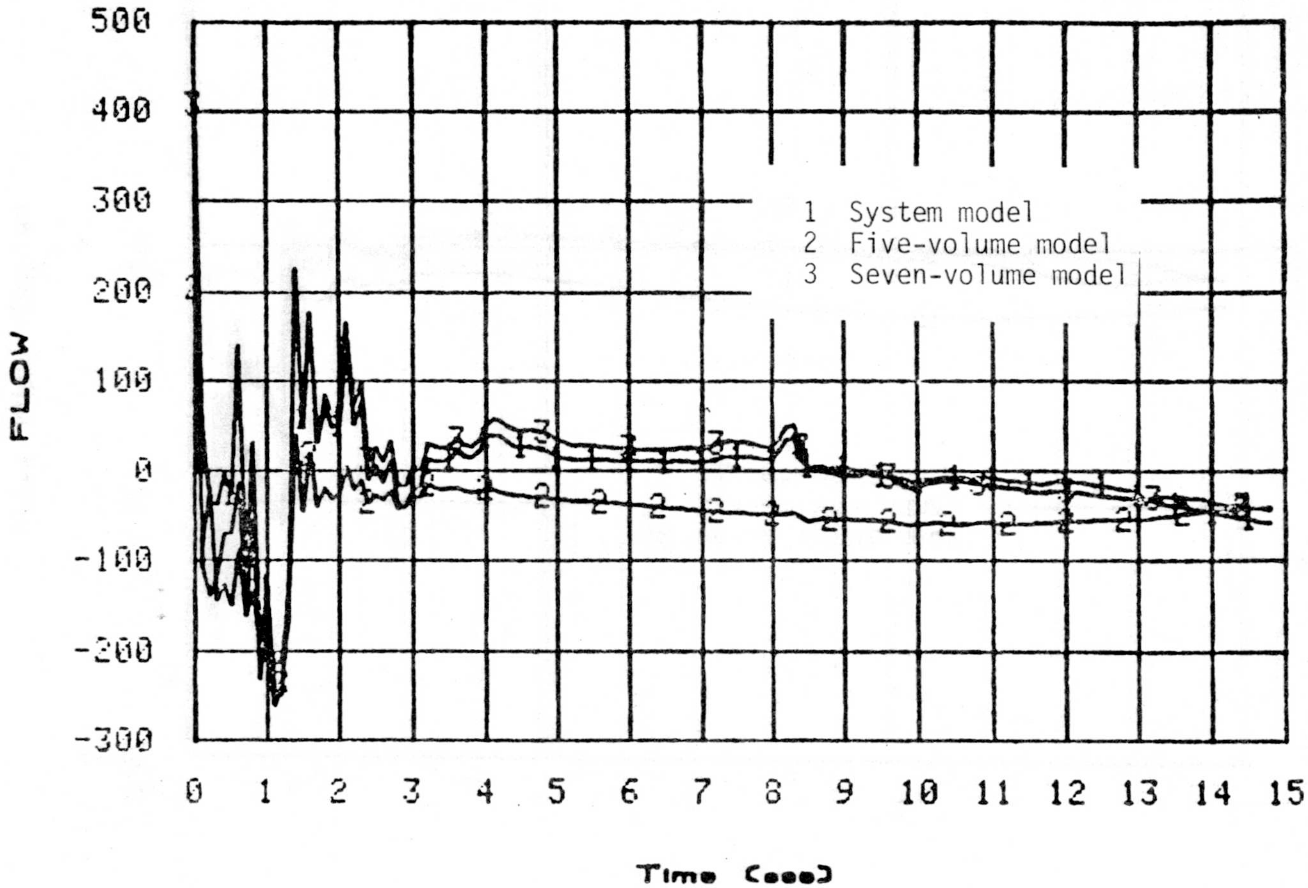

Fig. C-5 Volume-averaged velocity for volume above the core.

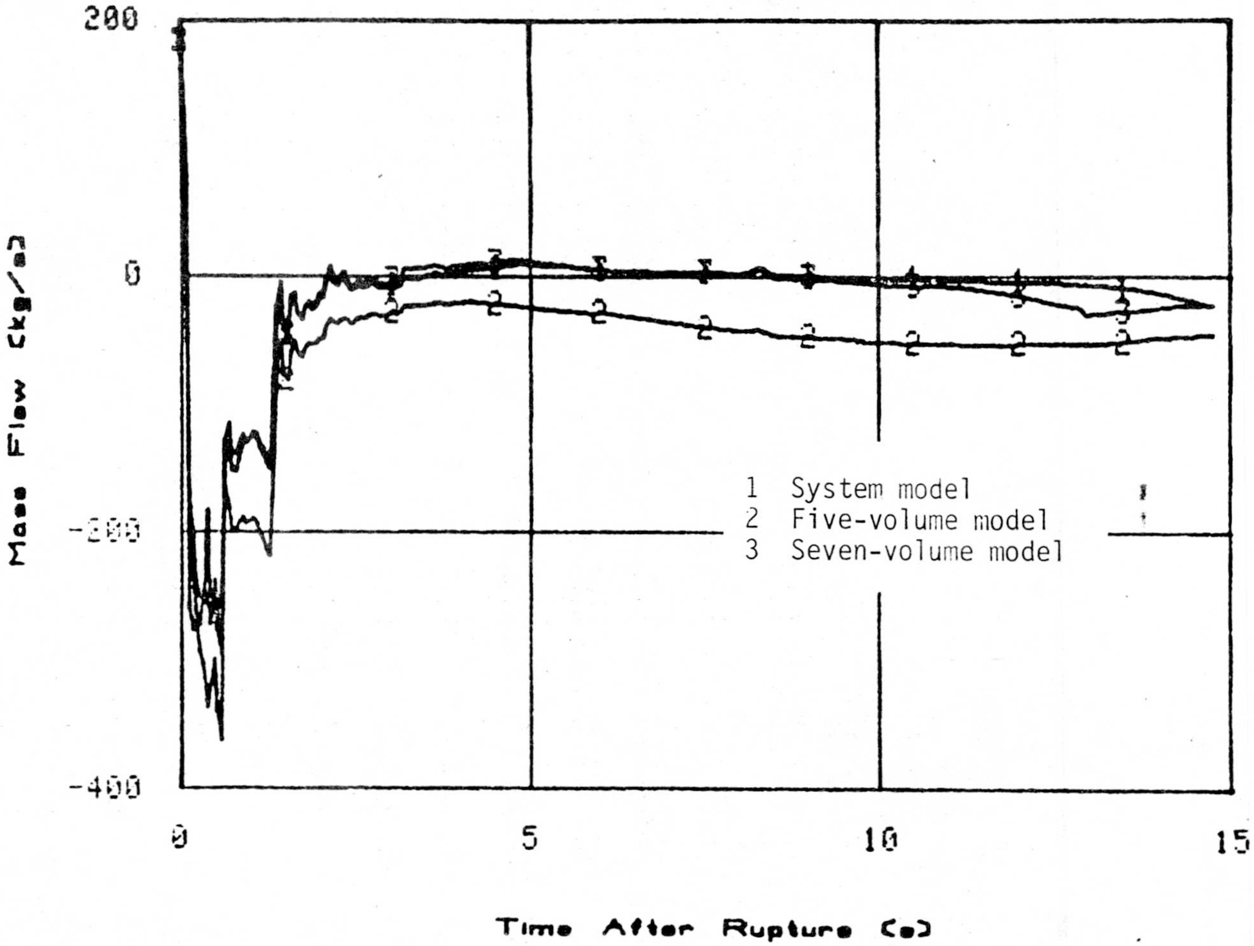

Fig. C-6 Mass flow rate in core inlet.

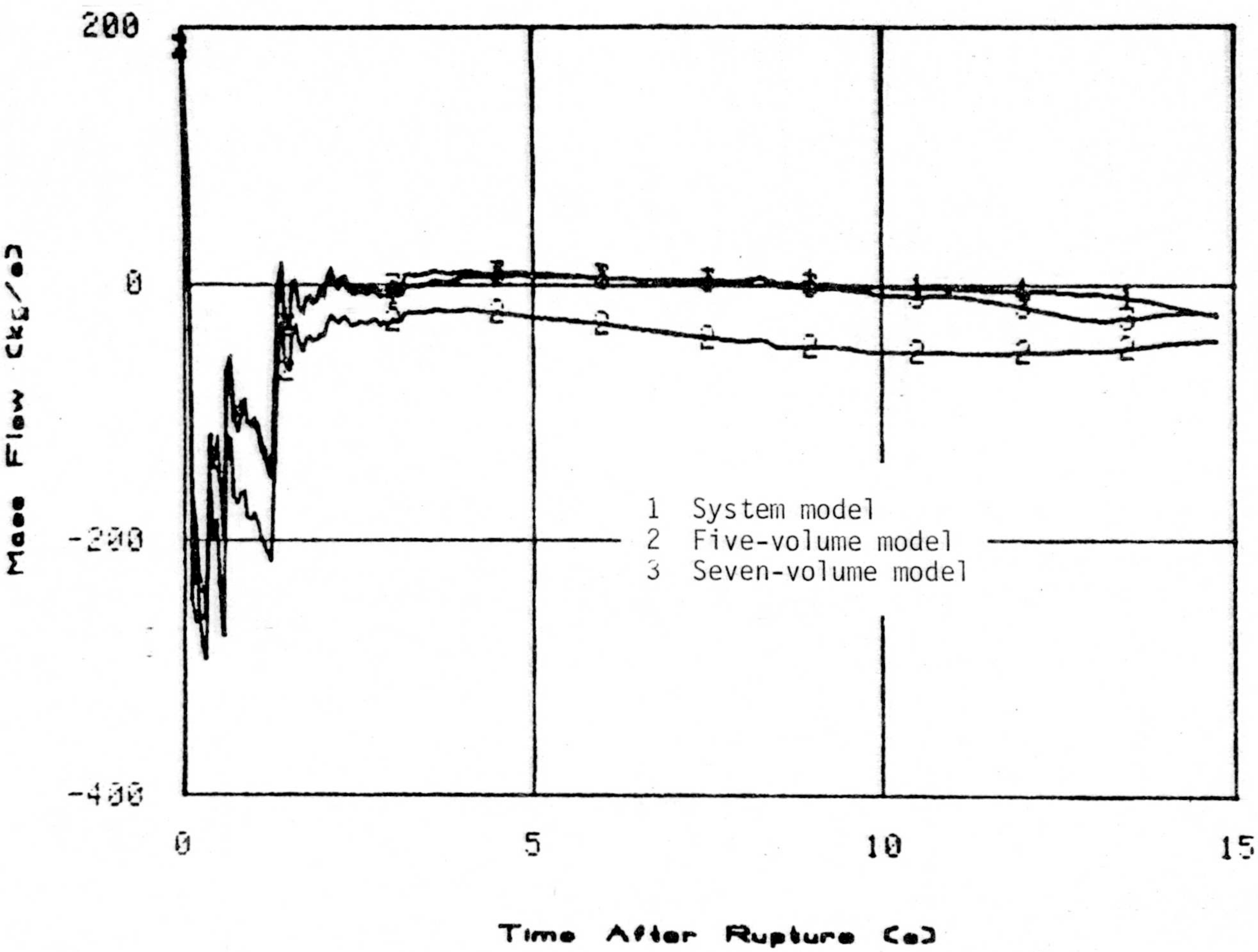

Fig. C-7 Mass flow rate in upper third of core.

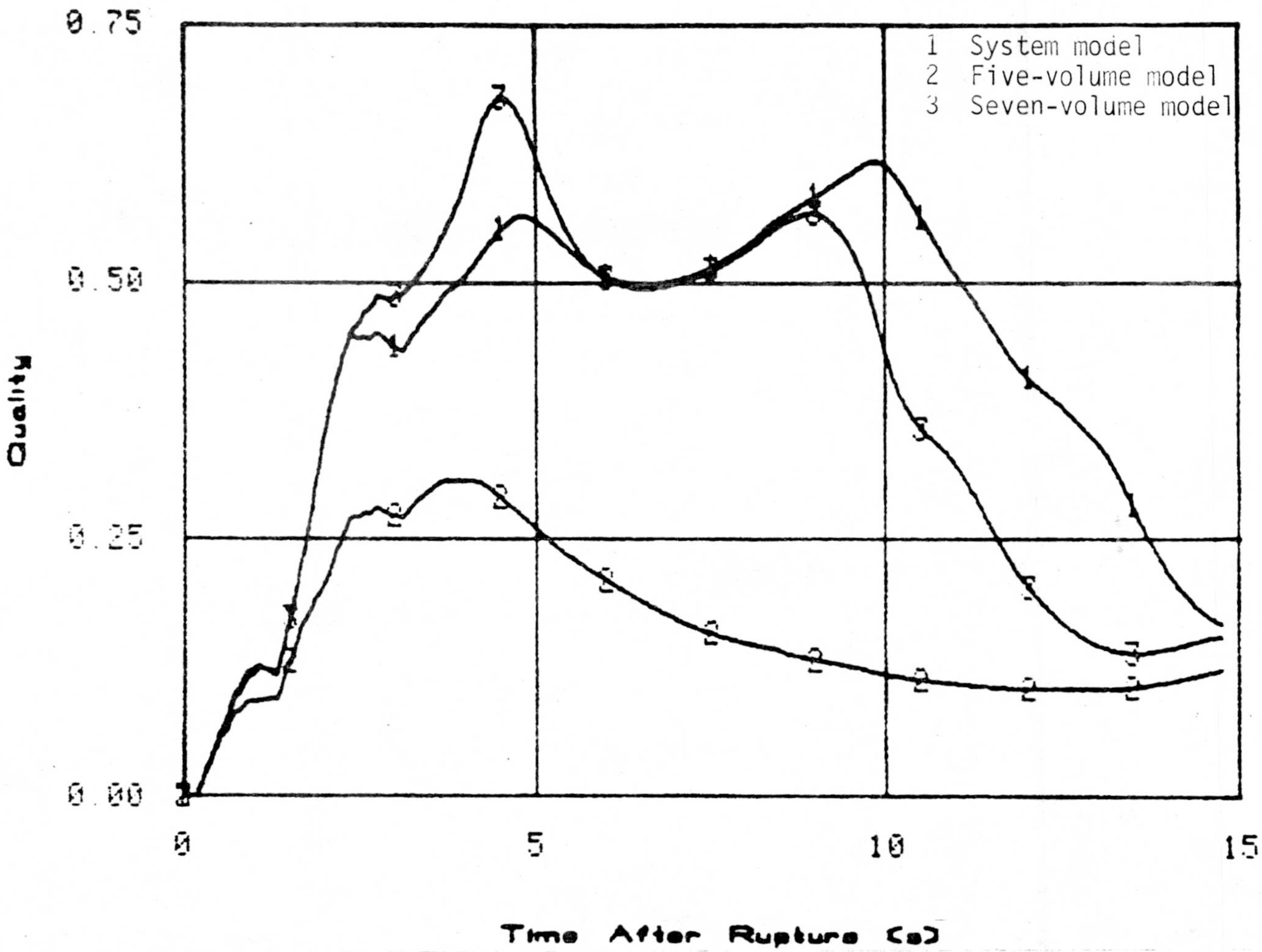

Fig. C-8 Volume quality in middle third of core.

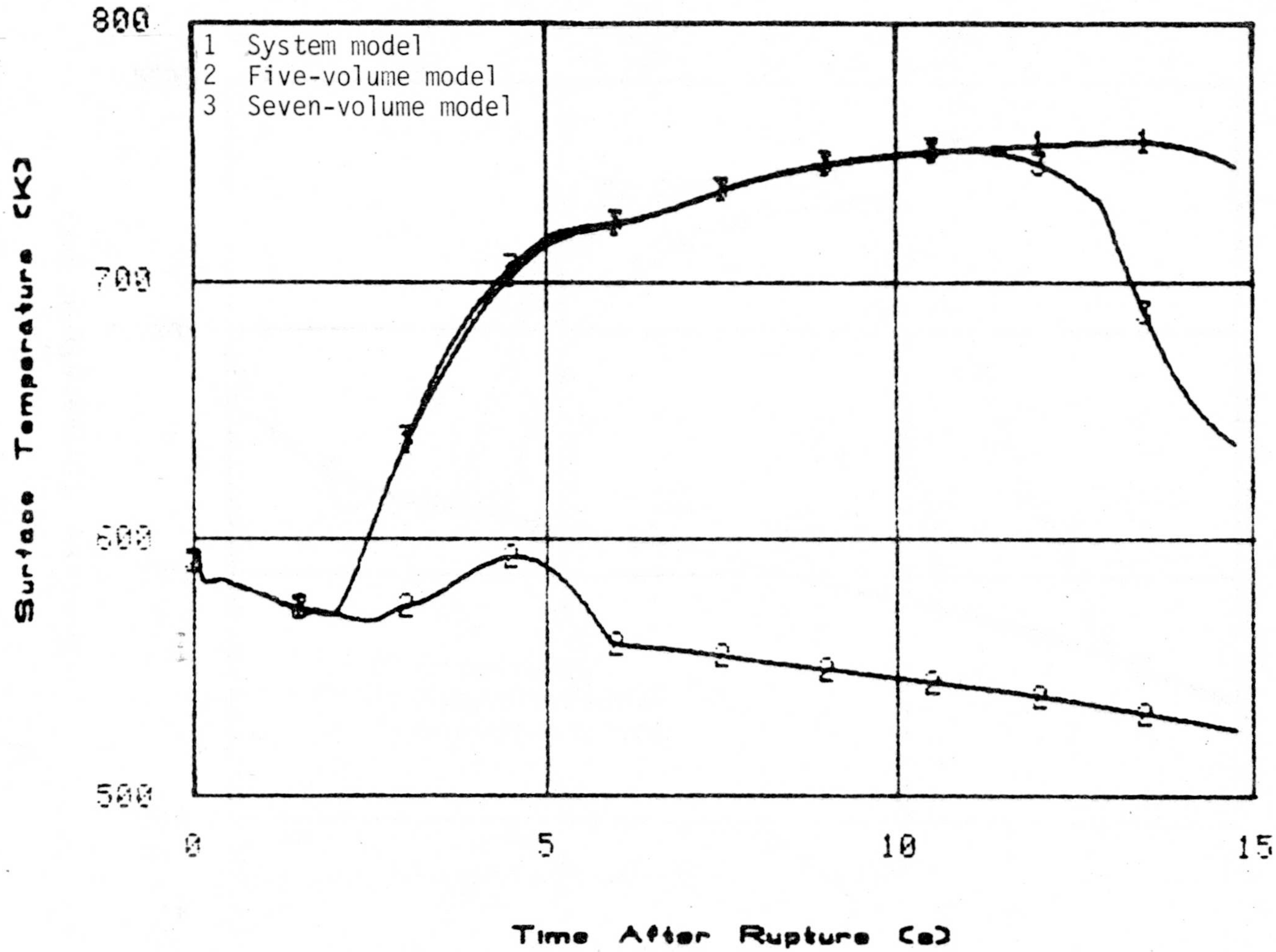

Fig. C-9 Fuel rod cladding surface temperature in lower third of core.

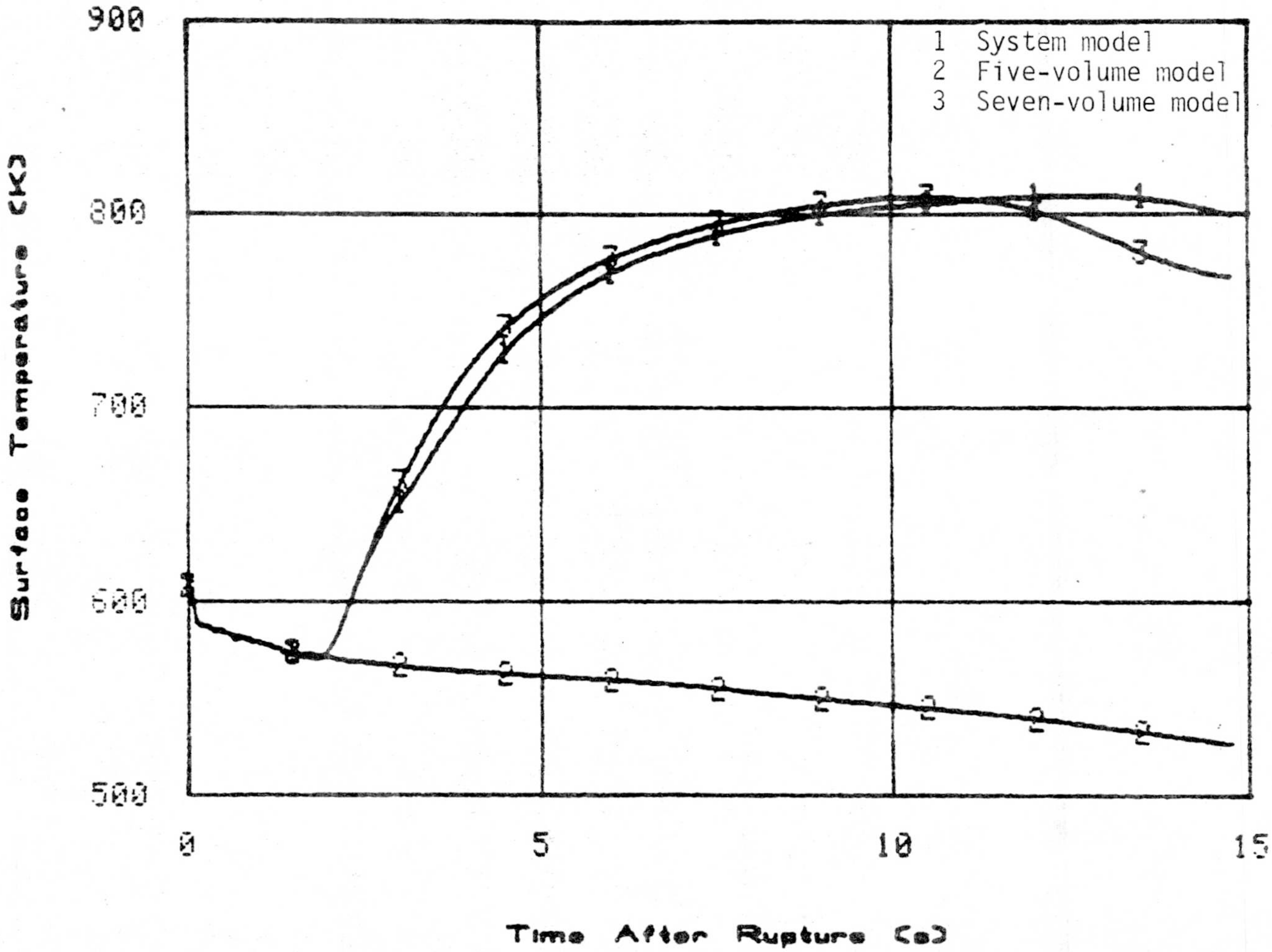

Fig. C-10 Fuel rod cladding surface temperature in middle third of core.

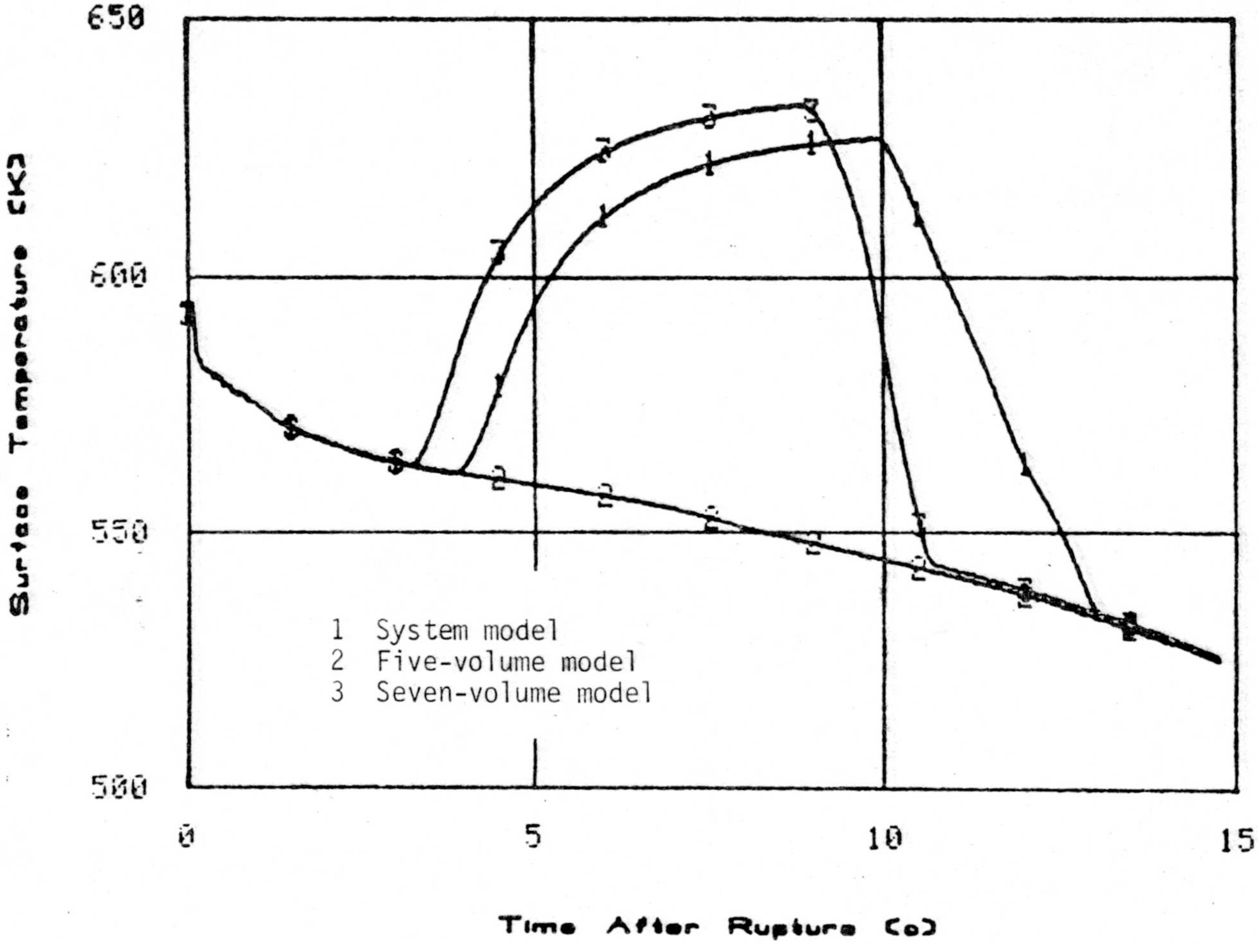

Fig. C-11 Fuel rod cladding surface temperature in upper third of core.

be caused by inadequate coupling (time step differences and interpolation between plot records) between the two runs. Efforts to reduce or eliminate these differences are continuing. When the coupling problem is resolved, the elegant hot rod computational method will be applied to single-channel hot rod analysis.

Although the elegant hot rod computation scheme provides a correct initial solution to the momentum equation at the core junctions, the erroneous WVBAR calculation in the end volumes may still affect the transient solution. A better solution to this problem is to reduce the WVBAR error by either:

(1) Nodalizing the time-dependent volumes with large flow areas so that the WVBAR is small

(2) Eliminating the WVBAR from the solution by using the incompressible form of the momentum equation at the core inlet and exit volumes and using a large hydraulic diameter in the time-dependent volume so that the friction term is small.

For the latter case, the junction loss coefficients should be adjusted to include the friction losses. These alternatives to the elegant hot rod computational scheme are being investigated.